U.S. DEPARTMENT OF ENERGY

JSA

USPAS June 2015

Rutgers

SURFACE & MATERIAL SCIENCE APPLIED TO SRF SURFACES- CASE STUDIES

Anne-Marie Valente-Feliciano

Thomas Jefferson National Accelerator Facility

CASE STUDY: N SURFACE DOPING OF BULK NB (JLAB/FNAL/CORNELL)

N doping

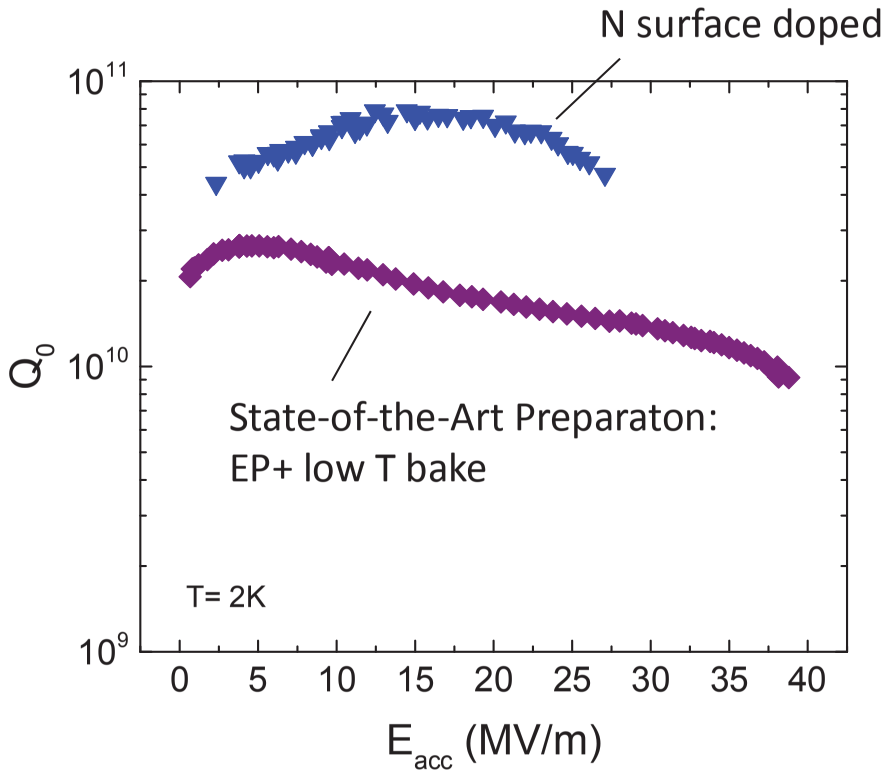

- Reacting bulk niobium cavities with N_2 gas (N_2 p.p ~$2x10^{-2}$ Torr) at 800°C in UHV furnace for ~20 min followed by 30 min with no N;
- Material removal via electropolishing (EP) followed by high-pressure water rinsing (HPR).

N doping: SEM, XRD & XPS

Nb samples processed parallel with cavities

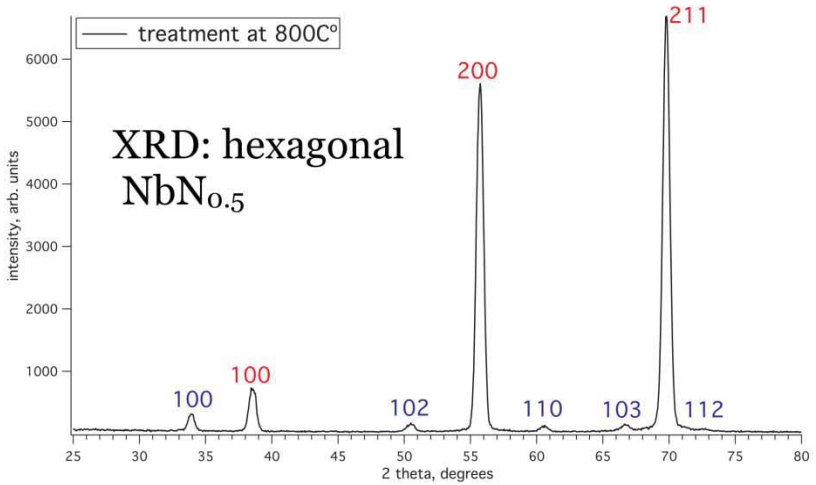

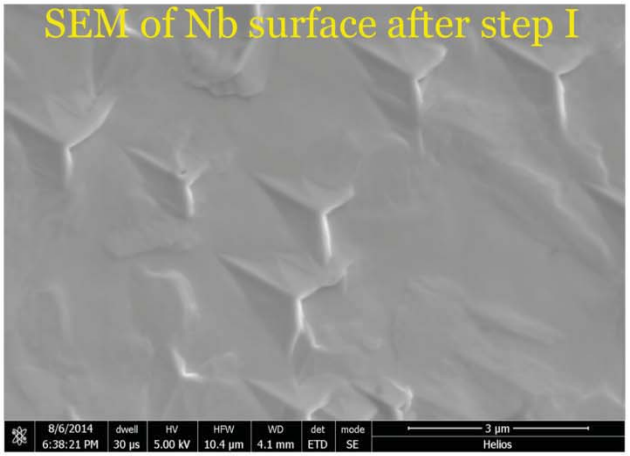

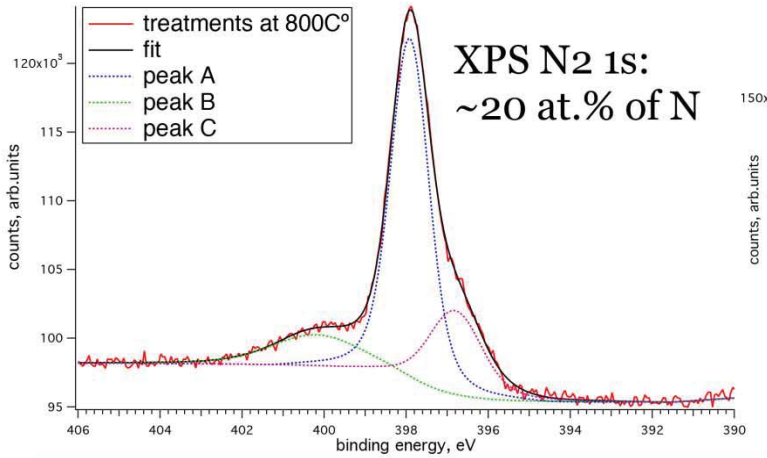

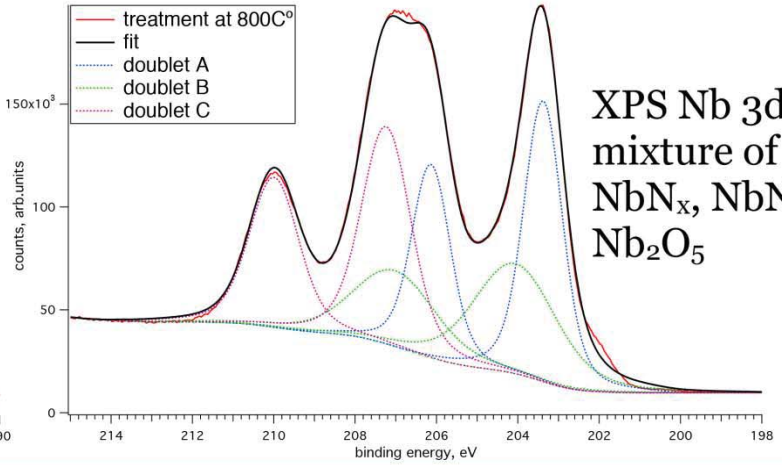

XRD, XPS, SEM: we have NbN_x (β-NbN) after the 1st step

N doping

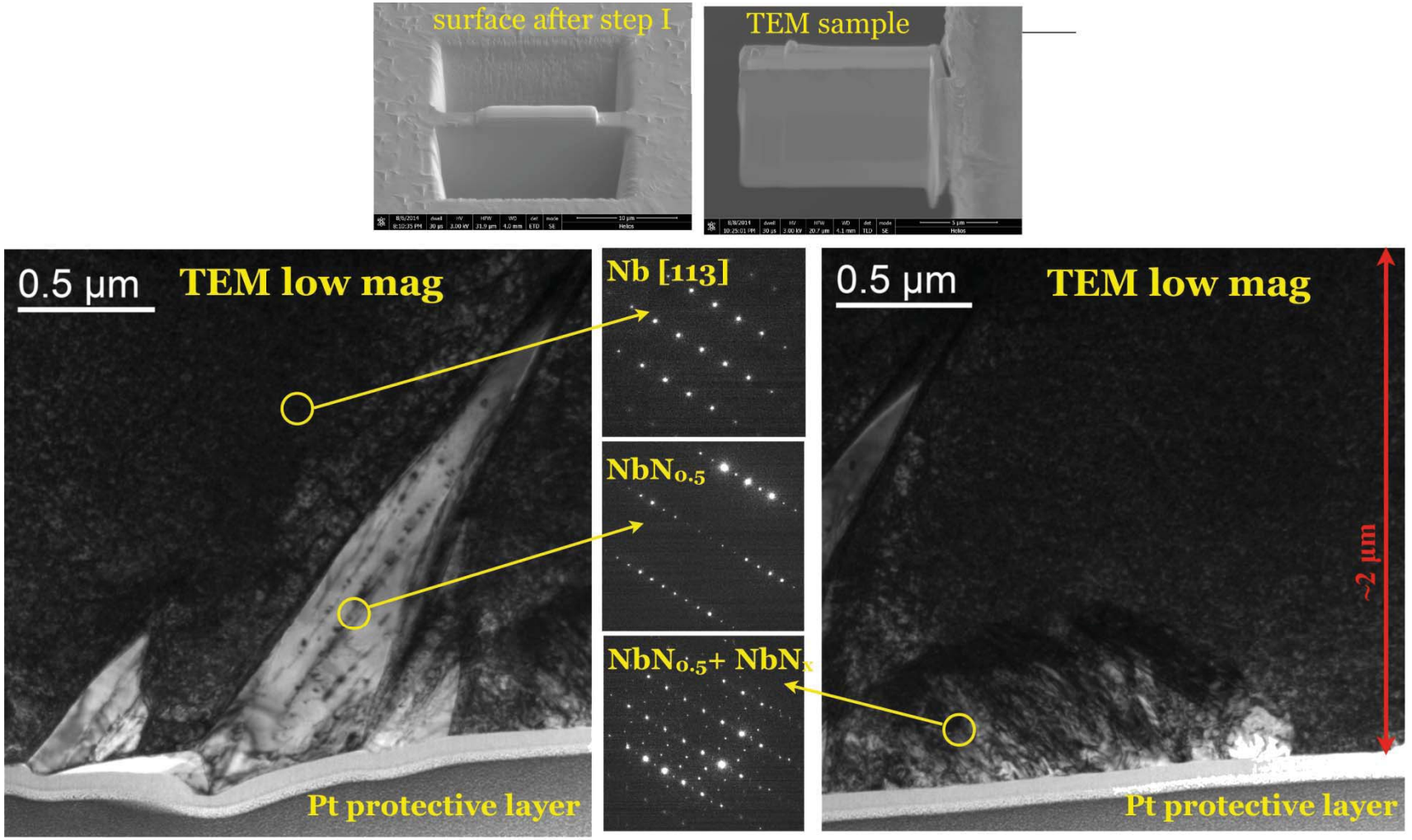

TEM, NED: $NbN_{0.5}$+NbN_x within at least first 2 µm.
Poor SRF performance after step I: Q~ 10^7

N doping

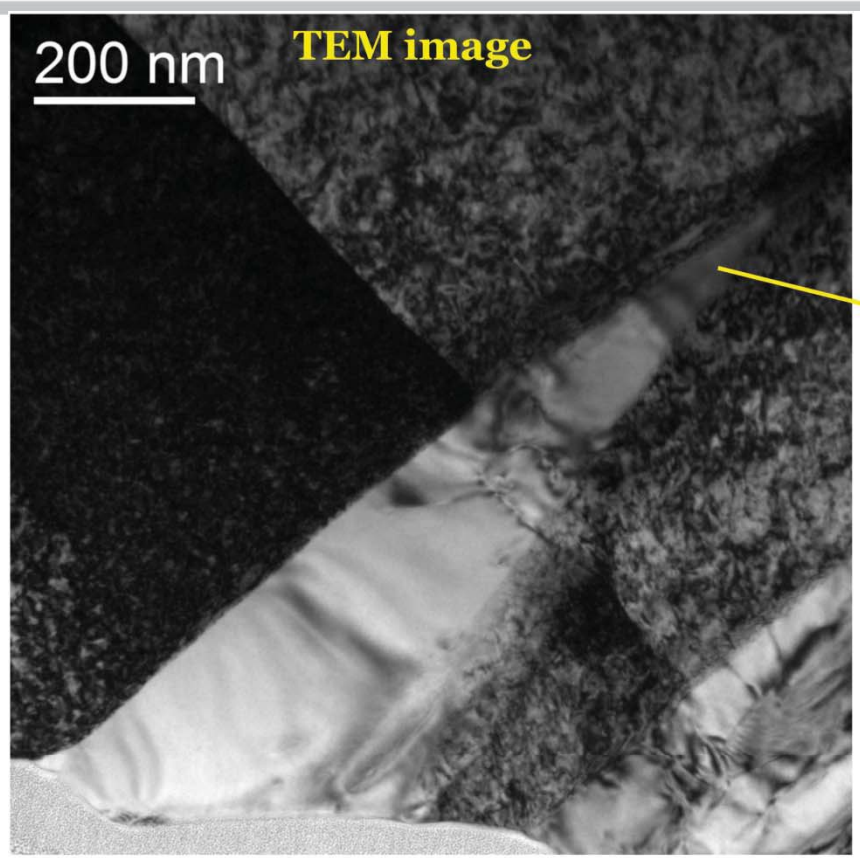

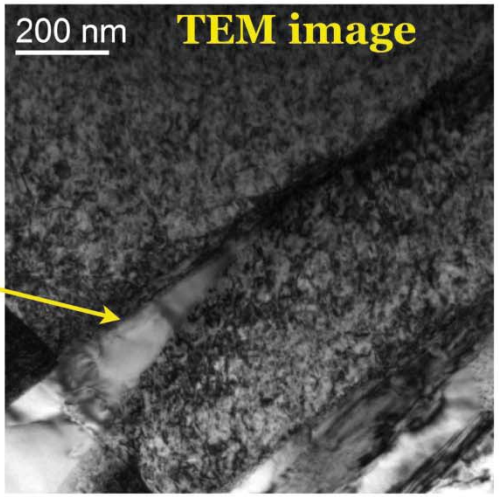

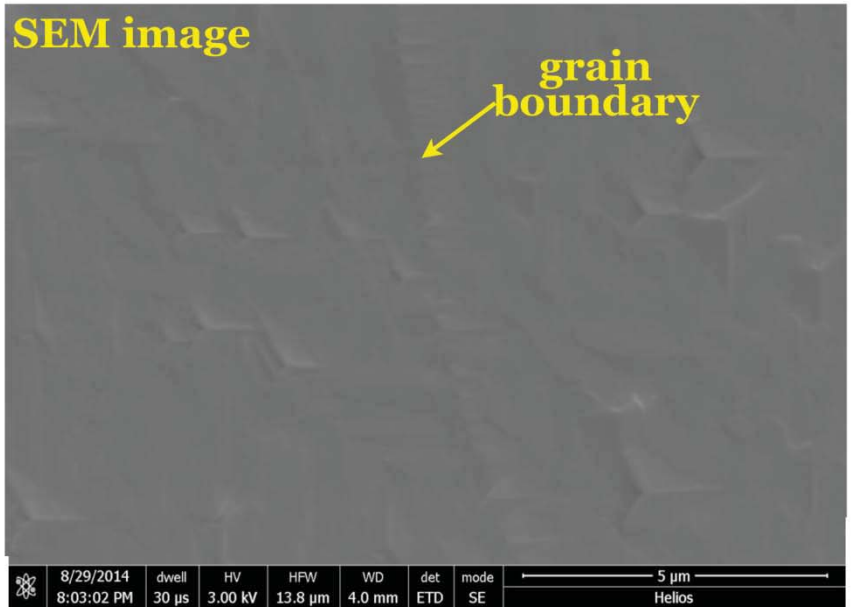

NbN_x extend ~2µm along GB

N doping

Cutout from N treated cavity

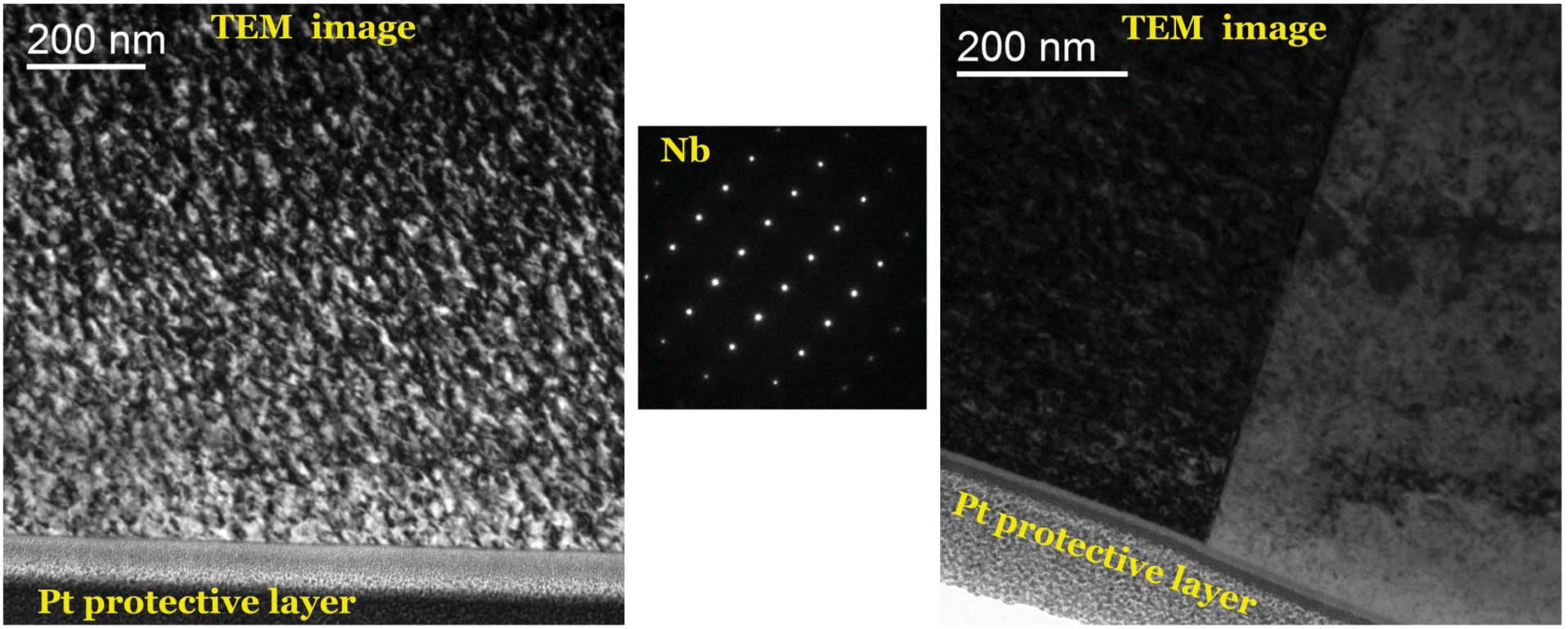

XRD, XPS, TEM: NO Nb nitrides after step II

(HPR).

N doping

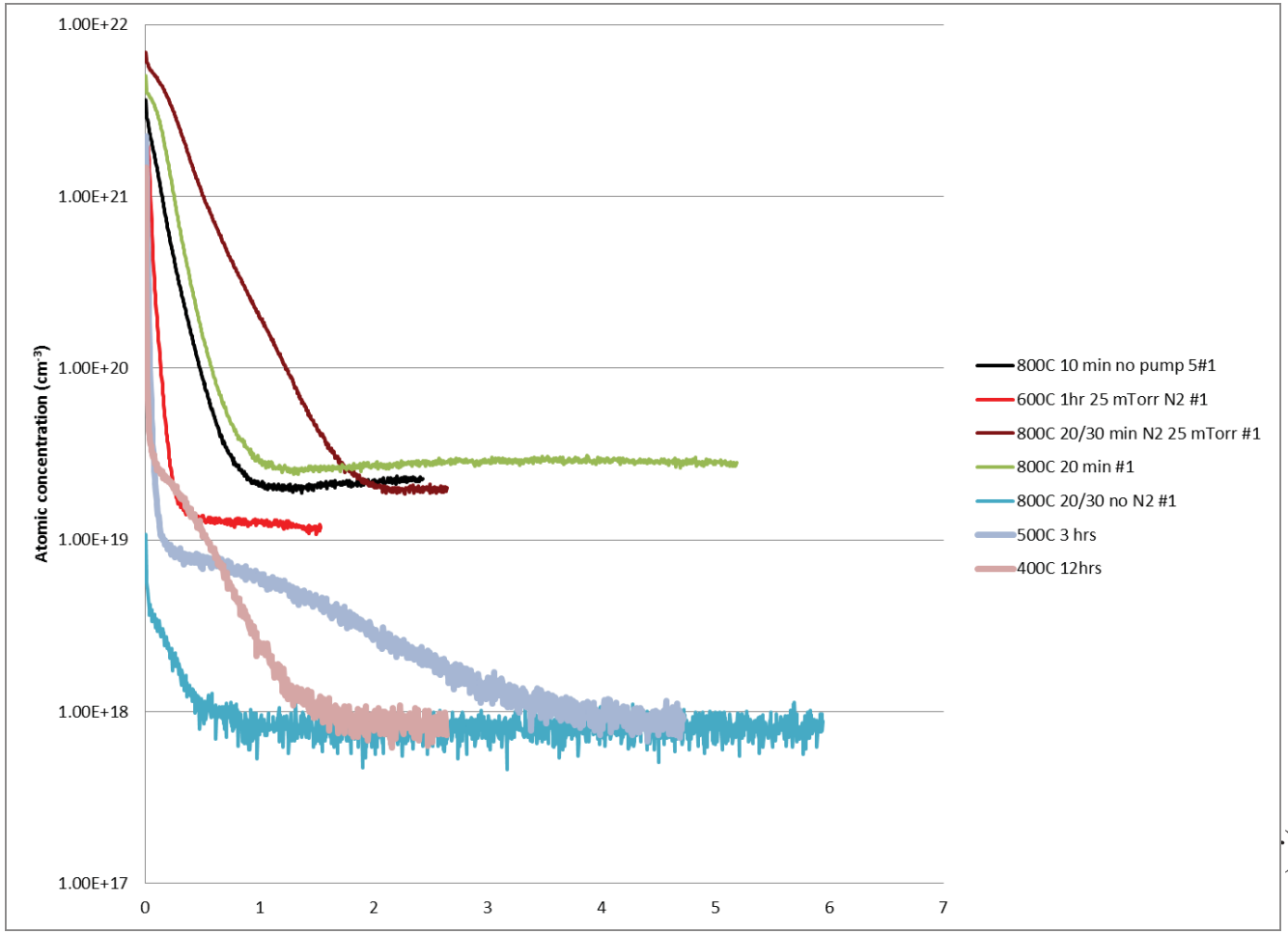

) at 800°C in UHV

- Material removal via electropolishing (EP) followed by high-pressure water rinsing (HPR).

CASE STUDY: STRAIN IN BULK NB (R. CROOKS, BLACK LAB LLC)

Problem & Solution

- Performance limits (~1/3 < 35 MV/m) for ILC cavities are related to defects
  - Hot spots
  - Thermal quenching due to pits in the heat-affected zone
- Recrystallization and grain growth occur during elevated temperature exposure of cold-worked metal (in the HAZ)
- Current production methods for SRF cavities produce high levels of stored strain energy near the equator.
  - increased interstitial content
  - unstable microstructures (to subsequent high temperatures)
- Higher performance srf cavities can be produced by using well-designed recrystallization processing

Low field quench AES001 ILC Cavity

Comparison of Q_0–E_{acc} curve between FNAL and KEK

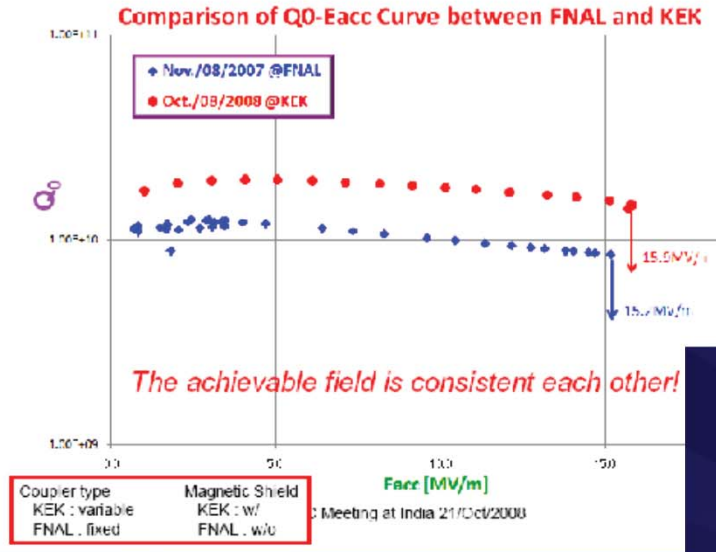

Y. Yamamoto, H. Hayano, E. Kako, S. Noguchi, M. Sato, T. Shishido, N.
K. Umemori, K. Watanabe(KEK), H. Sakai(ISSP, Univ. of Tokyo) and T. X
TTC Otober 21,2008

Positions of Hot Spots on AES001 Cell #3

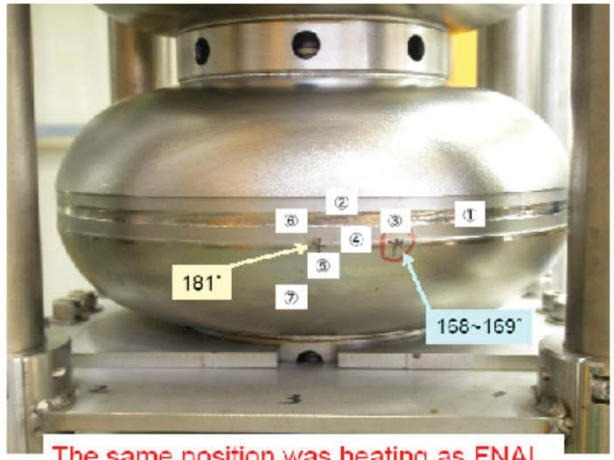

Y. Yamamoto, H. Hayano, E. Kako, S. Noguchi, M. Sato, T. Shishido, N. Toge,
K. Umemori, K. Watanabe(KEK), H. Sakai(ISSP, Univ. of Tokyo) and T. X. Zhao(IHEP)
TTC Otober 21,2008

Stored Strain Energy in Nb Cavities

Nb RRR sheet metal processing

- Rolled to sheet thickness
- Recrystallized
- Roller-leveled, surface cleaning
- Deep drawn
- Welded
- Chemically treated (BCP or EP), HPWR
- Heat treated

Post-recrystallization strain

Stored Strain Energy in Nb Cavities

- Stored energy is real
  - Dislocations are unstable defects
  - Heating causes increase in equilibrium vacancy content
  - Vacancies increase dislocation mobility, rearrangement to lower energy configurations
- Stored energy drives recrystallization

Measuring Strain: macroscopic technique

Aluminum alloy samples used in limit dome tests.

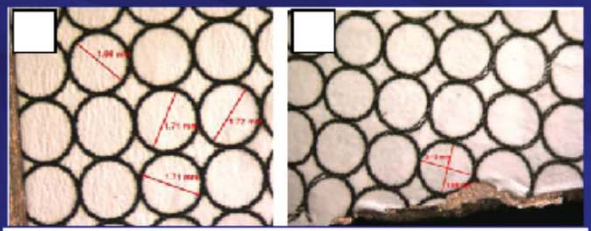

Grids on sheet metal surface viewed under a microscope: (a) before deformation, (b) after deformation (near a crack).

Prof. J
Northw

Engineering Strain in ILC Cavity – Saito 2004

Local Elongation

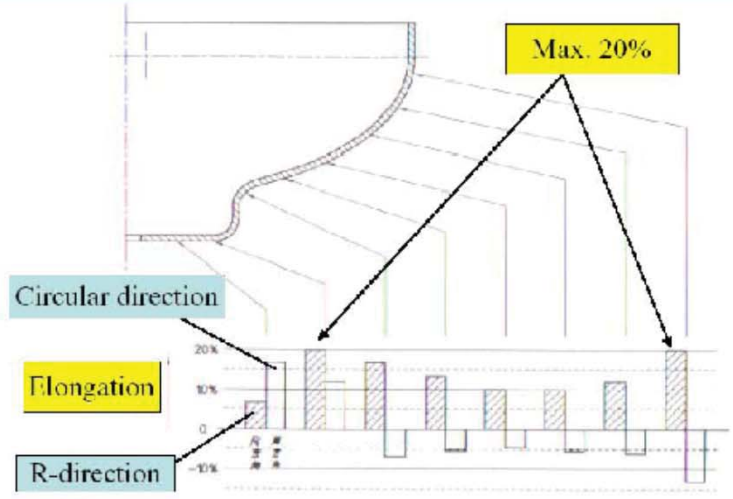

07/July/2004 K.Saito 名大物理集中講義ノート 137

Dependence on Deformation Strain

- Very low strains (< 10%): **secondary recrystallization**, driven by stored energy (surface energy effects also possible).
- Small strains (10-25%): "**strain induced boundary migration**" (SIBM), where new grains arise by fluctuations in position of existing grain boundaries.
- Medium strains (25-200%): **abnormal grain growth** of the subgrain structure (after recovery, polygonization).
- Also "**nucleation**" occurs from heterogeneities such as shear bands and coarse second phase particles.

Measuring Strain: EBSD

Deep draw

JLab 161
Mark III
CEBAF cavity

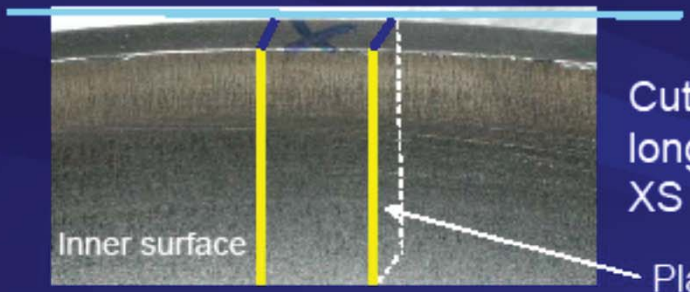

Cut
longitudinal
XS

Plane of
polish

mount

polish

Automatic polisher
to 0.05 μm colloidal silica

At NASA Langley

Longitudinal Section Etched 10s 1:1 Nitric:HF

3mm from top of cavity

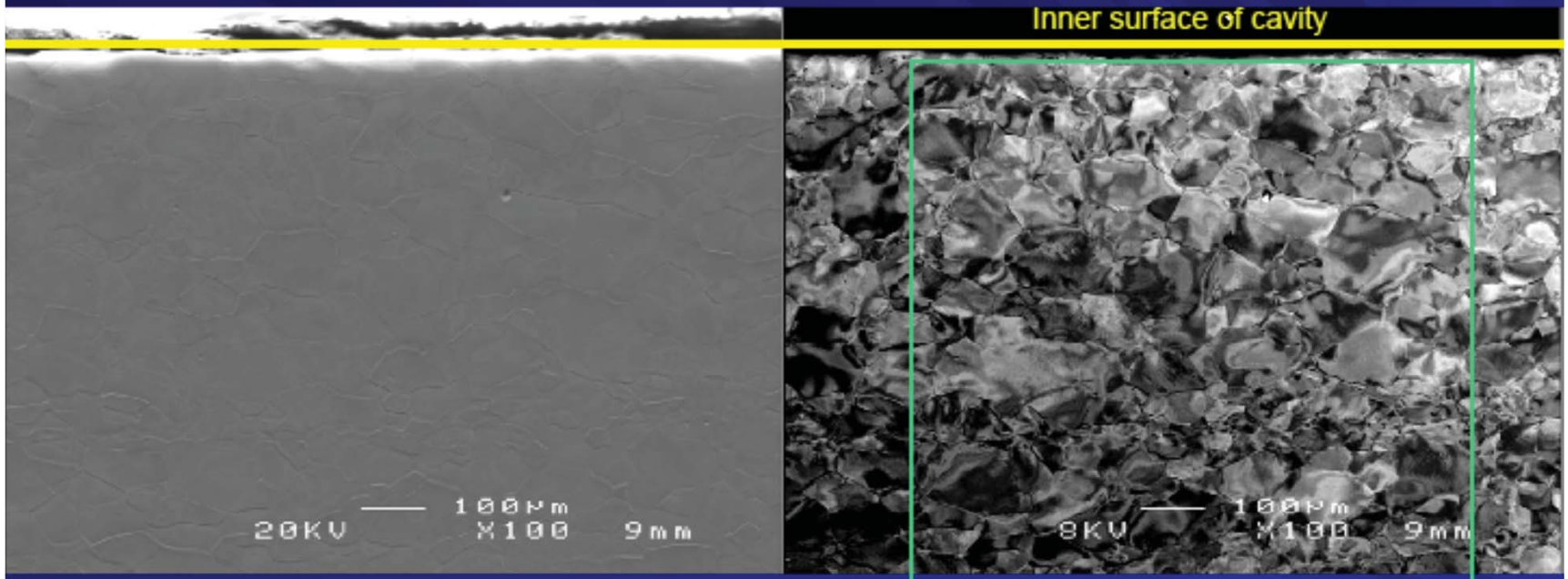

Secondary electron image

EBSD Grid

Backscattered electron image
(showing channeling contrast)

EBSD IPF Map

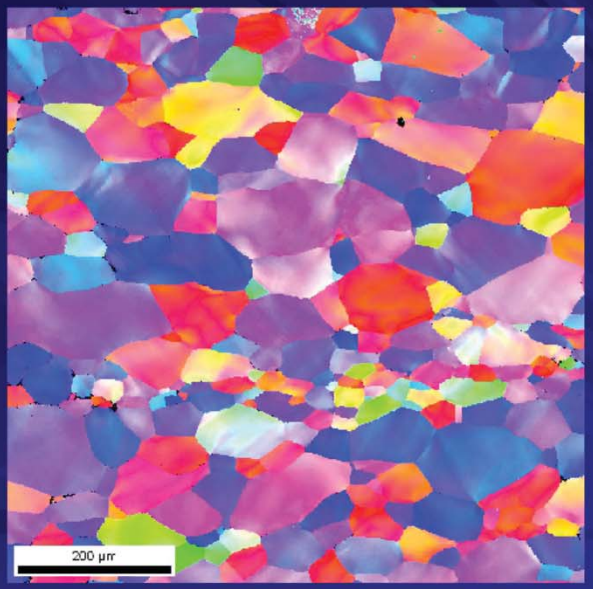

Crystal directions normal to sheet surface (interior surface)

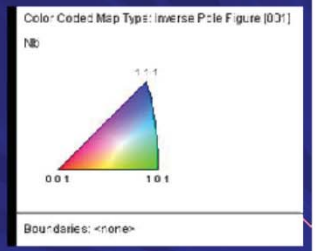

Color changes within grain show distortion of crystal

95% hit rate, 560,200 data points, 1 µm spatial resolution

22

EBSD GOS Map

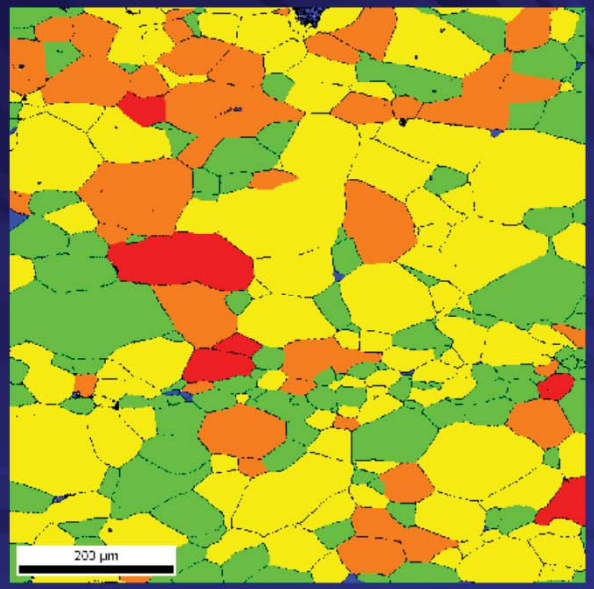

1 µm spatial resolution

Strain in isolated grains

GOS: The average orientation is first calculated for each grain. The spread is then the average deviation between the orientation of each point in the grain and the grain average.

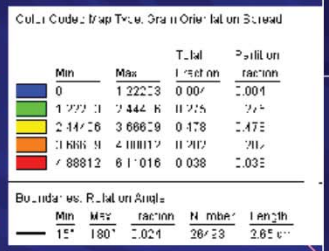

As-received sheet

23

EBSD KAM Map

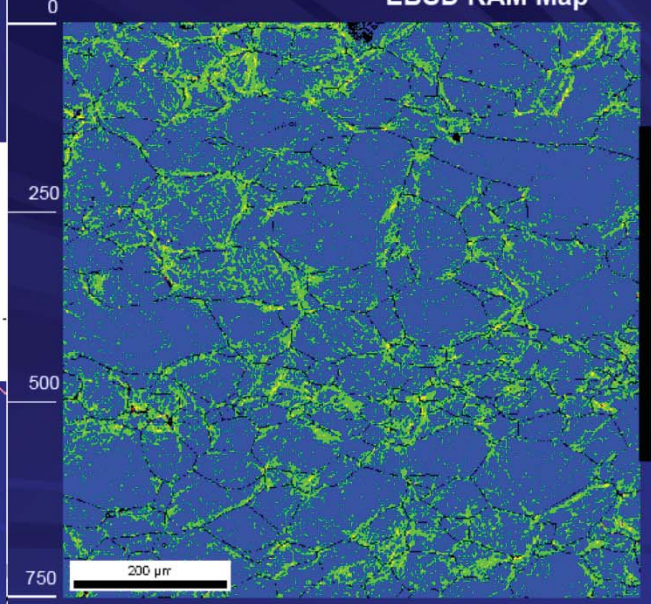

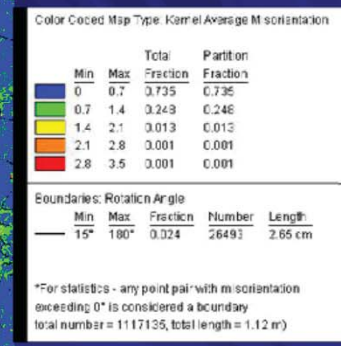

Stored Strain Energy Very High at 500 µm from inner surface

1 µm spatial resolution

24

EBSD IPF Map 500 μm deep

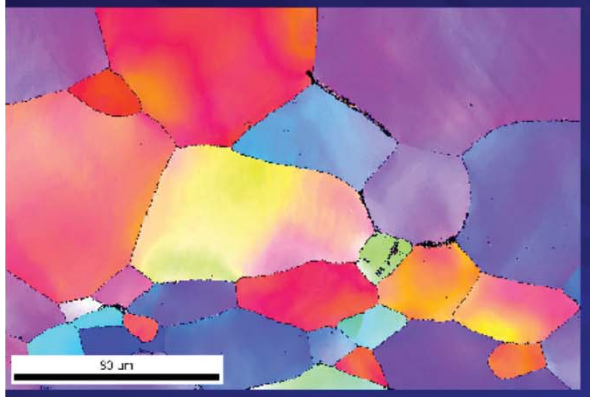

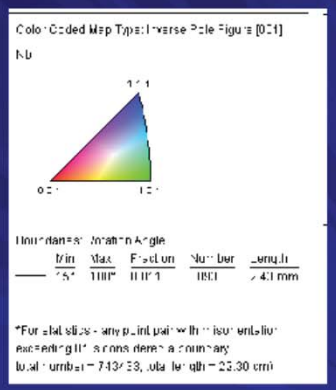

750 x 500, 0.3 μm spatial resolution

EBSD GOS Map 500 μm deep

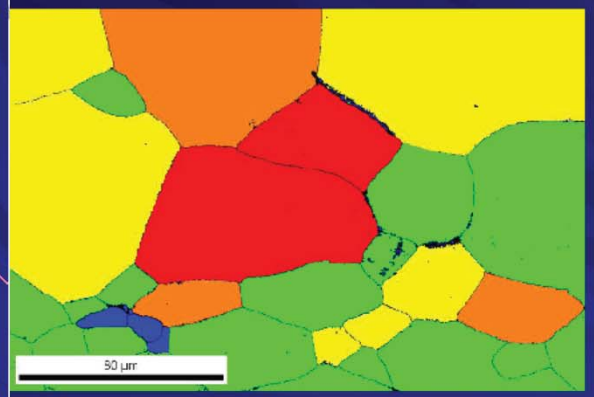

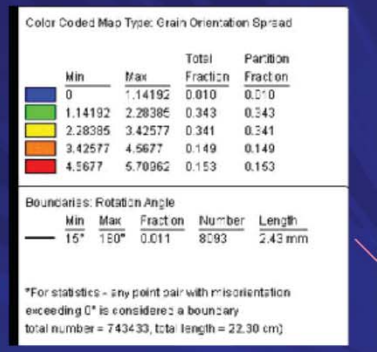

0.3 μm spatial resolution

EBSD KAM Map 500 μm deep

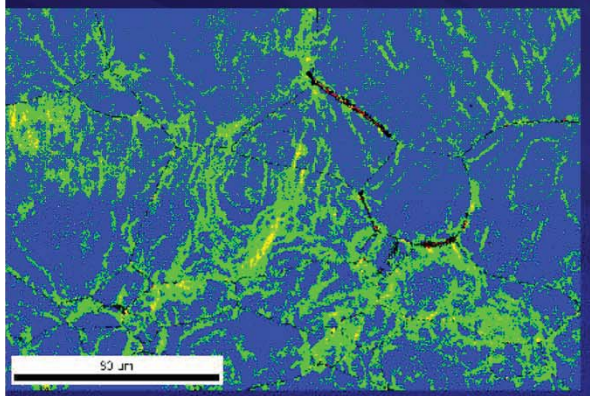

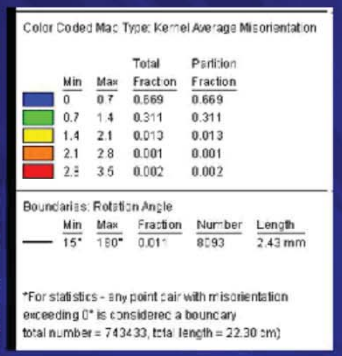

Stored Strain Energy

KAM 3rd neighbor x 0.3 μm spatial resolution

EBSD GROD Map 500 μm deep

Severely deformed, >15° in 50 μm

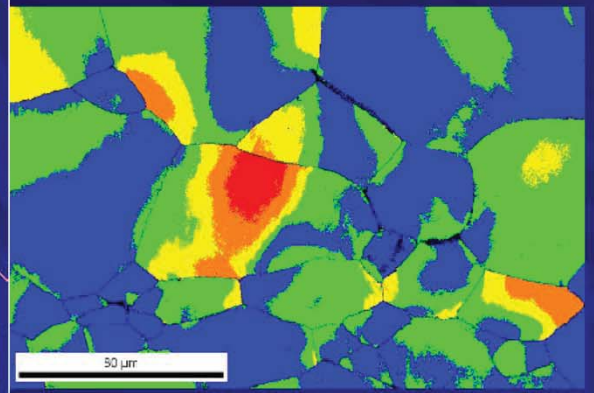

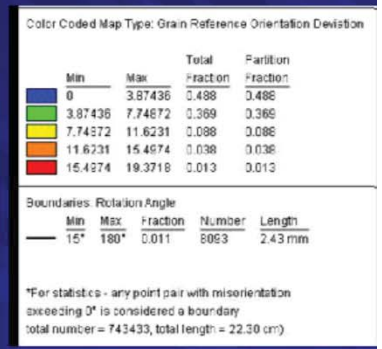

Deviation from grain minimum KAM

0.3 μm spatial resolution

Backscattered electron image

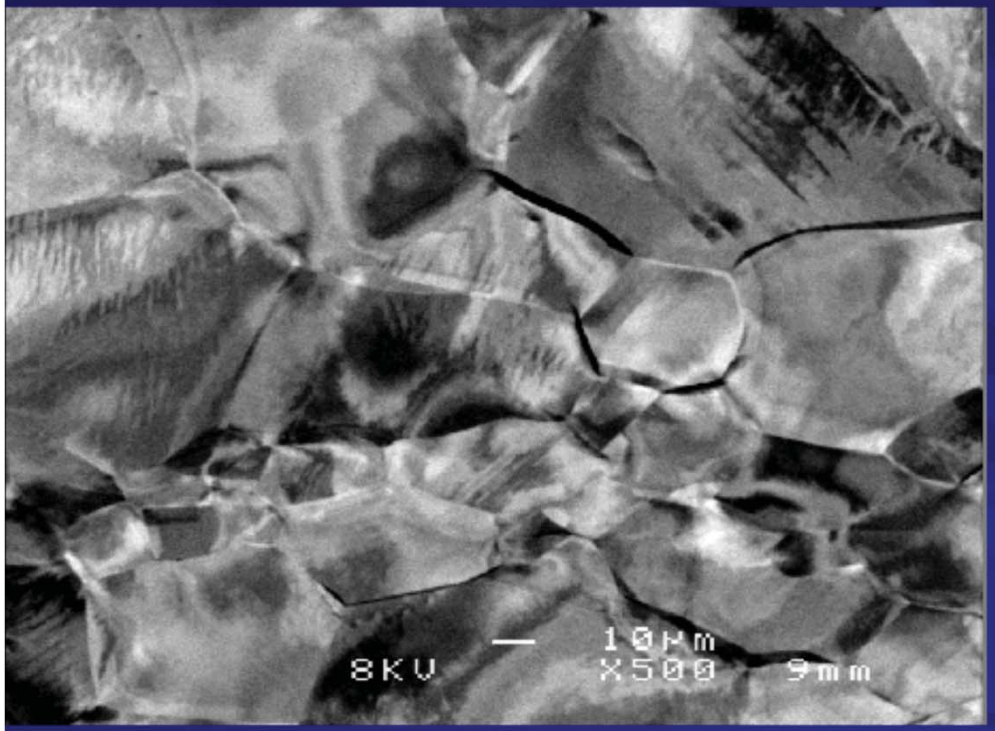

Channeling contrast of polished And etched surface resembles EBSD map

In as-deep-drawn condition, severe strain located in pockets through-thickness.

Greater strain at 300 and 500 µm than at surface.

Interstitials

- Stress fields of dislocations provide low energy sites for interstitial atoms—difficult to dislodge (Cottrell atmospheres)

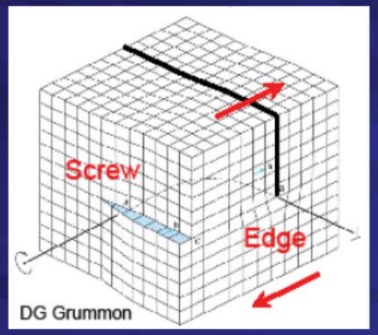

W. Singer, et all. Have suggested impurity atom contribution to pitting

Atomic Radii Size Comparison

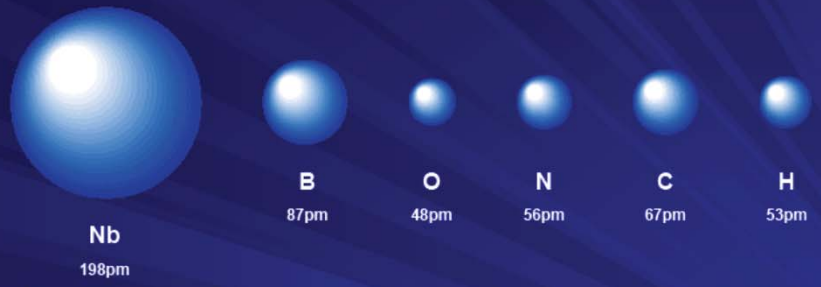

Atomic radii for each of the elements is specified in picometers. (Source: www.webelements.com).

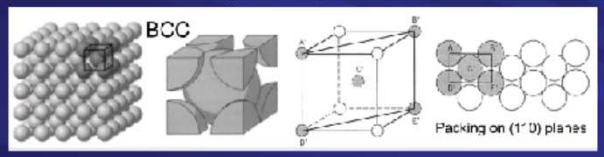

Callister, Materials Science and Engineering, An Introduction

Interstitials, e.g. O, lower superconductivity

Recrystallization Processing to eliminate stored strain energy

- Rolled to sheet thickness
- Recrystallized
- Roller-leveled
- Deep drawn
- Welded
- Chemically treated (BCP or EP), HPWR
- Heat treated

New

- Rolled to sheet thickness
- Recovery anneal
- Deep drawn
- *Recrystallized*
- Welded
- Chemically treated (BCP or EP), HPWR
- Heat treated

CASE STUDY: HOT SPOTS &ETCHING PITS (X. ZHAO, JLAB/A. ROMANENKO, CORNELL)

Abnormal Q-slope of a Large Grain SRF Cavity Motivated Surface Analysis of "Hotspots"

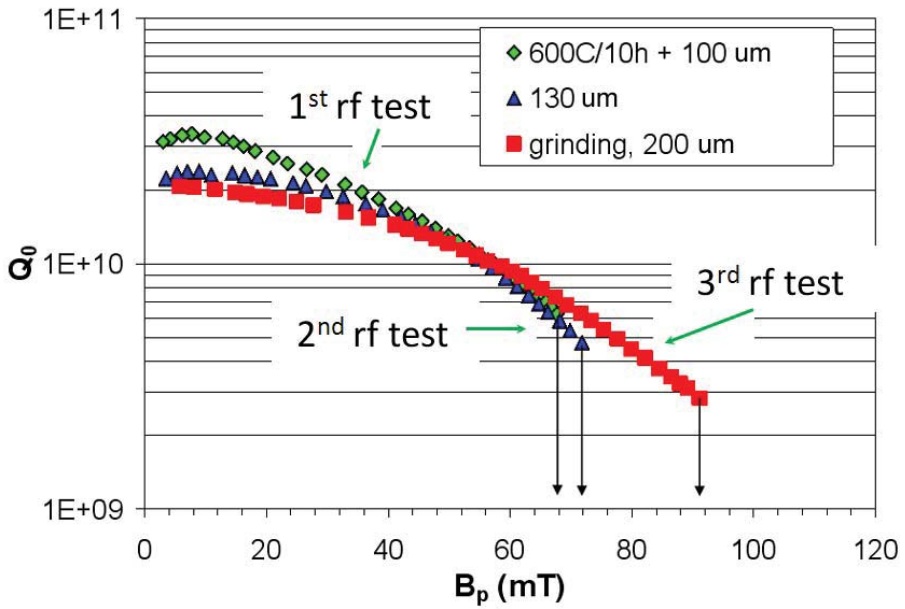

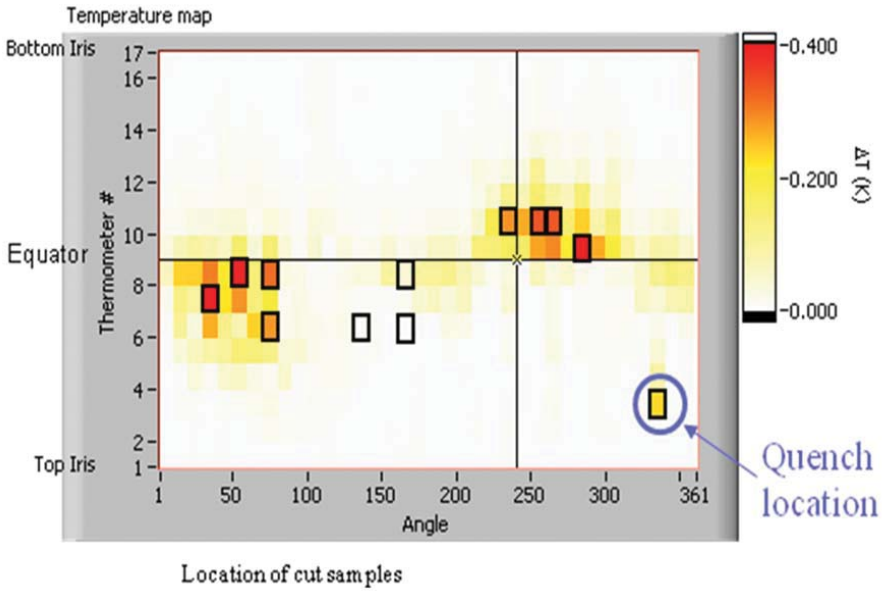

Q_o vs. B_p at 1.7 K after successive material removal showing a strong medium field Q-slope. The total material removal is indicated in the legend. (G. Ciovati, P. Kneisel)

Twelve samples (nine from "hotspots" and three from "cold spots") were cut from the cavity by milling for surface analysis.

New Approaches Applied to "Hotspots" Study

EBSD, SEM and Optical microscope

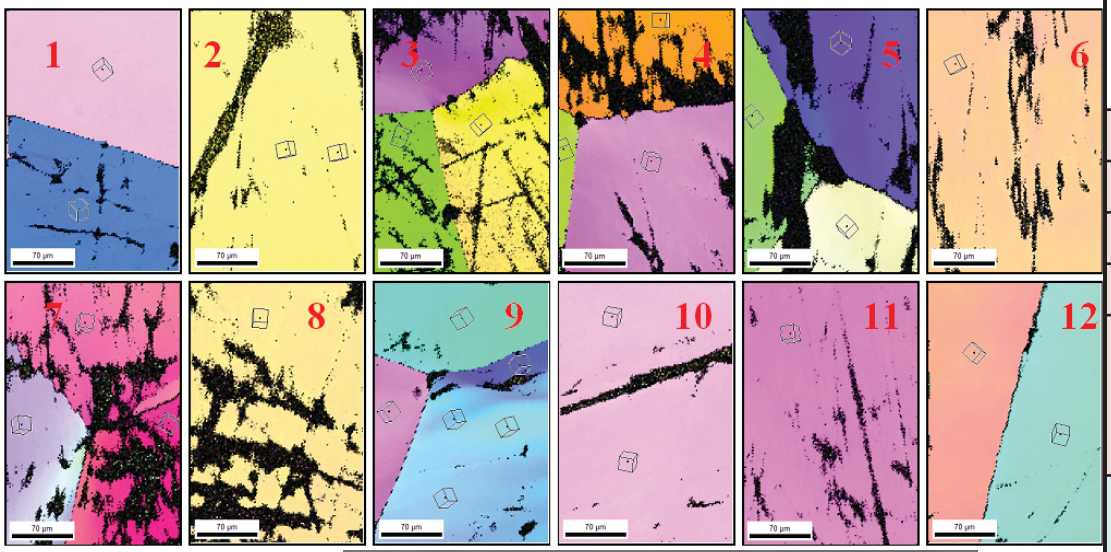

Nb IPF legend

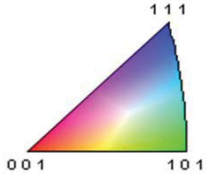

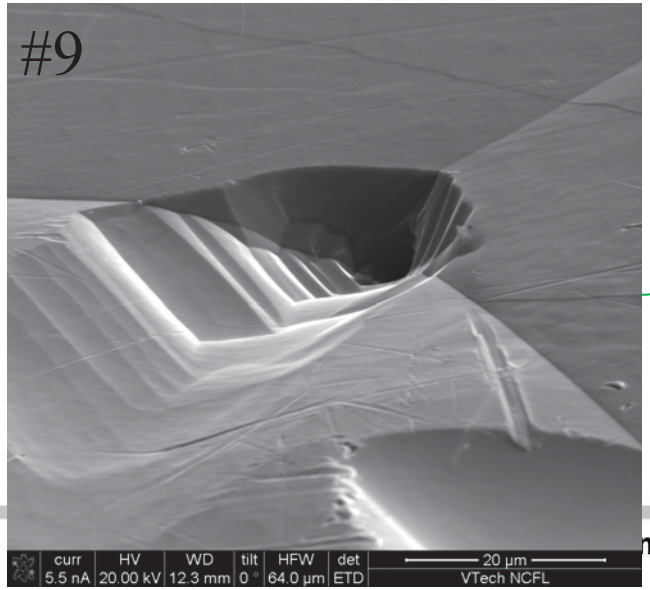

Sample No.	Grain Count	RF Character	Pit Density (No./mm²)	Etch-pit Features
1	2	Hotspot	34.2	
2	1	Hotspot	29.1	Quench site
3	3	Hotspot		
4	3	Hotspot		
5	3	Hotspot	61.7	A very deep pit on tri-crystal junction; on {110} plane, hi den of elongated etching pits
6	1	Cold spot	6.3	
7	3	Cold spot	19.7	A shallow pit on tri-crystal junction
8	1	Cold spot	17.6	
9	3	Hotspot		A very deep pit on tri-crystal junction
10	1	Hotspot		
11	1	Hotspot		
12	2	Hotspot		

Features of Etch Pits on the LG SRF Cavity

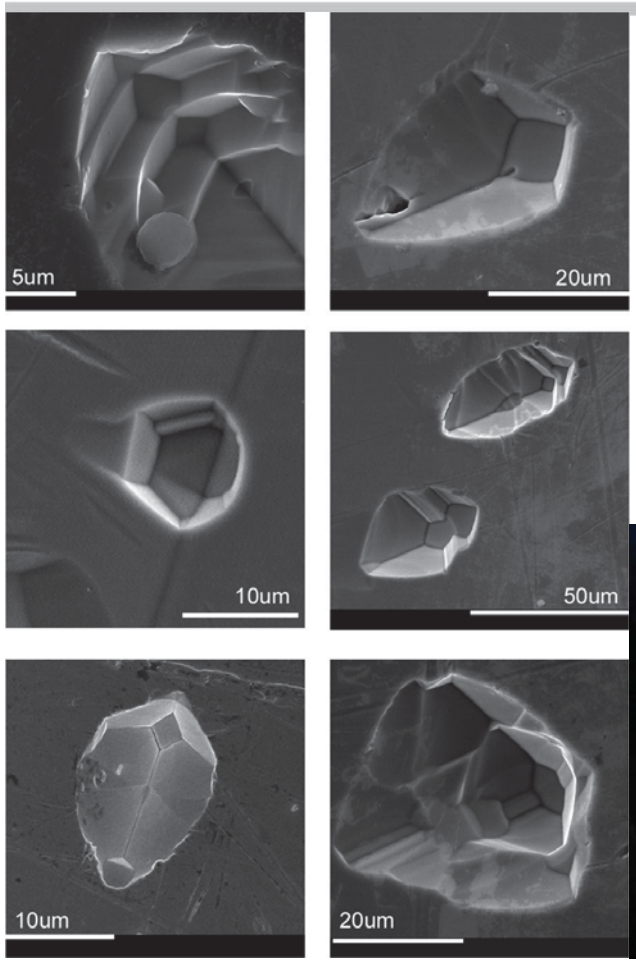

SEM figures of atypical pits which have elaborated symmetrical geometry. Their geometry deviates from the classic tetrahedral etching pits described in Cai's study

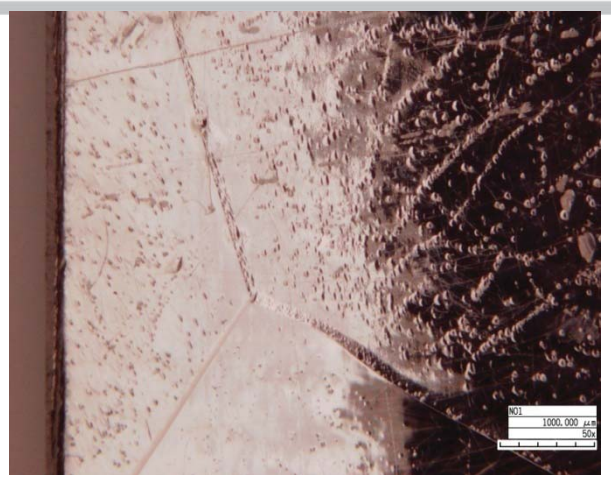

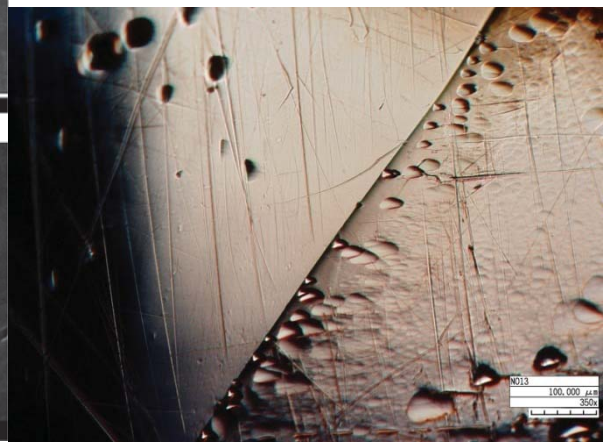

Optical microscopy images of sample # 9, showing high density of etching pits (left) and non-uniform pit distribution (right) on different crystal grains.

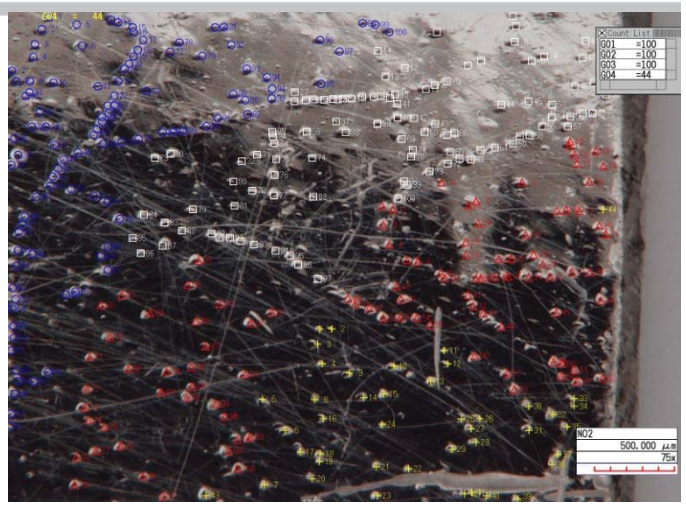

Etch pits networking on #1. Pits are in on grain (see EBSD)

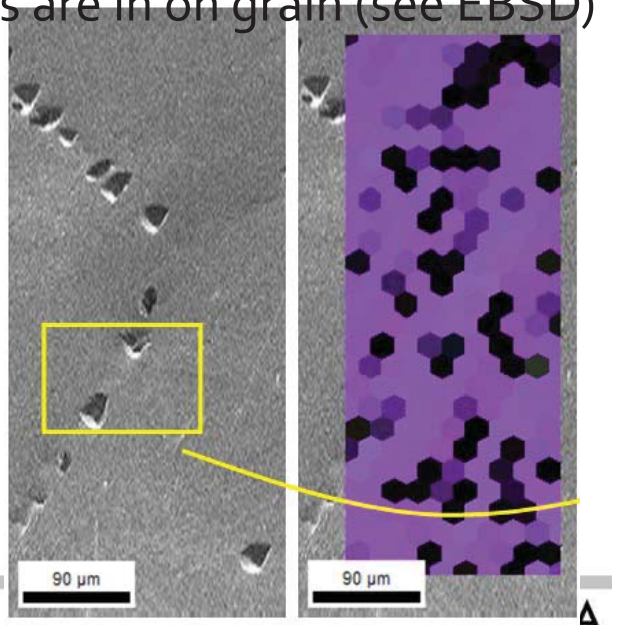

Edge or Corner Observed by SEM (CBMM-2 #2)

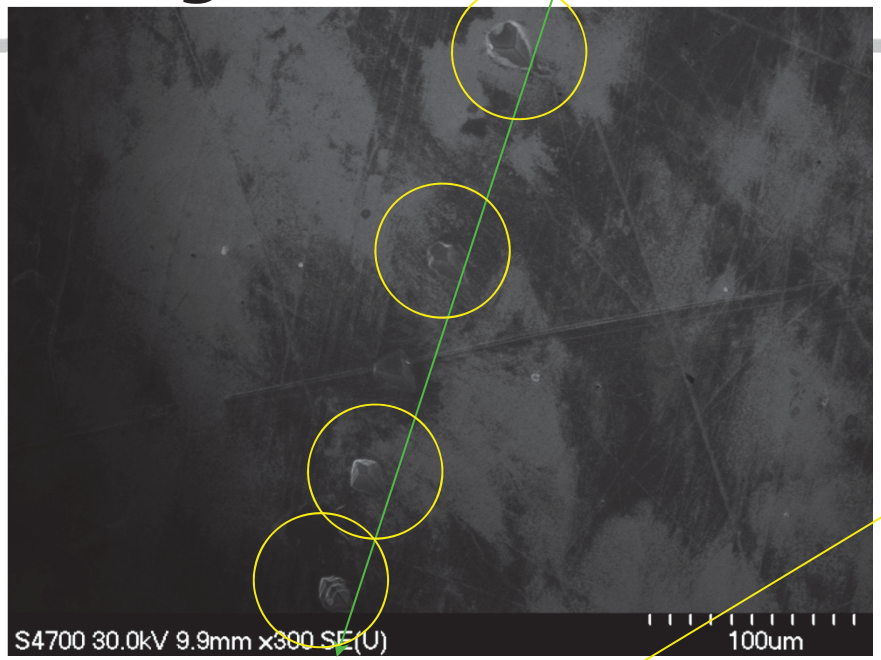

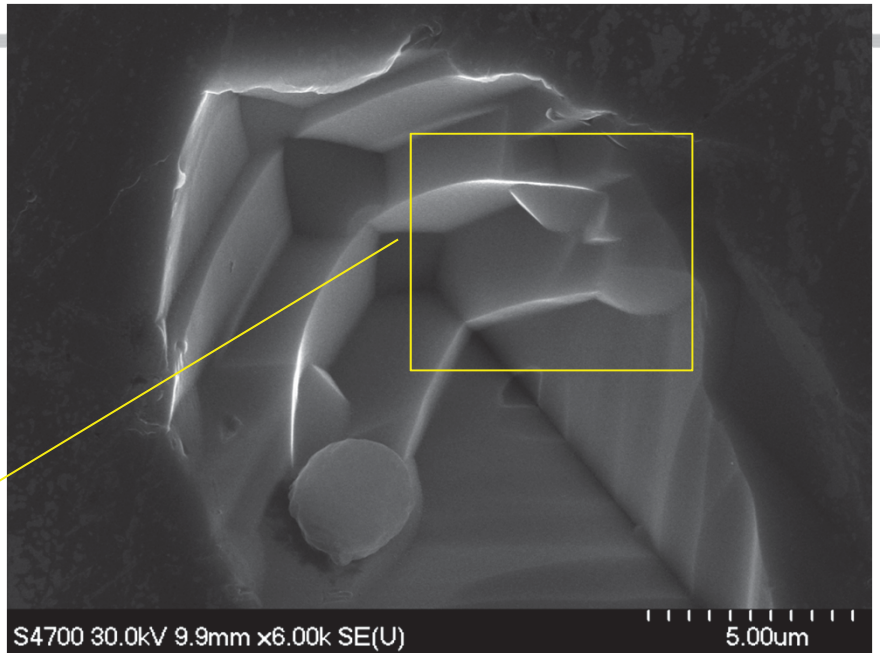

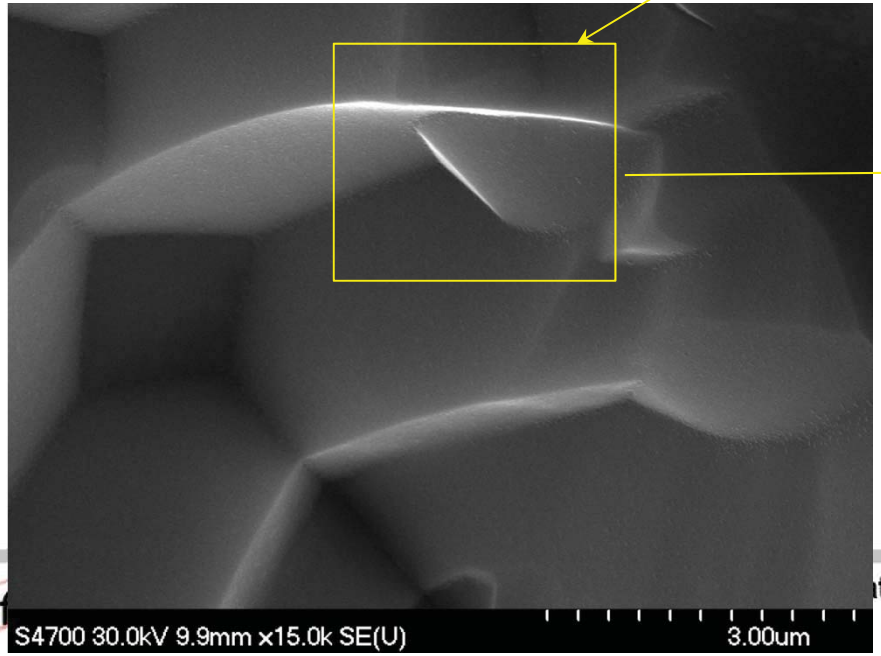

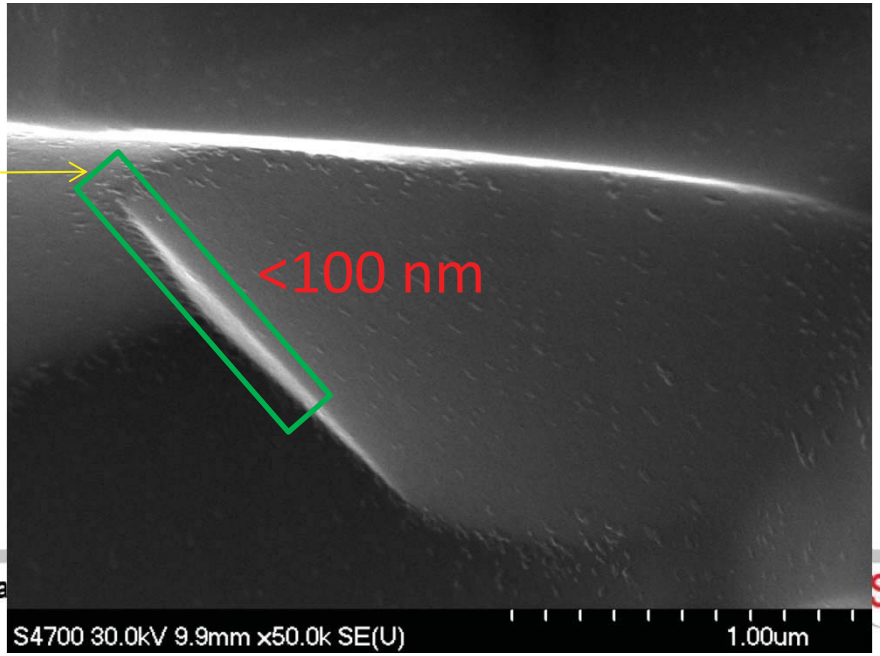

Etch Pits Formation Mechanism

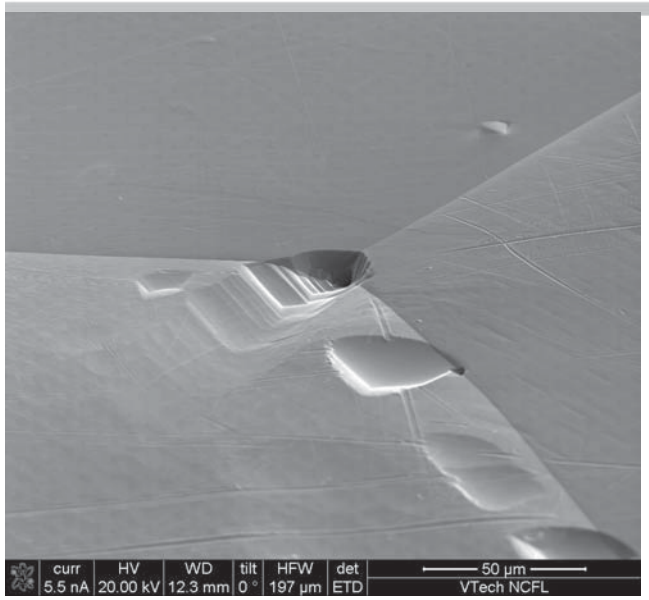

Buffered-Chemical-Polishing (BCP) is

Etching

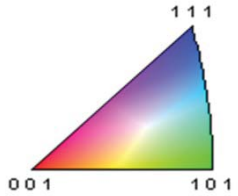

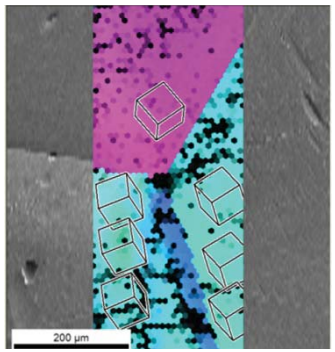

Different Etch Rates Involved in the formation of an etch pits at **ONE** dislocation site.

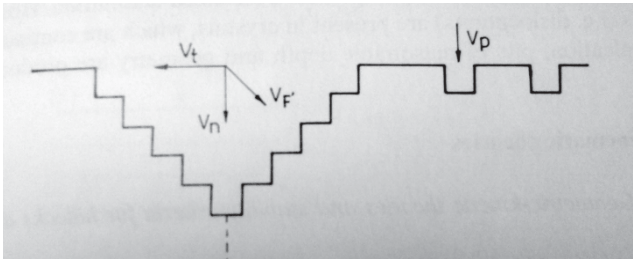

The tri-crystal etching pit on sample No. 5. The pit has deep, sharp profiles. The pit diameter is ~5 µm and its edge curvature radius ~50 nm.

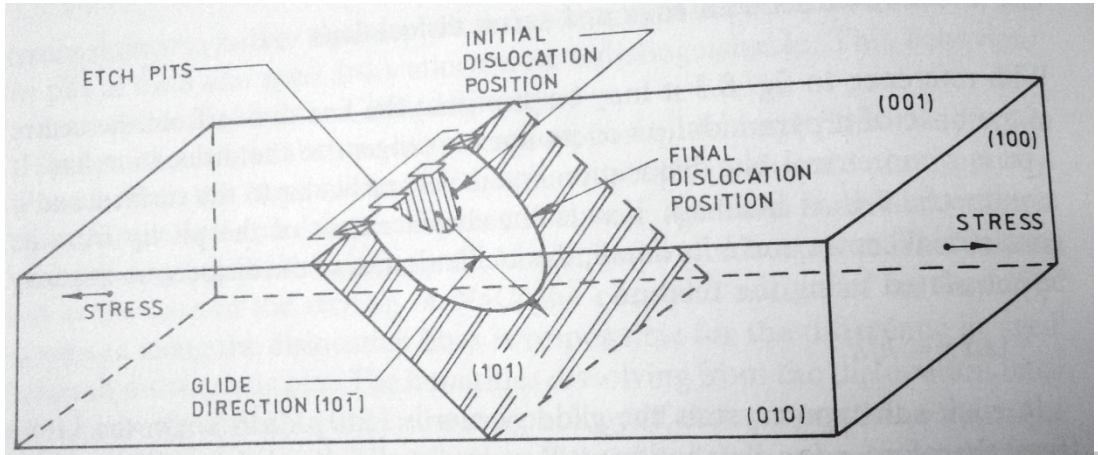

Fig. 8.4. Sketch of glide-plane orientation and movement of a dislocation half loop on the (100) face of a rock-salt-type crystal under an applied tensile stress (Gilman and Johnston 1957a).

Lattice Defects, Vacancies, Impurities and dislocations server as sites of initial dissolution

If Dislocation-Etch Pit is **One-to-One**, Etch Pits Distances are larger than 10 um. Then the dislocations will NOT impact SRF performance. **Too far**!

Dislocation Etching Pits

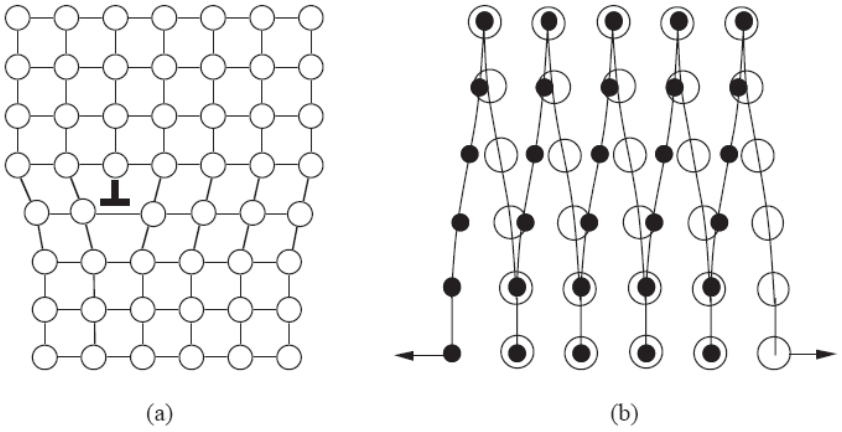

The atomic structure of the (a) edge dislocation and the (b) screw dislocation.
In (b) the smaller filled circles are in the same plane (above the paper) and the larger
open circles are in a different plane (below the paper).

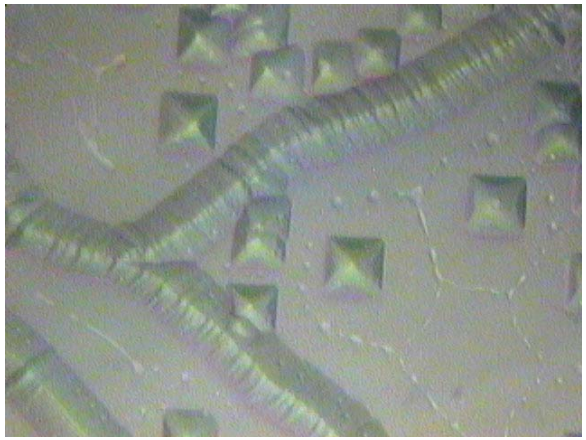

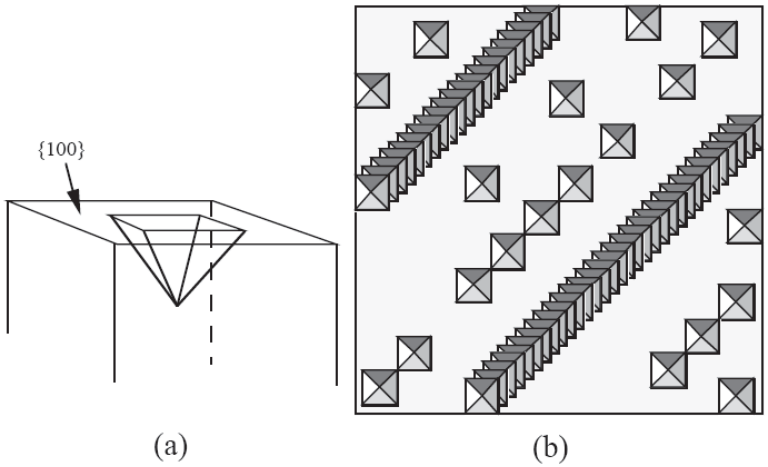

NaCl Dislocation etch pits. (a) a three dimensional view of a pit with square pyramidal facets. (b) Projection showing schematic distribution on the surface.

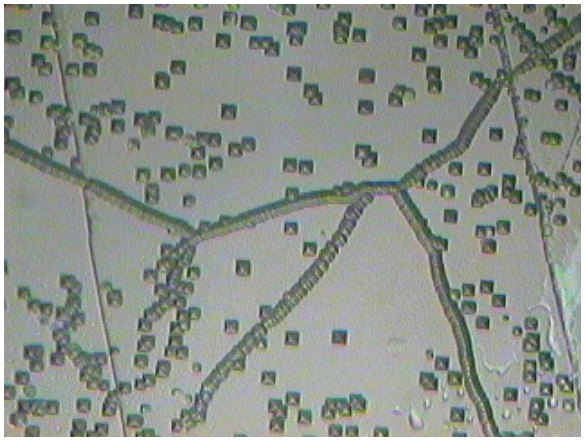

The top micrographs illustrate typical dislocation etch pits on cleaved rock salt (NaCl) surfaces

Orientation Dependence of Etch Pits Shapes

Fig. 6. Schematic representation of a three-dimensional etch pit. The tetrahedral pit is composed of three {110} planes with a {111} plane as the etching surface.

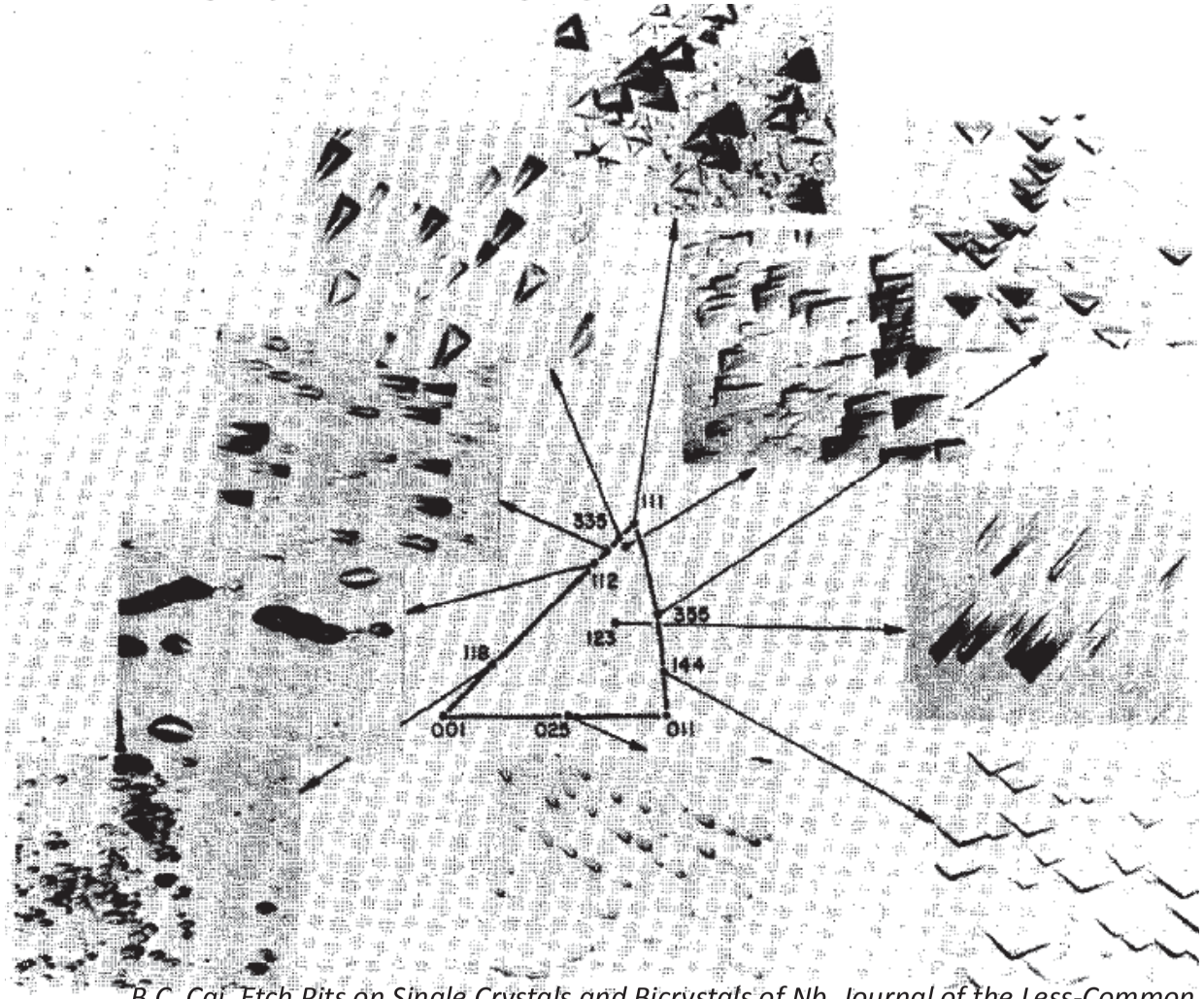

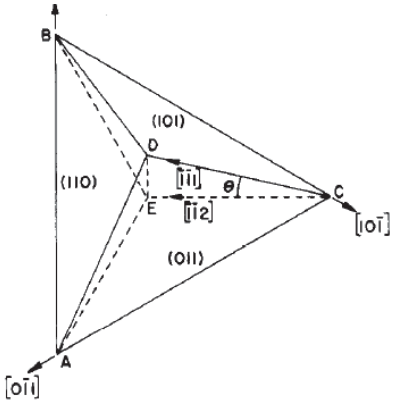

Schematic representation of 3-D etch pit. The tetrahedral pit is composed of 3 {110} planes with a {111} as etching surface

B.C. Cai, Etch Pits on Single Crystals and Bicrystals of Nb, Journal of the Less-Common Metals, 90 (1983) 37-47

Possible SRF Impact by Etch Pits

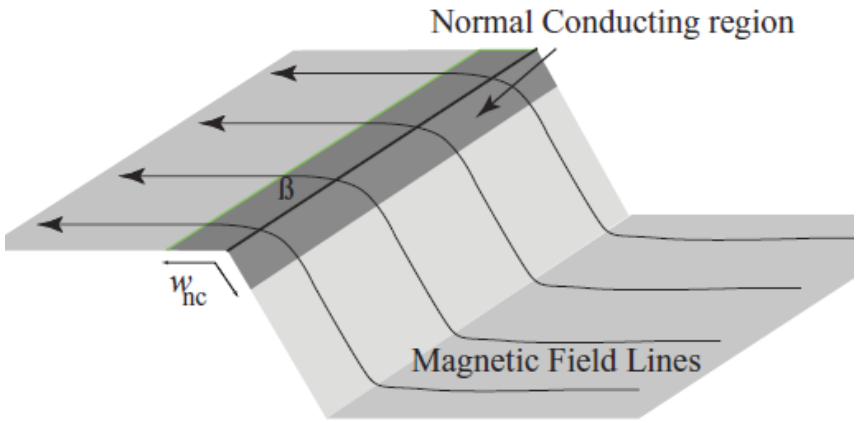

SEM showed pits with sharp edges but with aspect ratio of only about **100**. Therefore it seems that losses occurring at such low field **may not** be simply explained by local magnetic field enhancement.

Schematic of a grain boundary that has quenched due to magnetic field enhancement at the grain boundary.

-Shemelin and Padamsee

- J. Knobloch, R.L. Geng

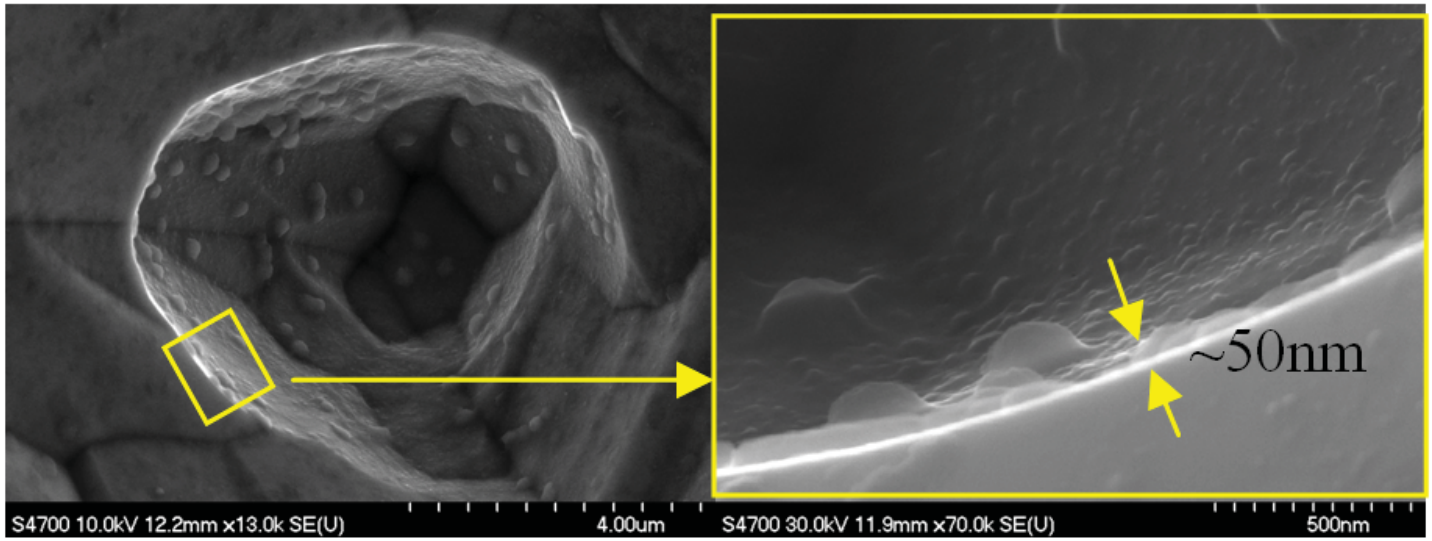

a) b)

BAKING EFFECT (A. ROMANENKO)

Typical fine grain EP cavity test result

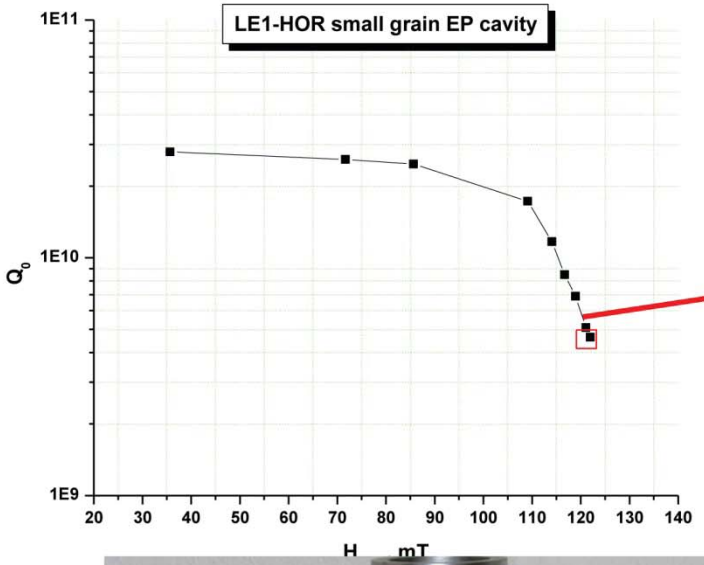

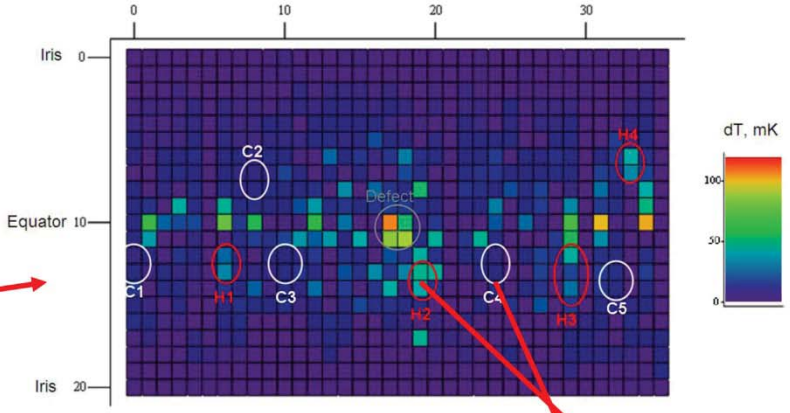

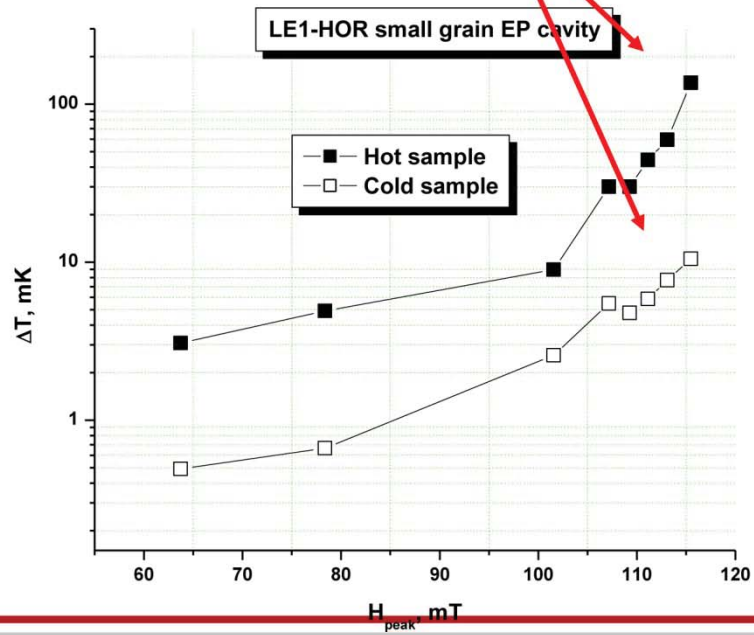

Microroughness

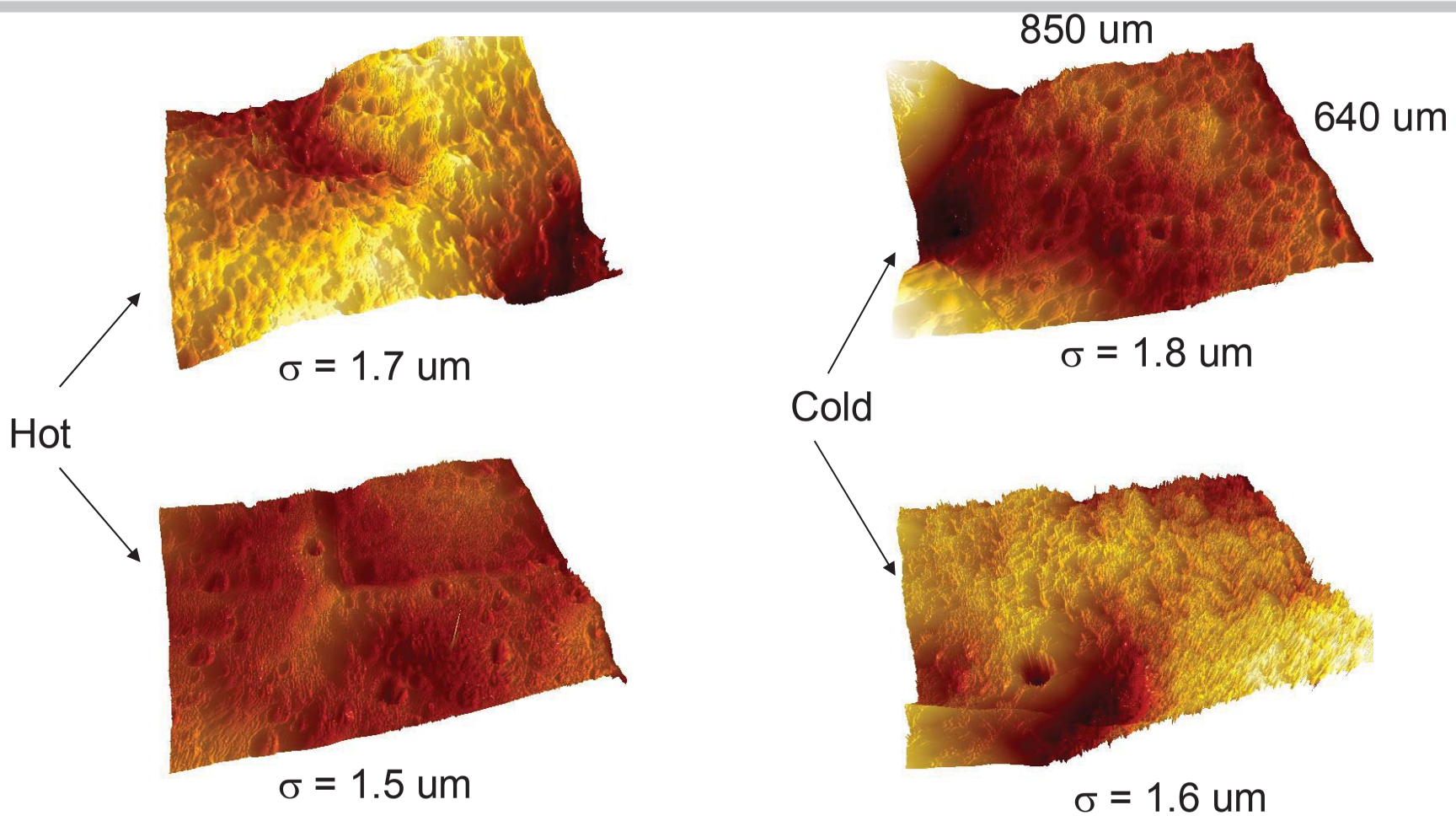

- Average roughness – σ = 1.5-1.8 μm is the same

Optical Profilometry

Hot

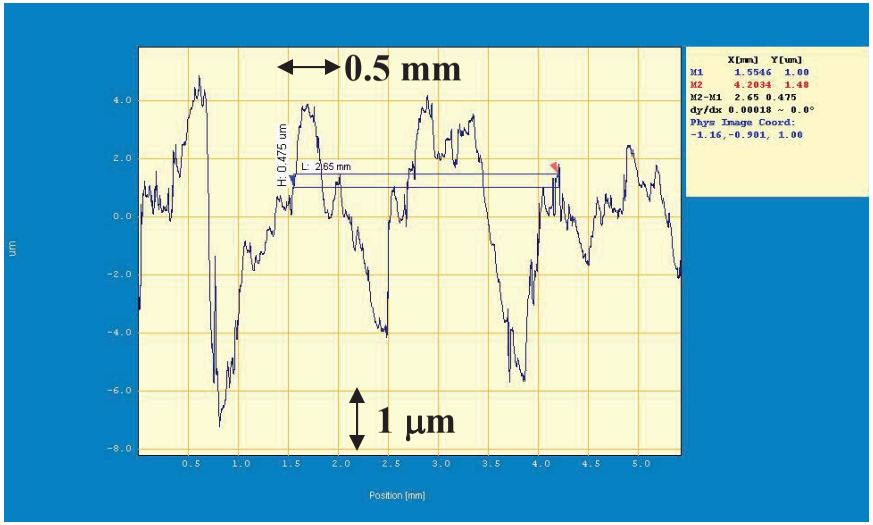

"Cold"

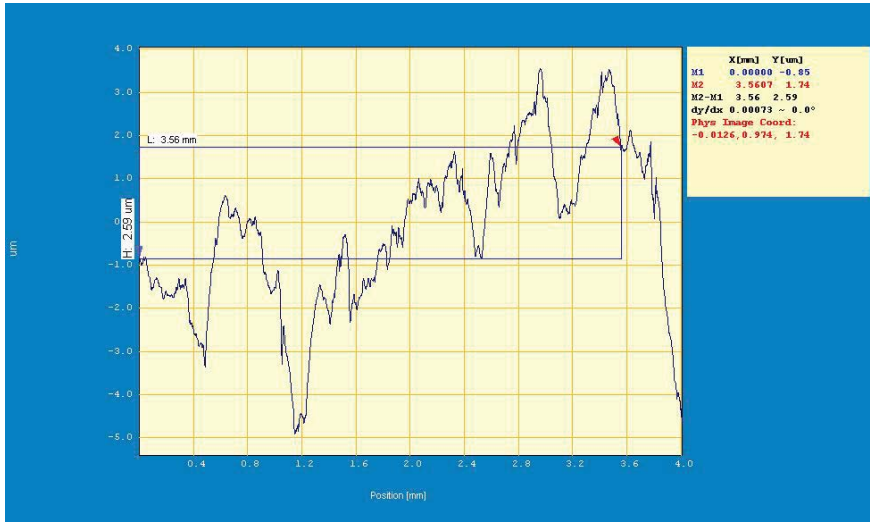

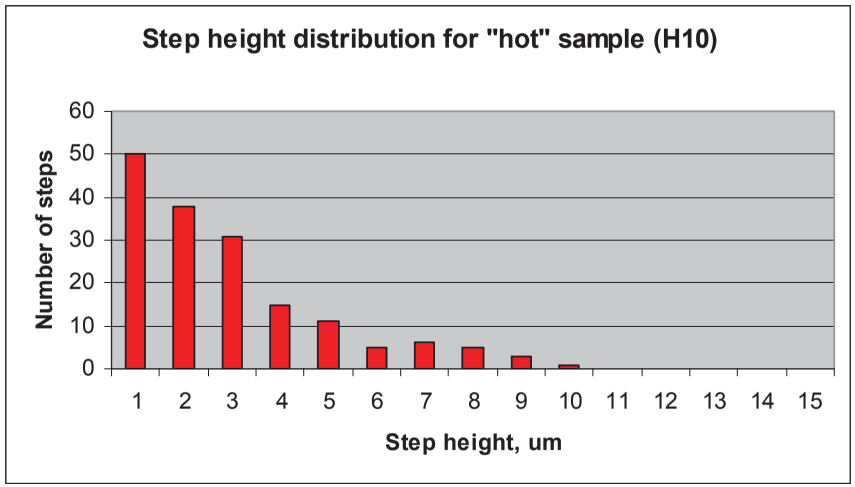

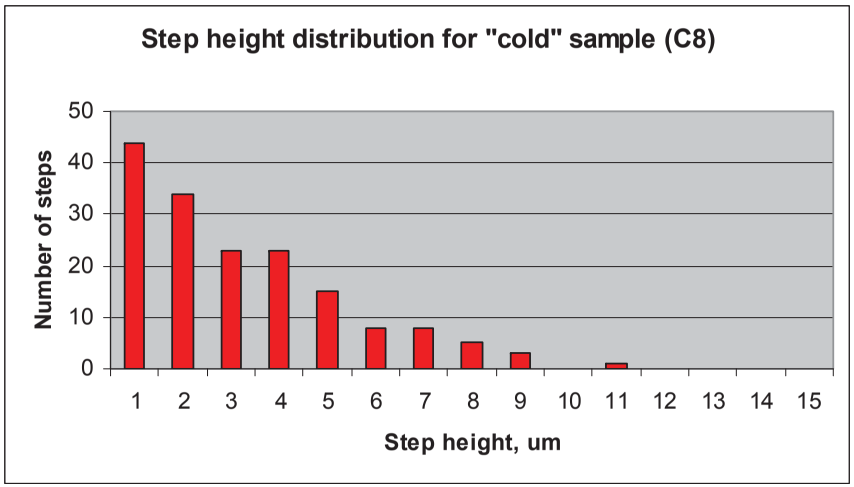

EBSD characterization

EBSD raw data:
crystalline orientation map

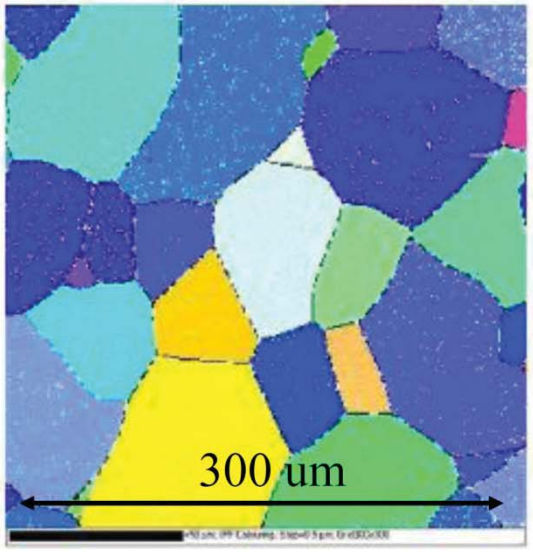

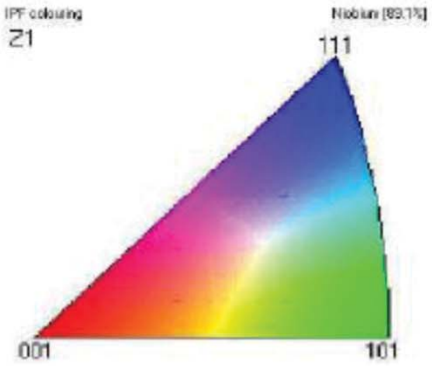

Local misorientation map

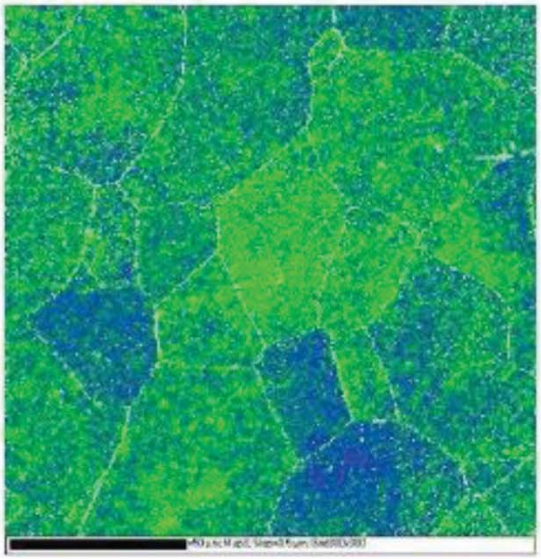

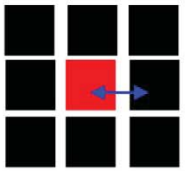

$\Delta\alpha_i$ – angle to rotate the unit cell to make orientations equal

Local misorientation = $1/8 * \Sigma(\Delta\alpha_i)$

Dislocation density & local misorientation – extreme case

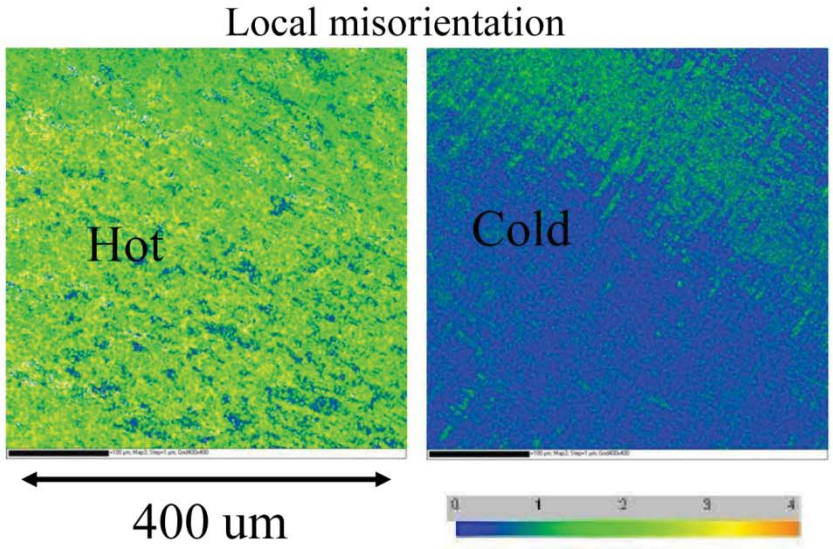

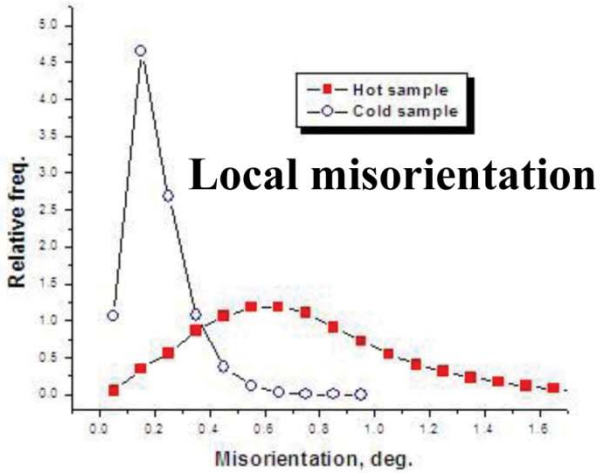

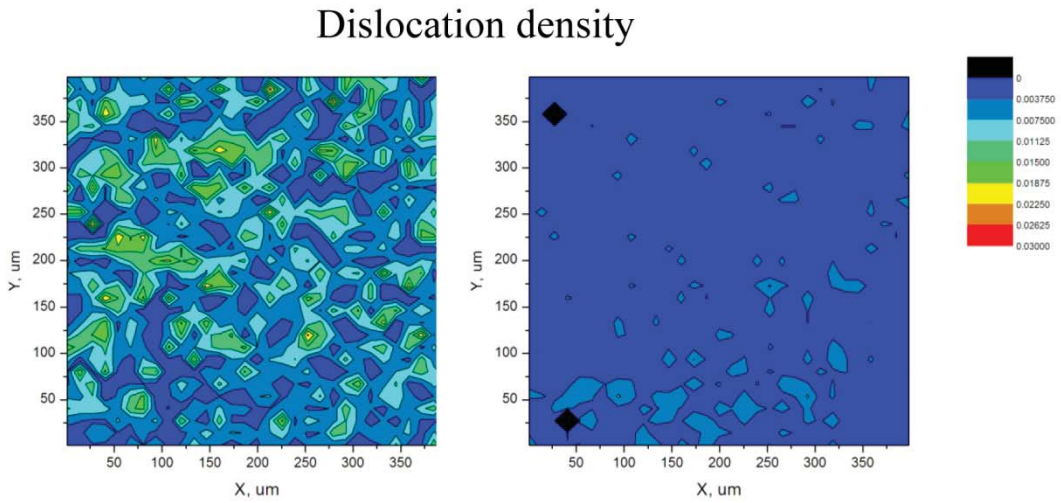

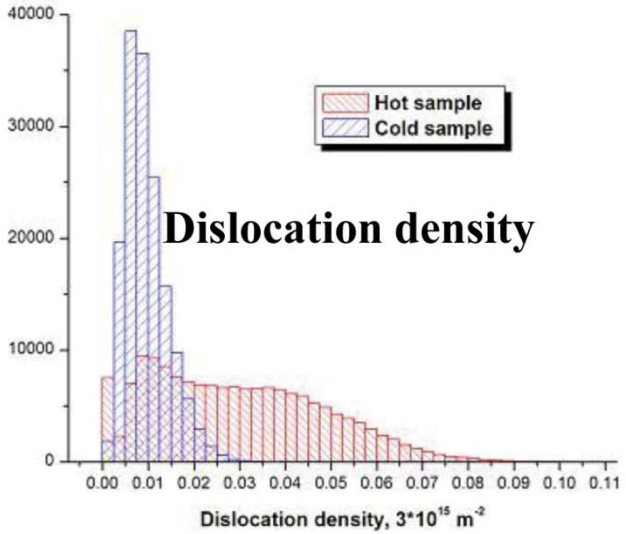

EBSD summary for hot/cold samples

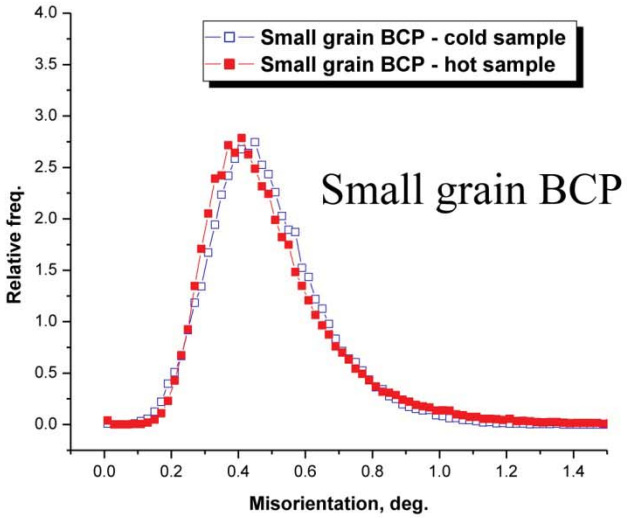

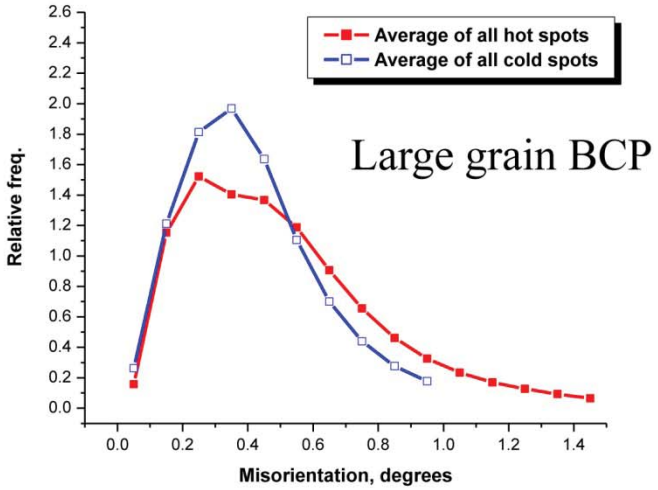

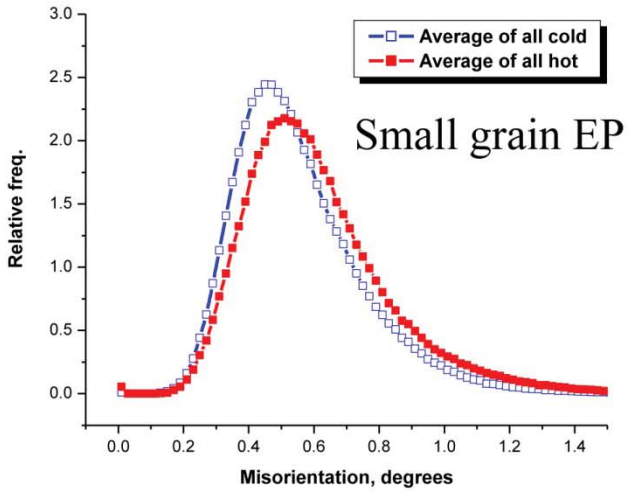

- Hot areas on average have misorientations shifted toward higher angles
- Difference hot/cold is largest in the case of large grain BCP, which is consistent with thermometry
- Motivated annealing of the samples at 100-120C and subsequent EBSD analysis

Baking of fine/large grain BCP Nb

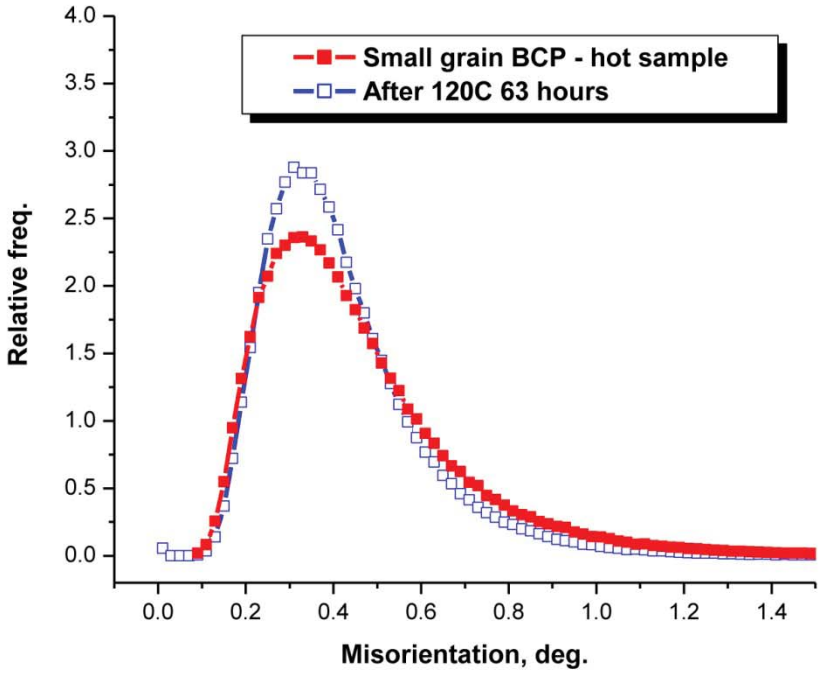

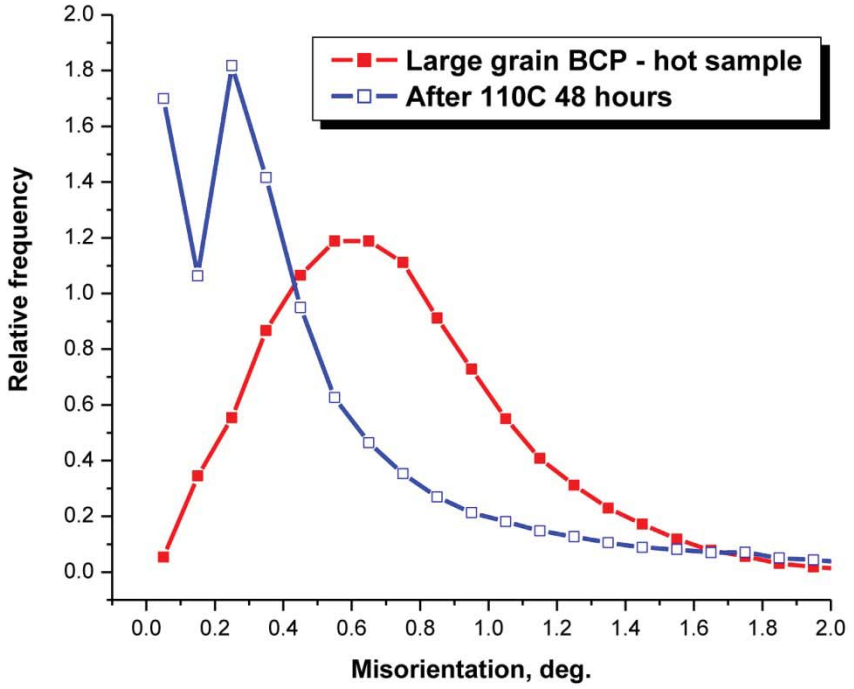

Baking of fine grain EP Nb

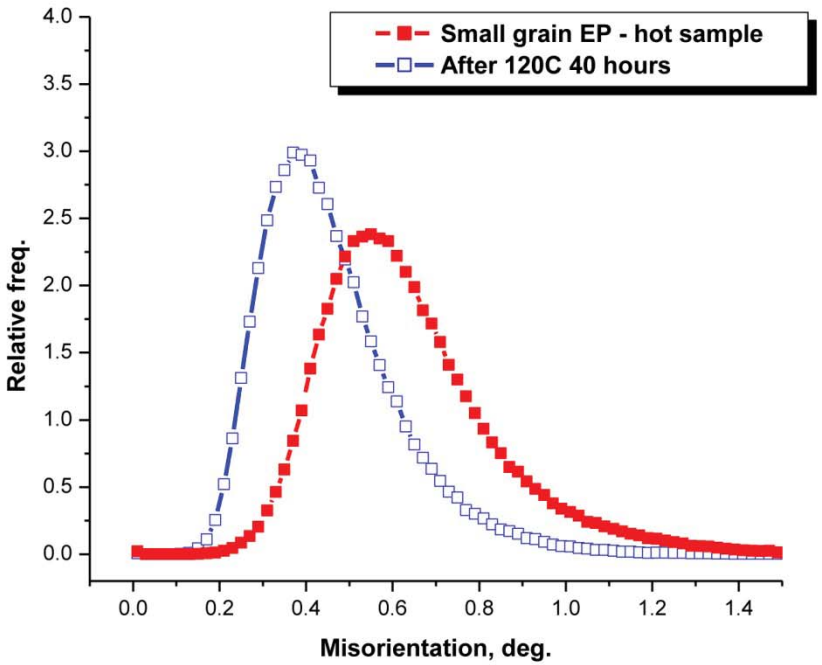

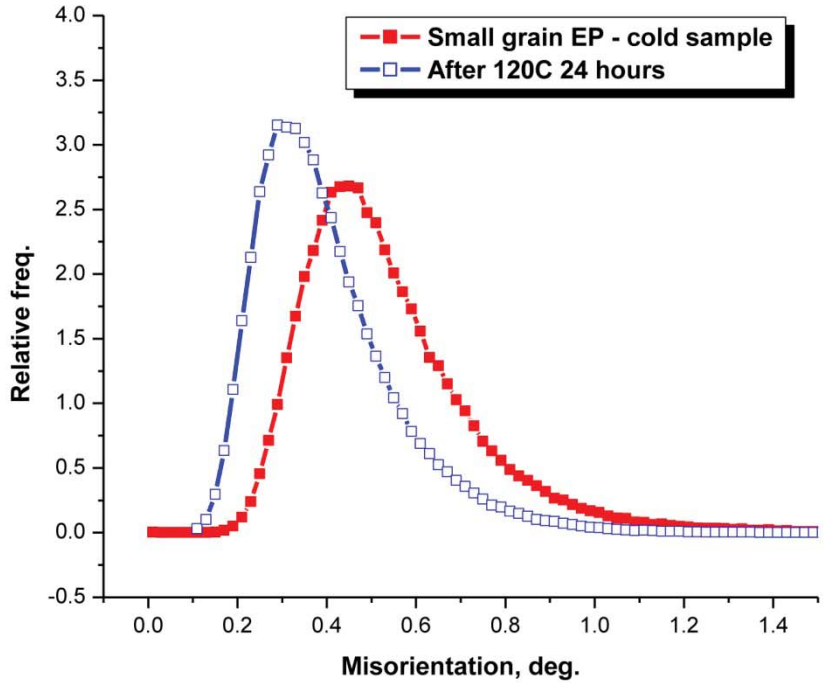

- Strong shift due to baking is observed in local misorientation distributions of both hot and cold samples
- Dislocation density maps were obtained to confirm and to get more info on distribution

Average screw dislocation density maps

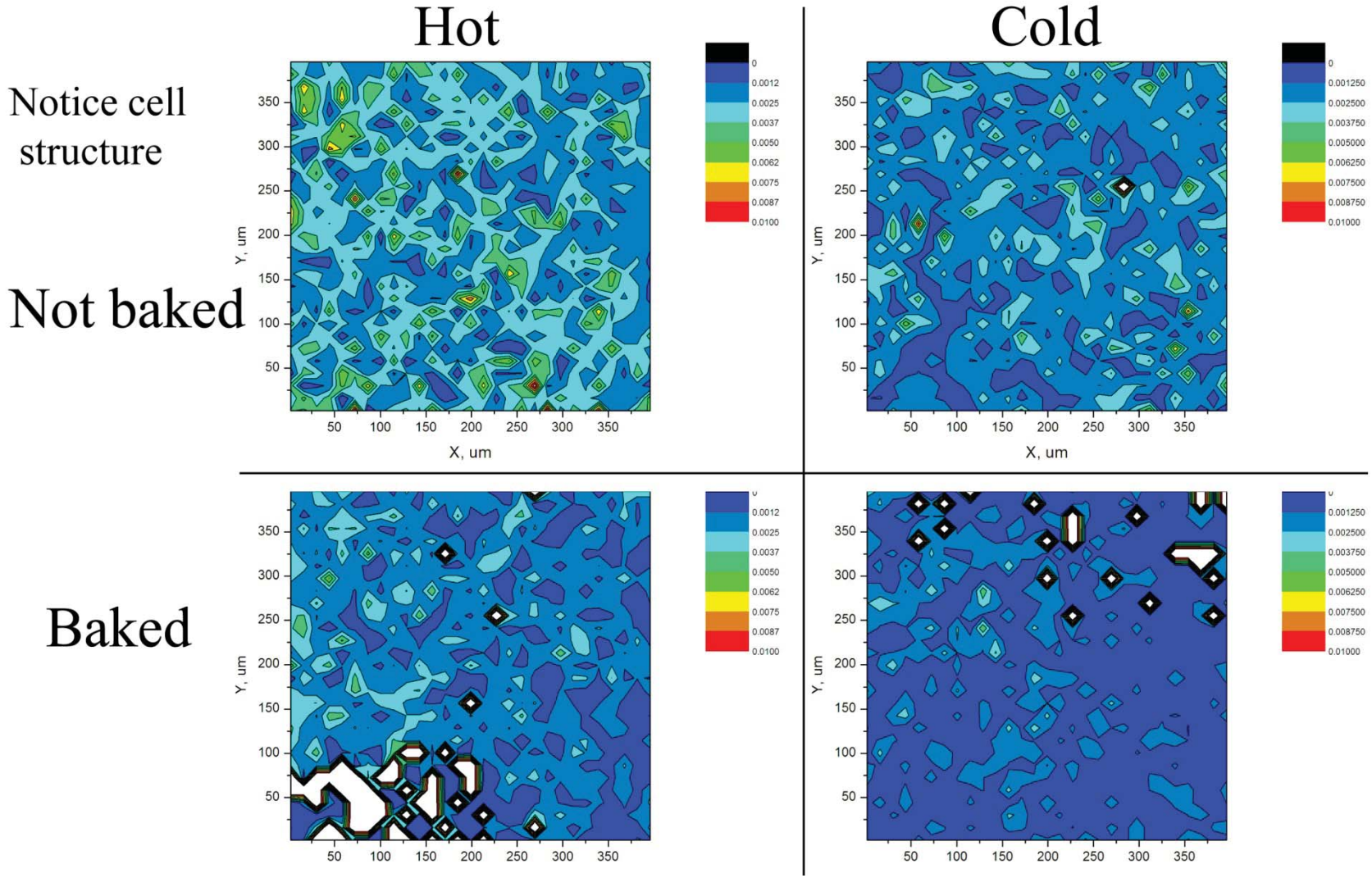

Average screw dislocation density maps

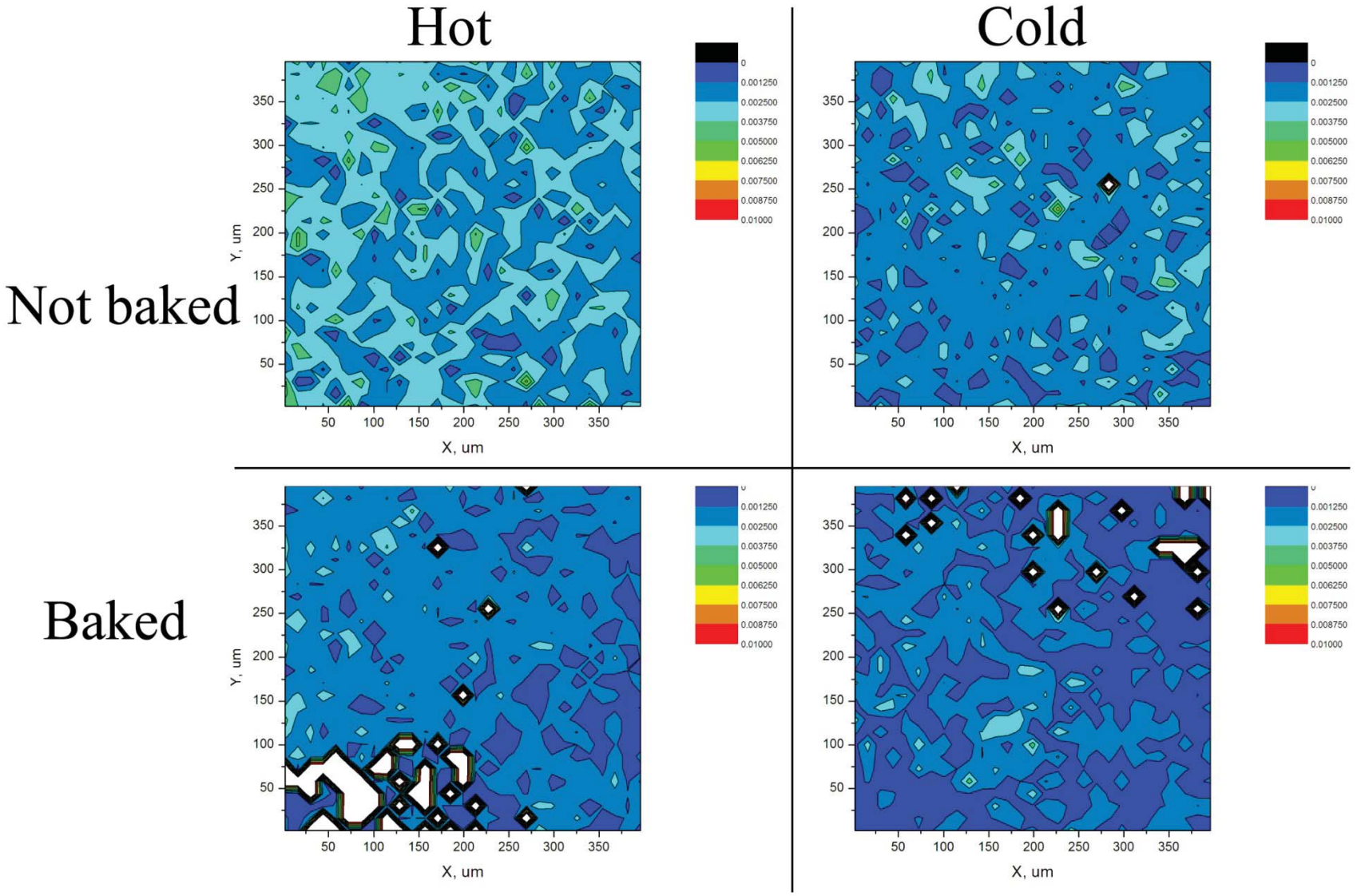

Baking summary - EBSD

- Significantly reduced dislocation density in small grain EP and large grain BCP samples after 120C baking
  - Consistent with the strong baking benefit on EP and large grain BCP cavities
- Almost no change in the small grain BCP sample due to baking
  - Consistent with the lack of baking effect on the small grain BCP cavities

Baking mechanism – dislocation climb

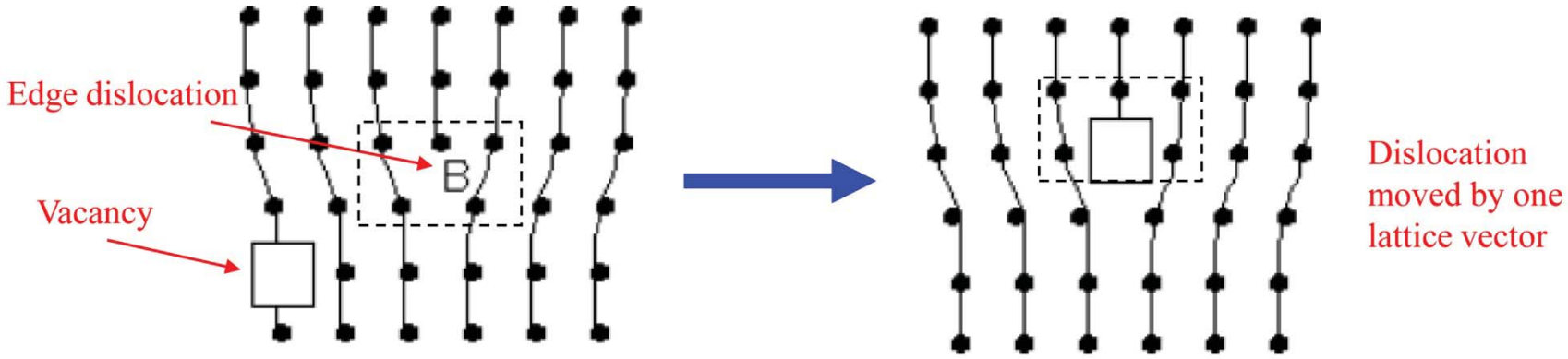

- Dislocation climb
  - Vacancies are necessary for the climb to occur
  - Vacancies in Nb become mobile around 100C due to Vacancy-H complexes dissociation – see next slide for positron annihilation studies [*Phys. Rev. B*, 32(7):4326–4331, 1985]
- Possibly - reduction in the dislocation density near the surface due to climb and annihilation of dislocations

Dissociation of vacancy-H complex

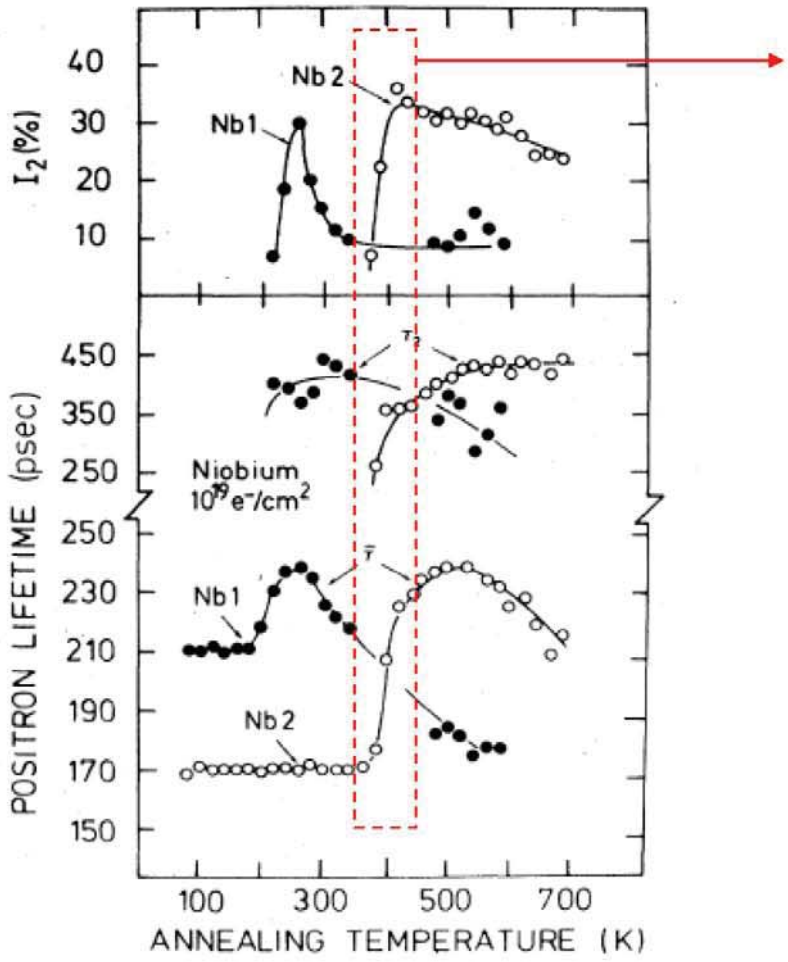

- Vac-H complexes in niobium containing some H (Nb2 in plots) dissociate at ~380K (107C) – compare to baking temperatures
- Mobile vacancies => dislocation climb becomes possible

[P. Hautojarvi et al., Phys. Rev. B., Vol.35, Num.7, 1985]

Dislocation & RF superconductivity

- Dislocation tangles, dislocation cell walls might serve as sites for magnetic flux penetration at lower fields due to
  - Lower surface barrier
  - Higher κ => lower H_{c1}
- After flux penetrates – losses due to oscillatory flux motion

Baking effect – TEM/EELS

A. Romanenko, J. Mundy, P. Ercius, J. Grazul – details eslewhere

- FIB prepared samples from "hot" spot before and after 120C baking
- EELS elemental analysis with atomic scale resolution
- **No oxygen-enriched layer**
- **No oxygen diffussion**
- **No oxide modification**
- **No cracks or suboxide clusters –**

very nice and uniform oxide

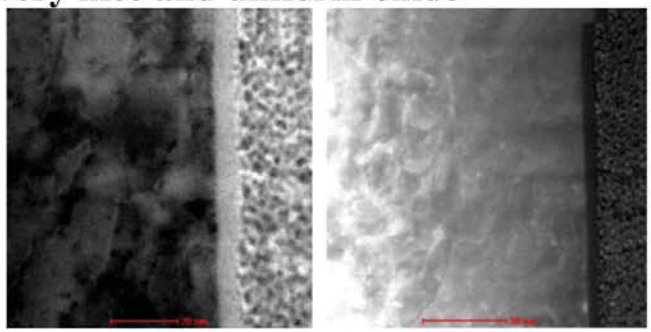

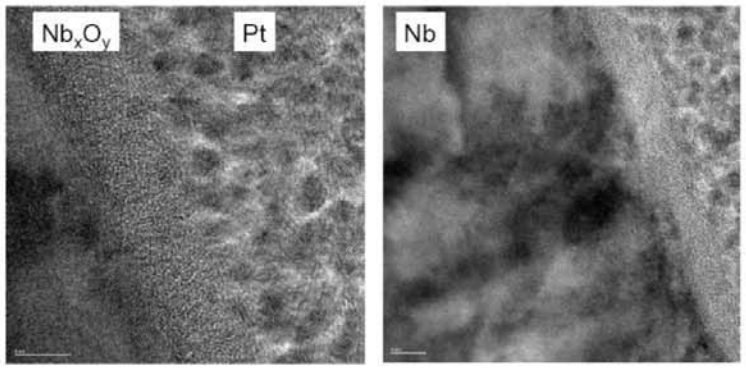

Not baked

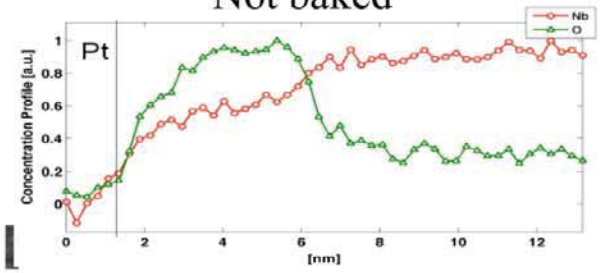

Baked

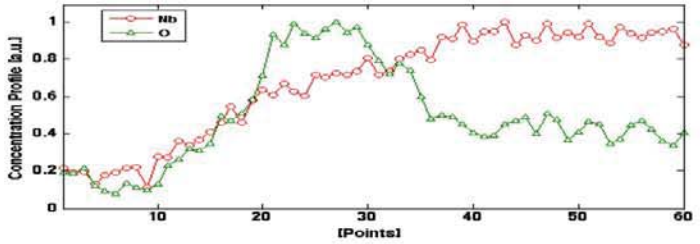

Conclusions

- Lattice defects (i.e. dislocations) may be the cause of the HFQS based on:
  - Difference between hot and cold samples
  - Change with 100-120C baking
- Dislocation climb as a possible mechanism
  - Vacations immobilized by H up to ~ 100C
- FIB/TEM + EELS disqualify oxygen diffusion-related and/or oxide modification baking mechanisms

CASE STUDY : HIGH RESOLUTION XPS OF NB OXIDE LAYER (H.TIAN, JLAB)

Introduction

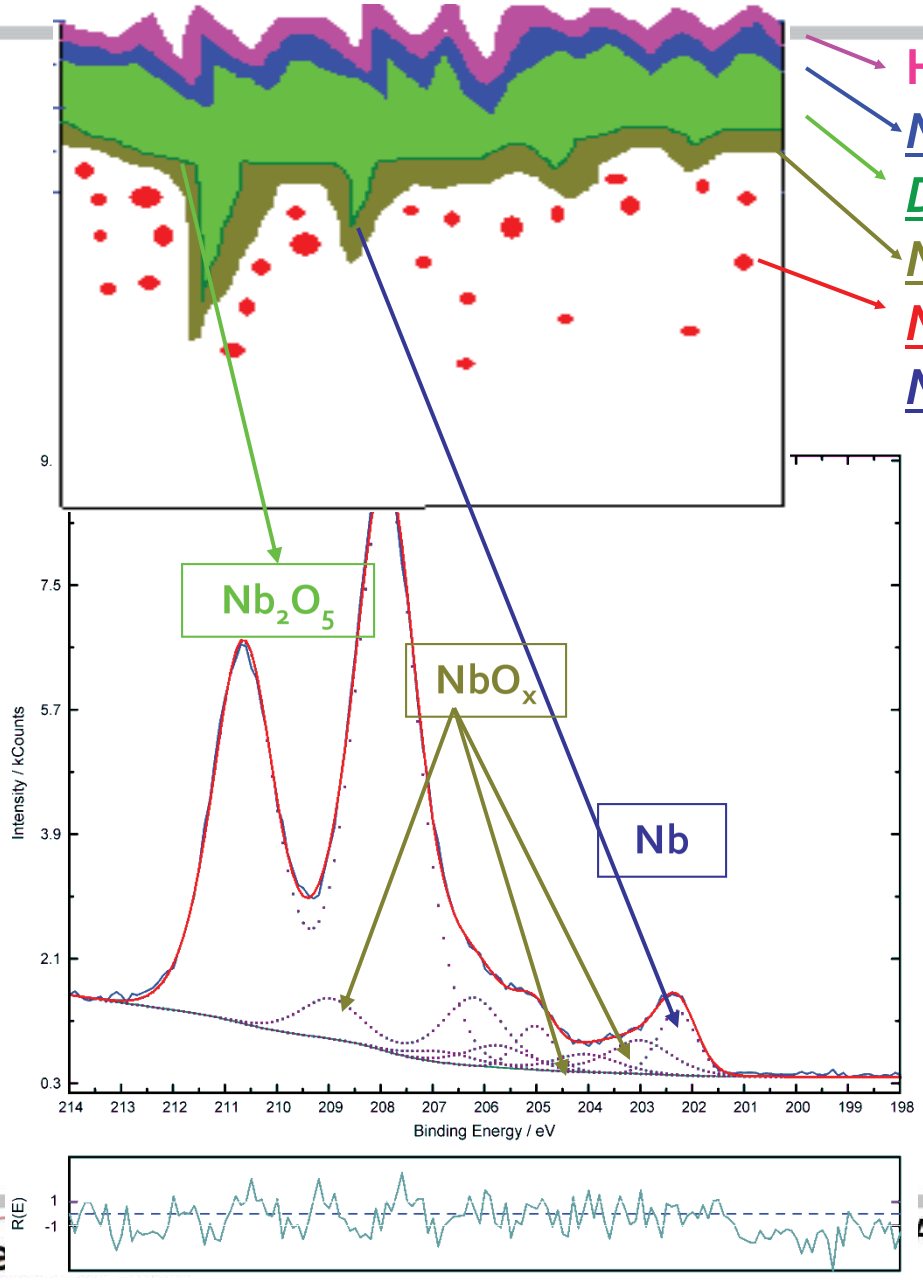

Hydrocarbons & impurities (<1nm)

Nb hydroxides (< 1 nm,?)

Dielectric Nb_2O_5 (3~8 nm)

$NbO_{x-(0.2 < x < 2)}$-metallic(1~2 nm,?)

NbO_x precipitates (0.02 < x < 0.2,?)

Nb (RF penetration depth : ~ 35 nm)

The surface chemistry of Nb is dominated by the high reactivity to oxygen; the outermost oxides layers are always found to be Nb_2O_5.

Suboxides in various combinations and morphologies are proposed to be between the Nb_2O_5 and the underlying metal.

Angle Resolved (AR) *vs.* Energy Resolved (ER)XPS

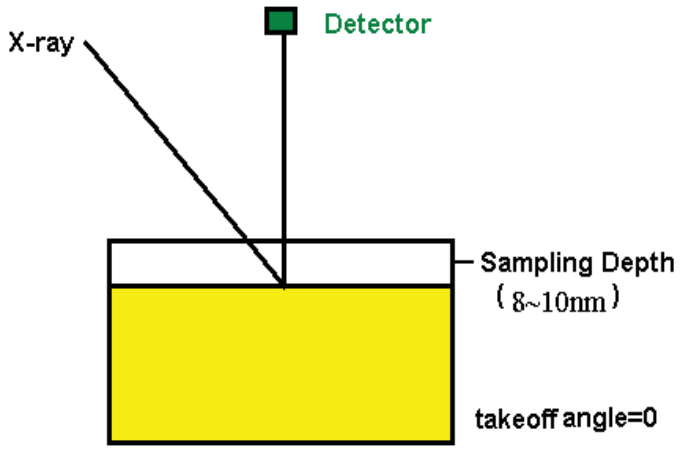

AR

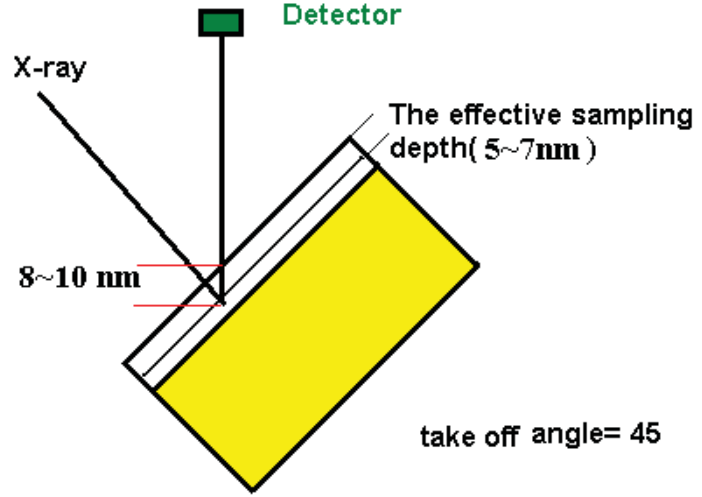

At the normal incident angle (Nb_2O_5: 3 ~ 8 nm+ metal)

$$\lambda = E / \{E_p^2[\beta_m \ln(\gamma E) - C/E + D/E^2]\}$$

E=hυ(eV)	Sampling Depth (nm) Nb_2O_5
300	2.8
550	4.2
750	5.3
1254(Mg)	8.1
1486(Al)	9

ER

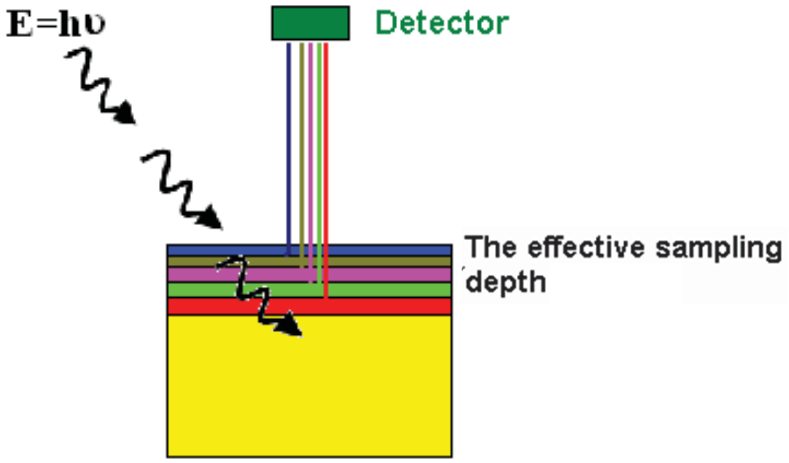

Surface topography has less impact on variable photon energy XPS.
AR + ER XPS provides the most surface sensitive information.

Energy Resolved XPS -BNL, NSLS, X1B

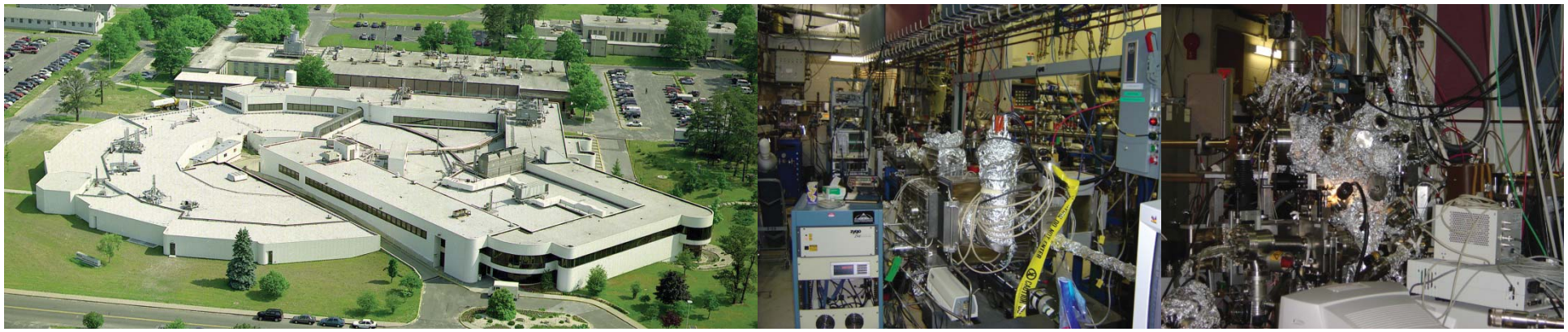

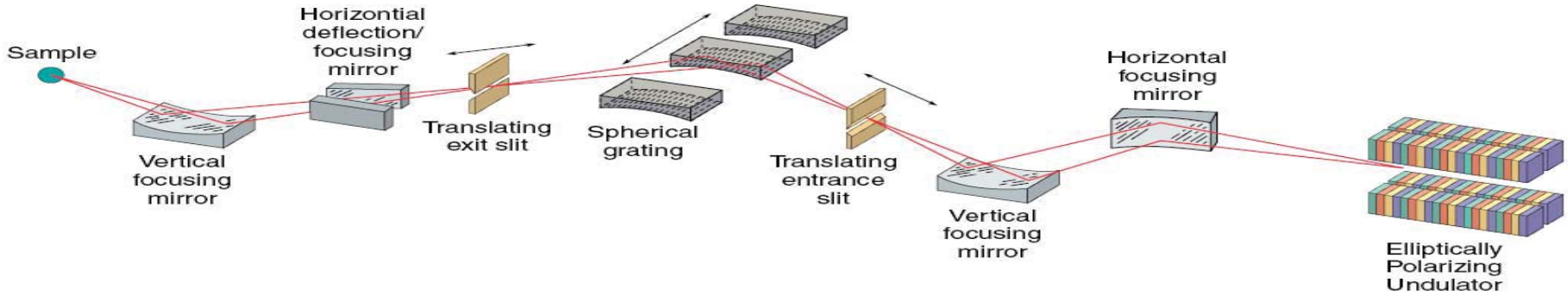

hυ = 300 eV, 550 eV , 750eV(100 ~ 1600 eV)- energy resolved XPS
Take off angle = 0°, 41°, 60°…-angle resolved XPS.
Spot size < 250 μm with enough intensity, total energy resolution can be less than 0.1eV.

Depth Profiling : Angle Resolved *vs.* Energy Resolved XPS

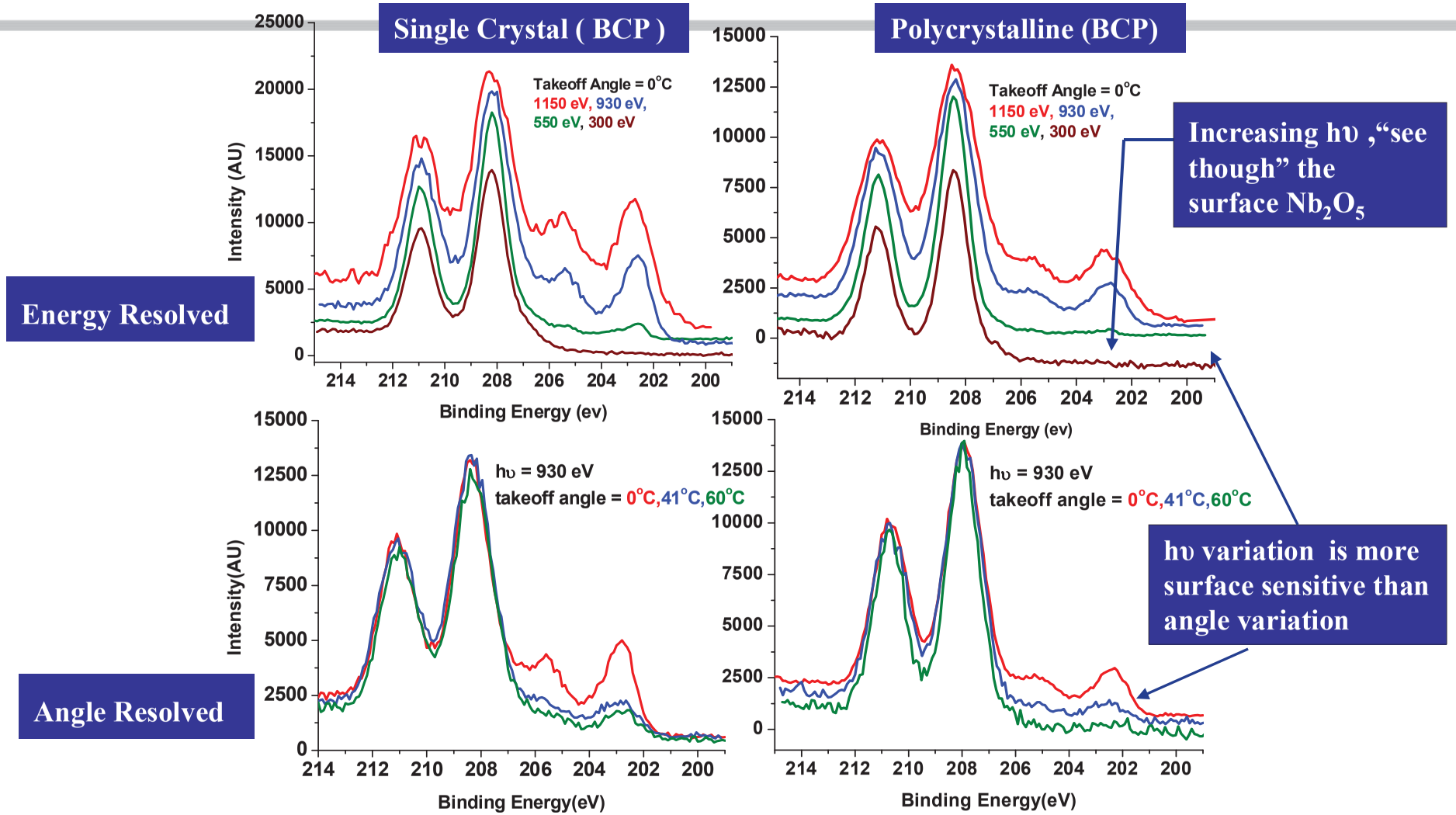

Variable photon energy XPS probes the near-surface composition more incisively and provides better depth analysis than angle-resolved XPS.

Niobium Oxide Profiling of Single Crystal Nb by Energy Resolved XPS

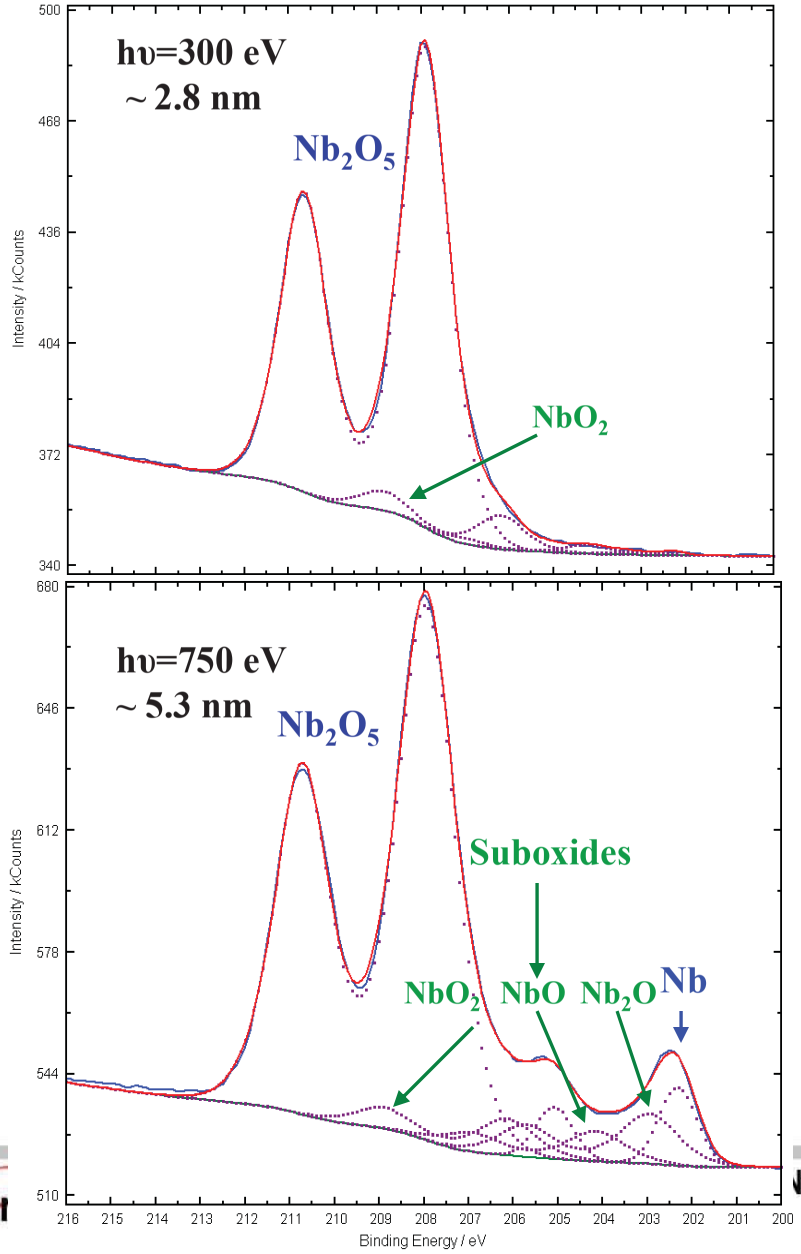

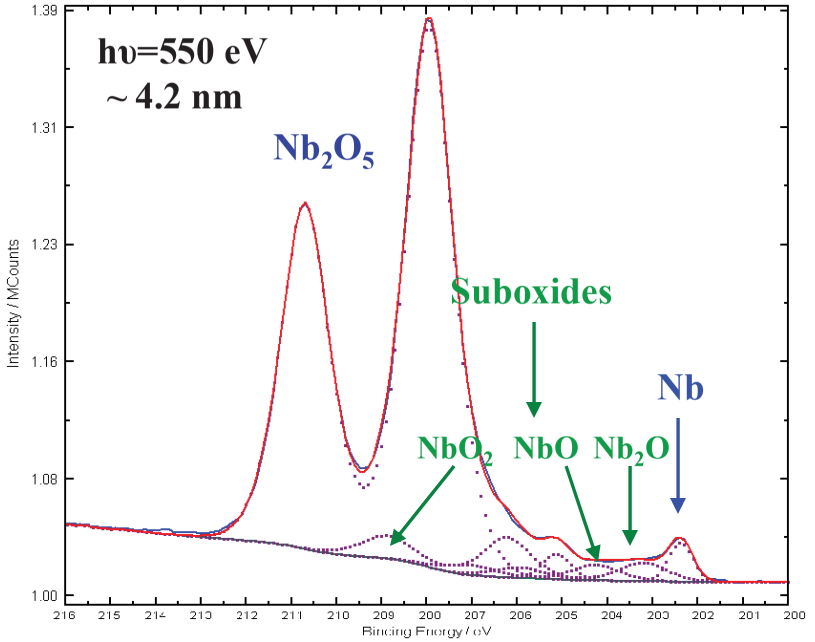

Energy Resolved XPS clearly reveals that between 2~3 nm Nb_2O_5 and the underlying metal is the structural transition zone of suboxides (NbO_2, NbO and Nb_2O) with a thickness not larger than one nanometer.

Where is the Hydroxides-ARXPS?

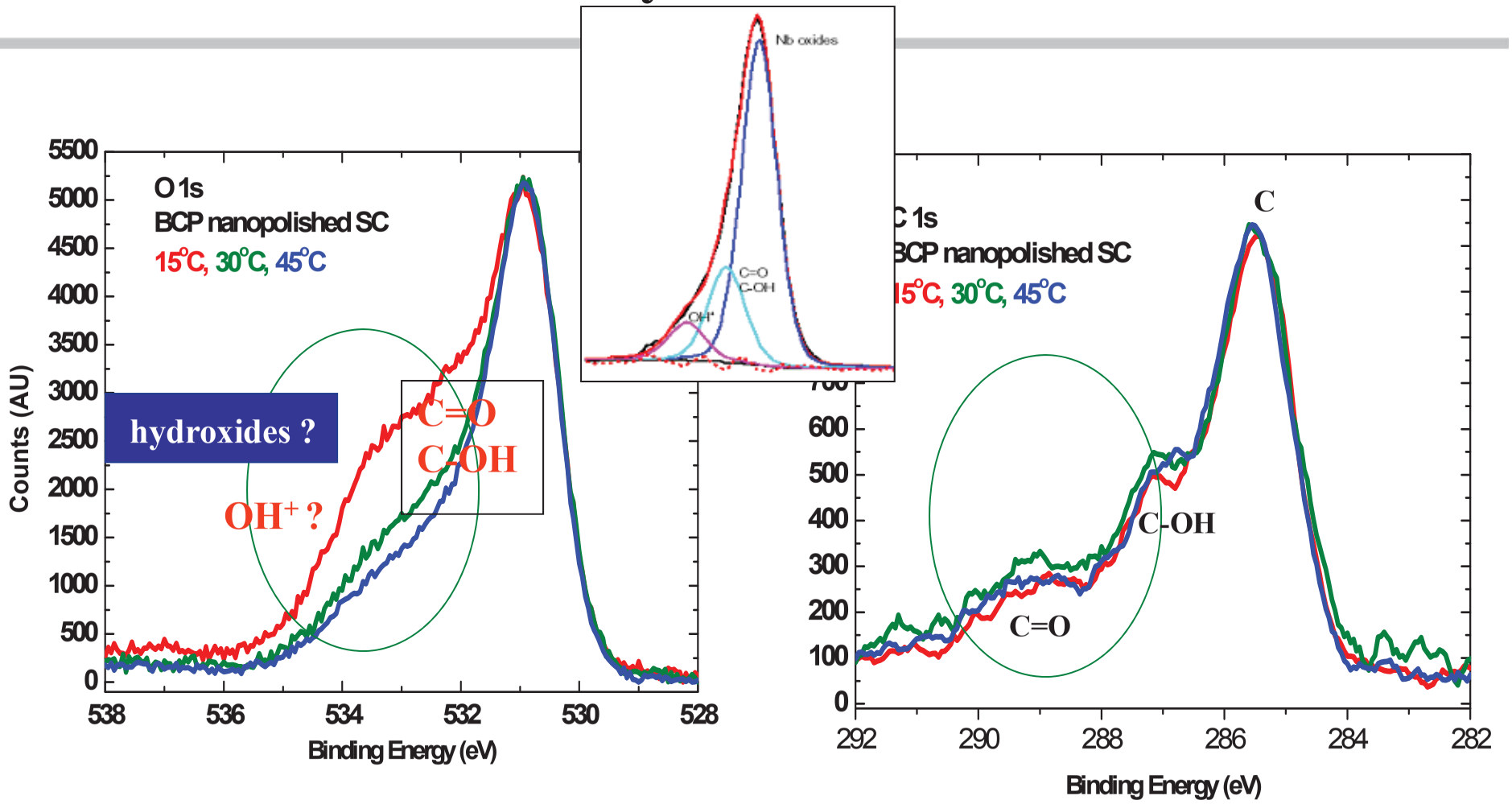

A less than nm hydroxide layer seems to lie below the hydrocarbons & impurities by ARXPS .

Possible Mechanisms about Q-drop & Low-T Baking

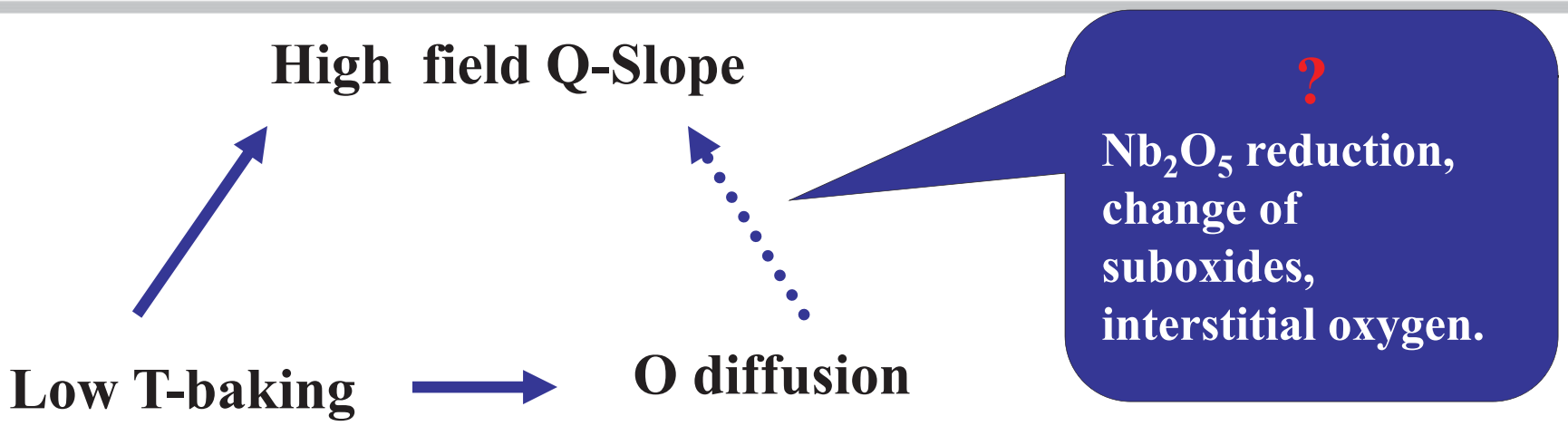

Low temperature (100~140°C, 12~ 24 hrs) baking at high vacuum becomes an indispensable process to be applied to high RRR bulk niobium cavities (BCP/EP, SC/ PC). The performance enhancement from baking remains even after several days of air exposure.

Present Baking Recipes :
Classic: 110~120°C (< 150°C), 24~48 hrs, high vacuum
B. Visentin et, Saclay: 145°C, 3 ~6 hrs, Air; 120°C, >24hrs, Ar.
G. Ciovati et, J-lab: 120°C, 3~6 hrs, large grain, high vacuum

Niobium Surface Oxide
Before/ After Low T Baking

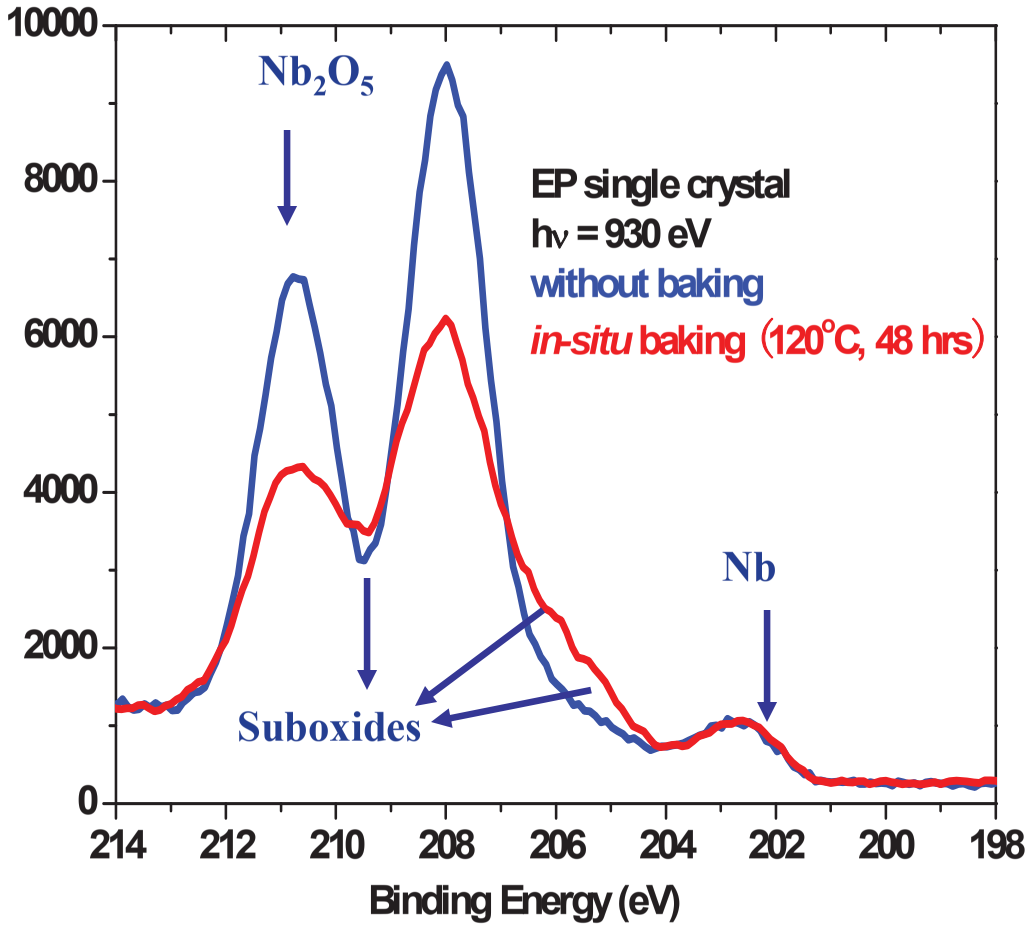

XPS study about BCP/ EP Nb surface show that Nb_2O_5 is partly transformed into suboxide.

Nb_2O_5 Reduction Increases with the Baking Time

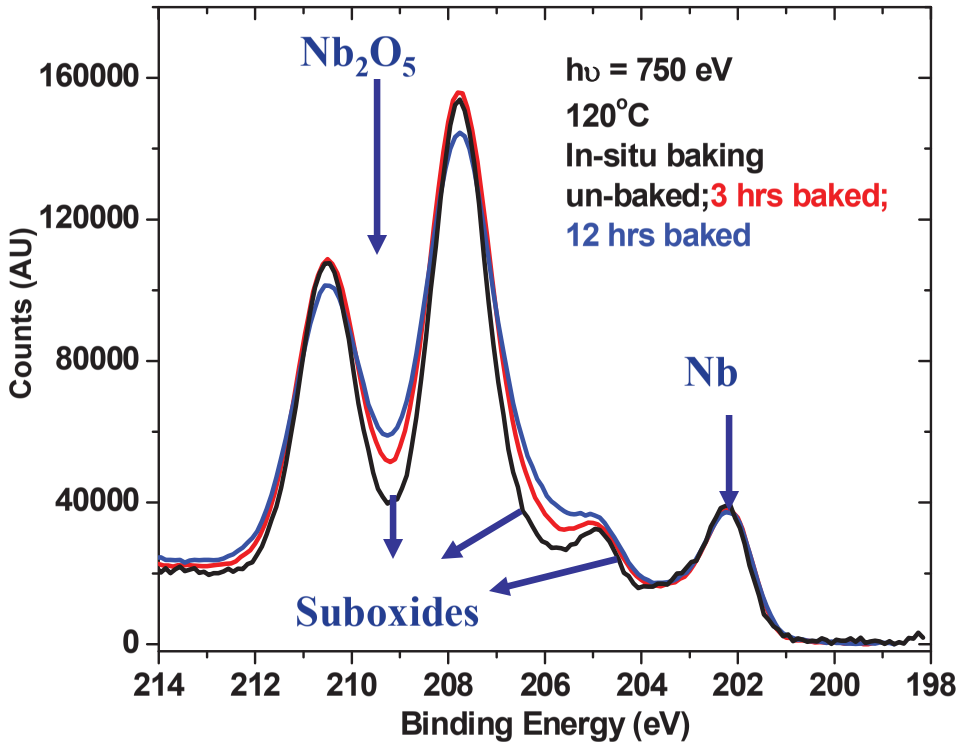

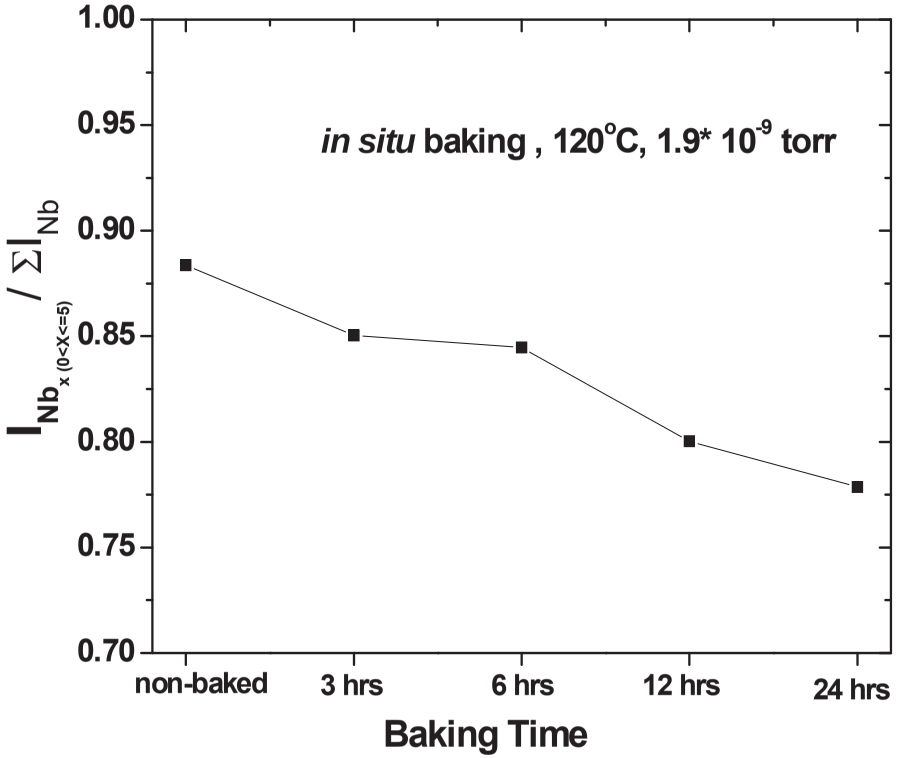

More Nb_2O_5 transforms into suboxides with the baking time

$I_{\text{total oxides}} / I_{Nb}$ decreases linearly with baking duration -surface oxide layer become thinner.

Air Exposure "Recovers" Nb Surface Oxide

The samples in this study were treated at the same condition: BCP 1:1:2, 120°C, 12hrs, air-exposure ~8hrs

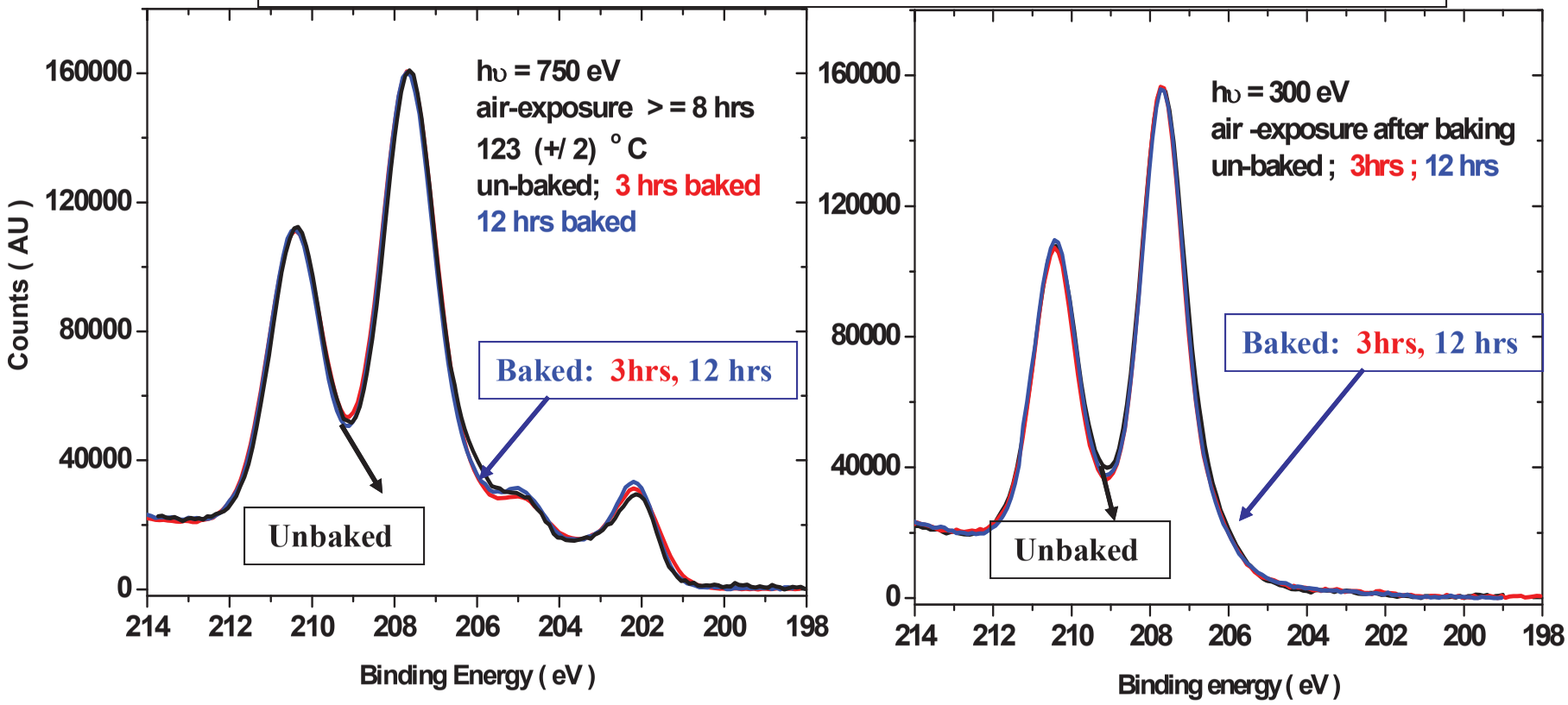

No significant change in surface oxide layer can be observed after air exposure

Air Baking Produce Thick Oxide Layer

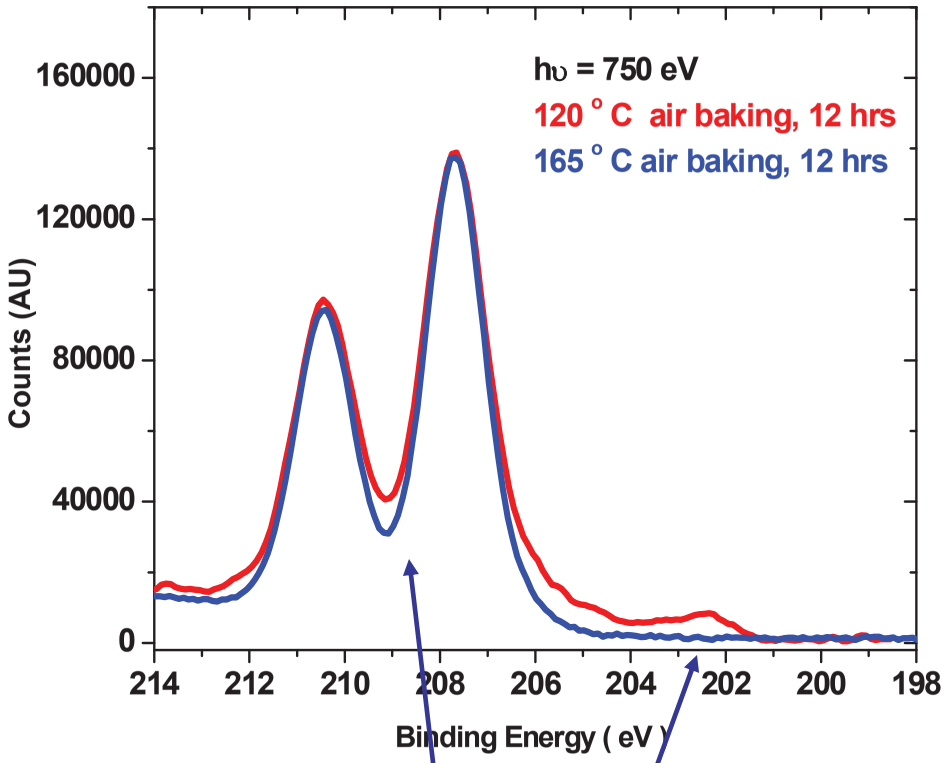

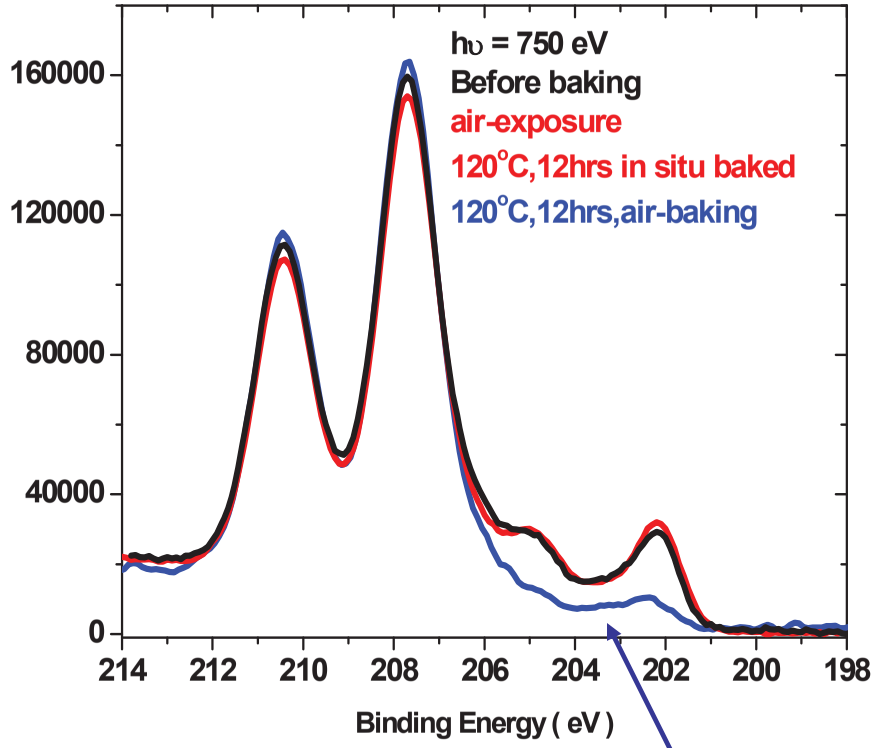

Higher temperature air baking helps make thicker oxide layer (165°C, ~ 9 nm Nb_2O_5), instead of the Nb_2O_5 dissociation .

Comparing with high vacuum in-situ baked sample at the same temperature (120°C), and durations (12 hrs) ,air baking makes thicker oxide layer

Where is the Hydroxides-ARXPS?

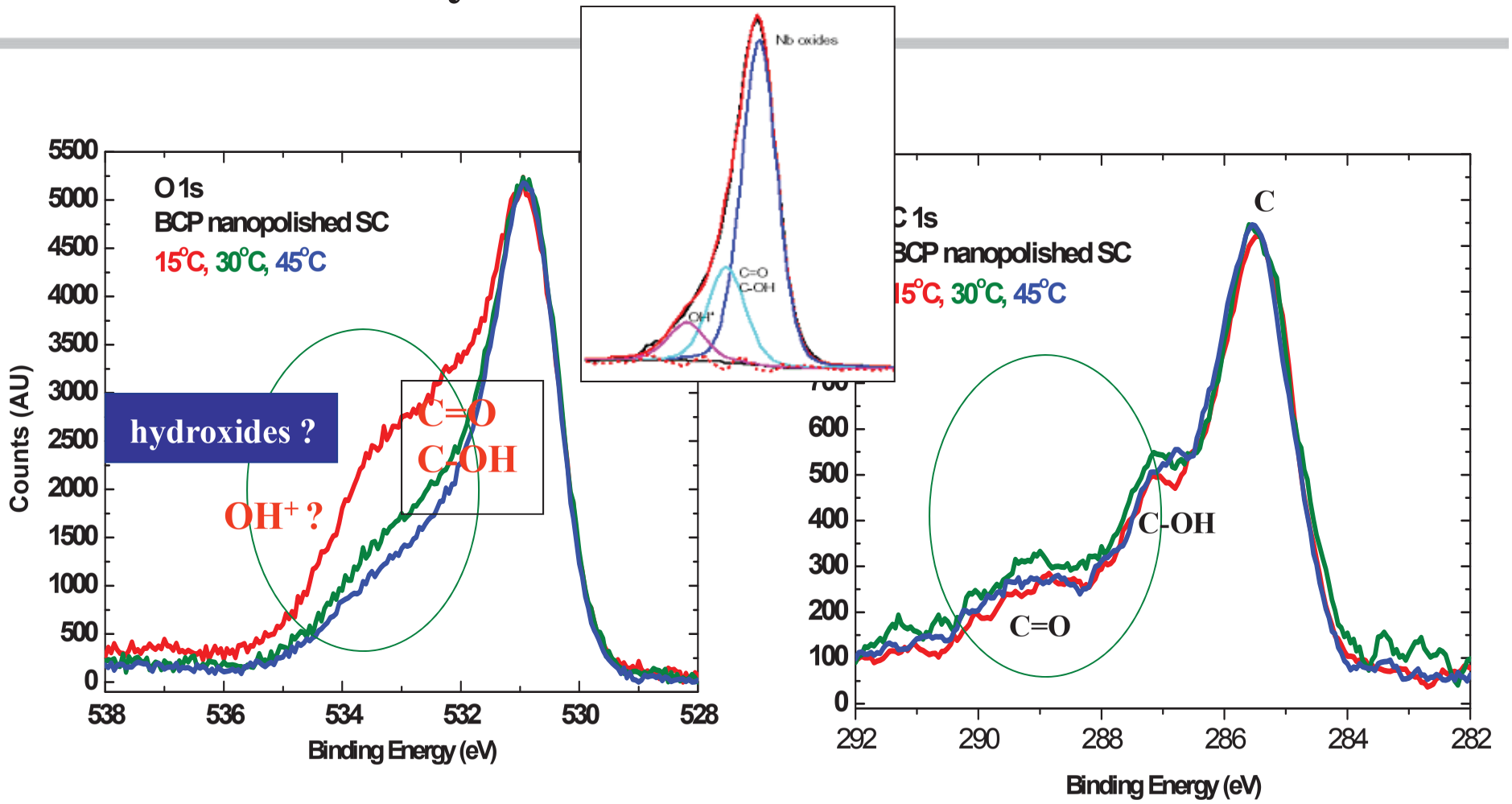

A less than nm hydroxide layer seems to lie below the hydrocarbons & impurities by ARXPS .

Where Does the Hydroxides Go After Baking & Air-exposure ?

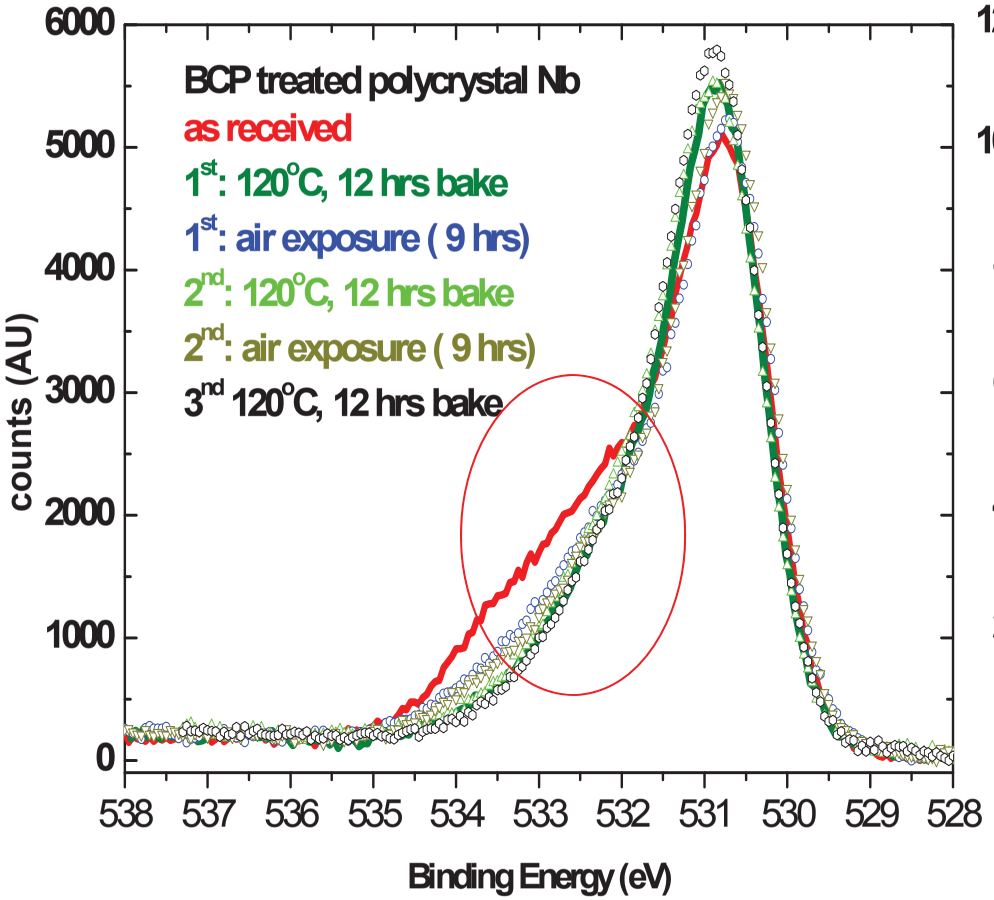

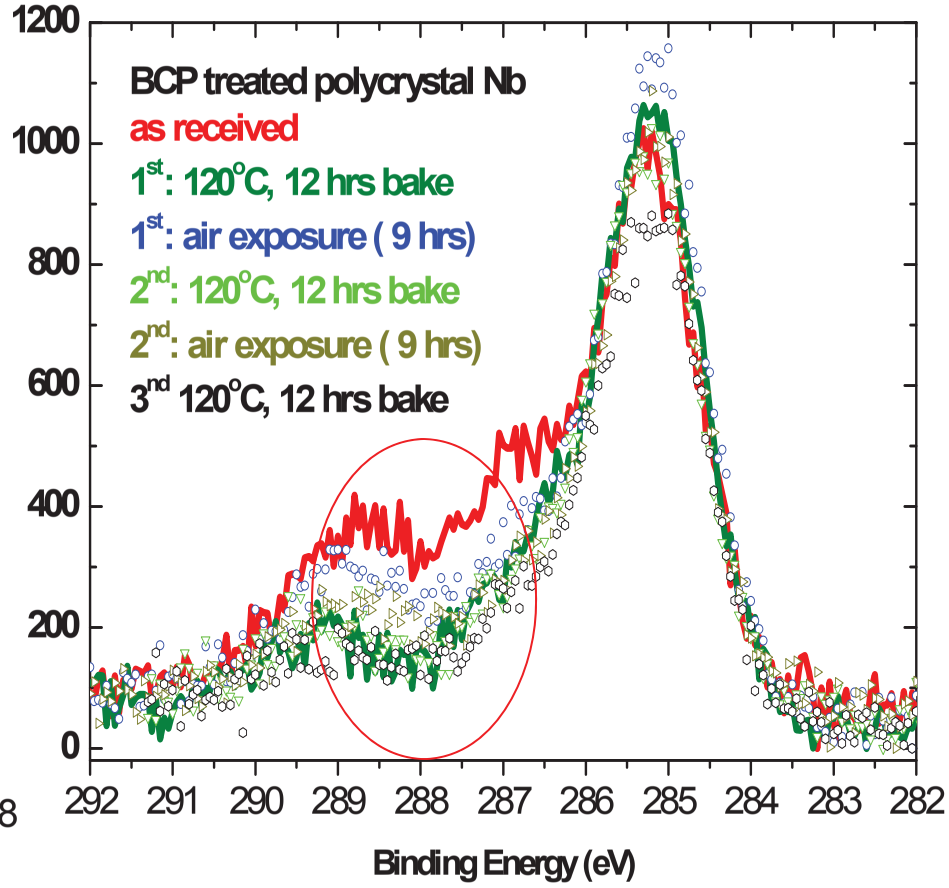

Low-T baking helps to "remove" the top hydrocarbon layer?

Systematic Surface Oxide Study in Parallel with Practical SRF Cavities Baking Process

After baking, Nb_2O_5 is partially transformed into suboxides, the total oxide layer becomes thinner. But upon air-exposure, the change of oxide layer observed after baking disappeared . Cavities still kept good performance, therefore the suboxides created by in situ bake is irrelevant to SRF cavity performance.

Longer baking time at 120°C increases Nb_2O_5 reduction & transformation
Large grain cavities after 3 hrs baking shows performance improvement, the reduction of Nb_2O_5 is irrelevant to SRF cavity performance.

Comparing with 120°C baking, higher baking temperature (160°C) helps more oxide transformation; Air baking produce thick oxide layer.

XPS studies show that the changes in the niobium oxide layer caused by low -T baking appears to not play a big role in cavities performance. H.Tian, C. Reece, M. Kelley, A. DeMasi, L. Pipe, K. Smith, Proceeding of 13th workshop on RF superconductivity

CASE STUDY: NIOBIUM THIN FILMS (JLAB/W&M)

Nb Thin Films Deposition

Deposition of Nb films with energetic condensation via ECR under UHV

Influence of substrate nature & treatment, coating temperature and ion energy

In-situ observation with RHEED & STM of the nucleation and subsequent growth with coating parameters, annealing… on single crystal and polycrystalline substrates.

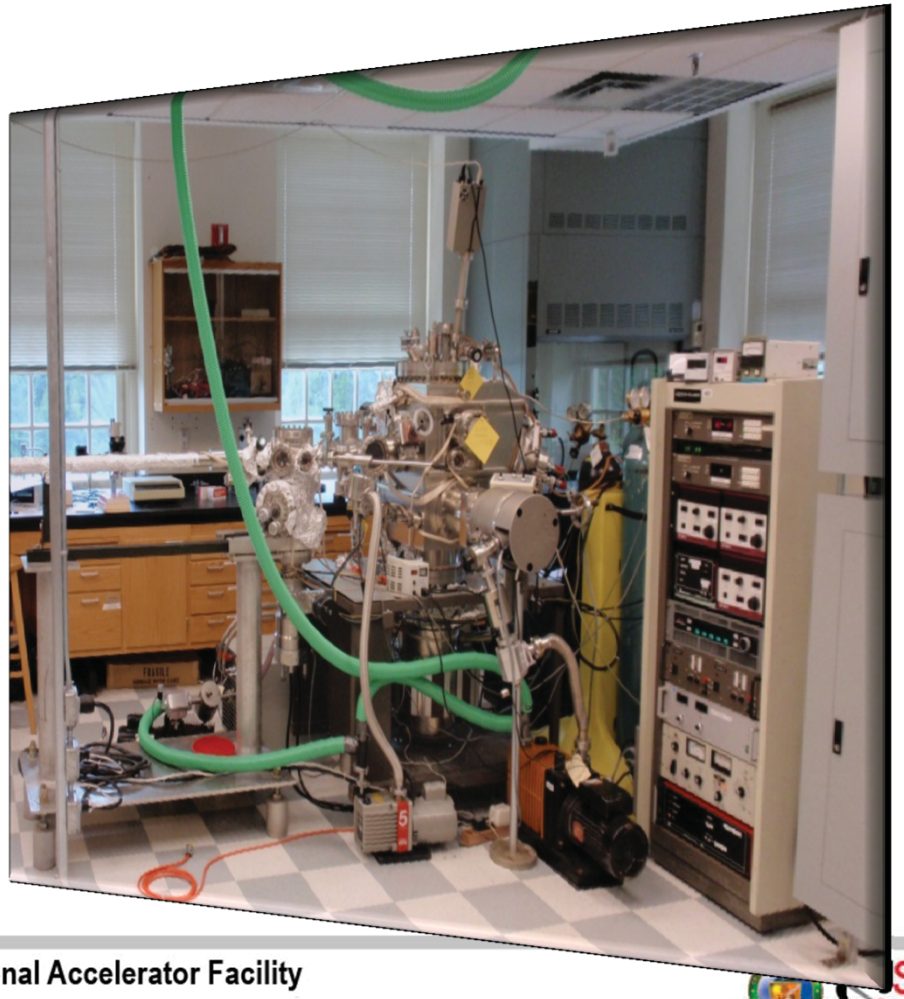

Nb Film Creation

Deposition of films in both systems
Investigation of effect of ion energy (bias), substrate nature & treatment, coating temperature

Film growth approach in 3 sequential phases:

- ✓Film nucleation on the substrate (Nb, Al_2O_3, Cu; single crystal & polycrystalline)
- ✓ Growth of an appropriate template for subsequent deposition of the final rf surface
- ✓Deposition of the final surface optimized for minimum defect density.

Nb/a-Al_2O_3 (11-20)

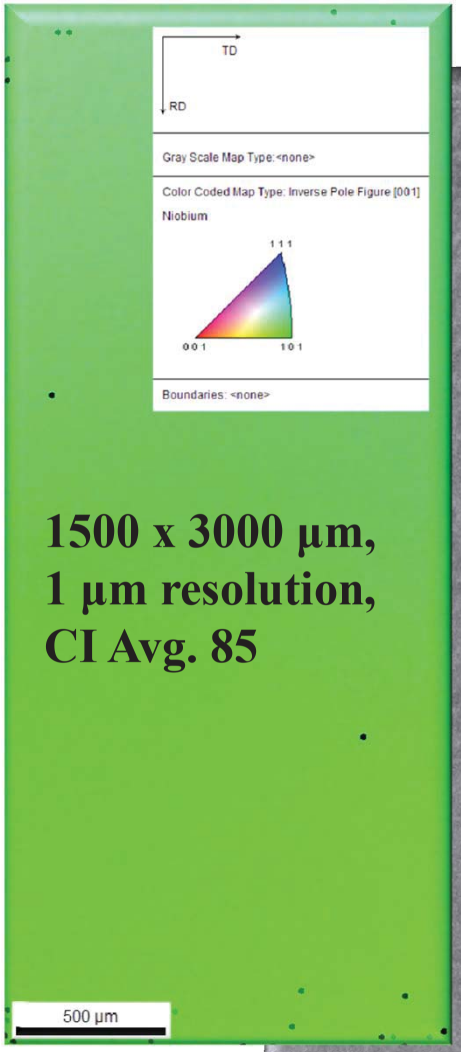

1500 x 3000 µm,
1 µm resolution,
CI Avg. 85

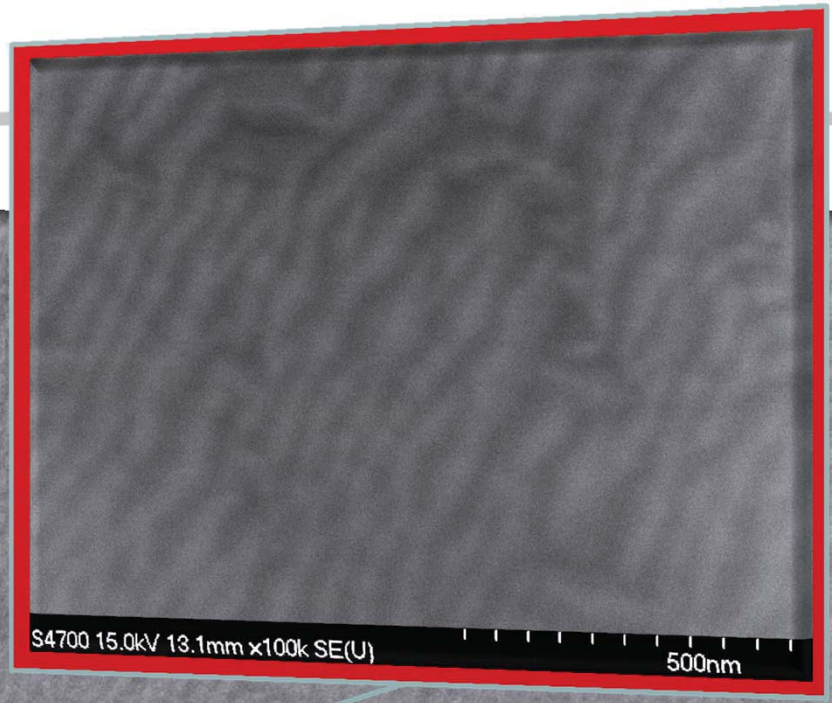

ECR, bias -120V, 20 minutes, Bake-out (18hrs) and coating at 450°C

S4700 15.0kV 13.1mm x20.0k SE(U) 2.00um

Jefferson Lab

Nb/c-Al_2O_3 (0001)

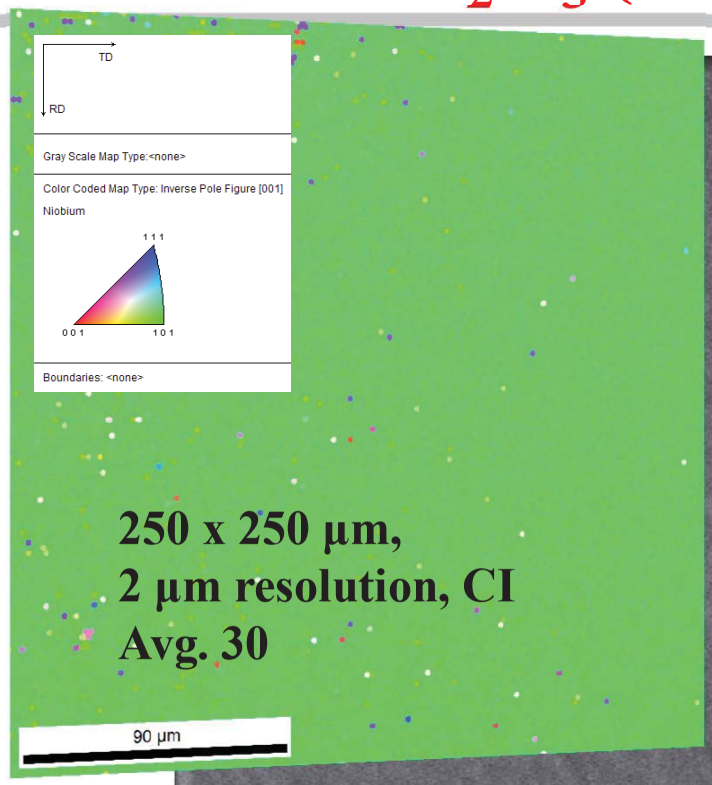

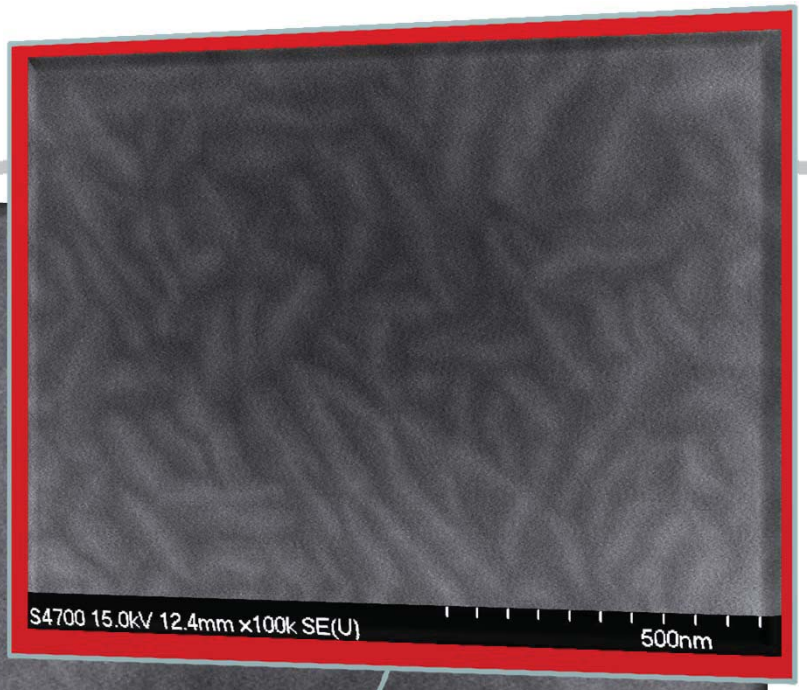

ECR, bias -120V, 20 minutes, bake-out (1.5hrs) and coating @450°C

Thin Films: niobium

Anticipated epitaxial relationships between Nb (bcc) and Al_2O_3 (hcp)

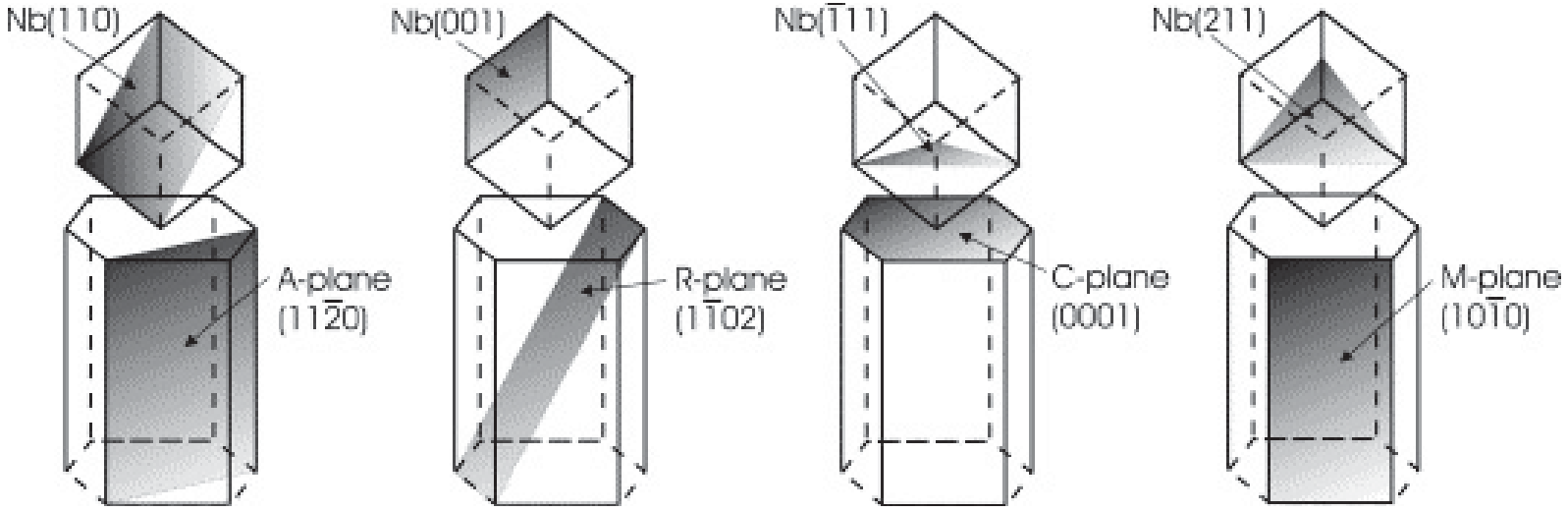

A. R. Wildes et al., Thin Solid Films, 401 7 (2001)

In all cases, Nb films grow along (110) on a-plane sapphire (11-20) for both magnetron sputtered films and ECR films with different bias voltages.

Nb films deposited by energetic condensation on c-plane sapphire (0001) grow along (110) not (111) as anticipated.
Due to higher ion incident energy? (T. Wagner et al., J. Mat. Res. Vol. 11, n°5, pp. 1255-1264 (1996), Mat. Res. Symp. Proc, Vol. 440, pp.151-156, (1997)

Nb/Al2O3 (11-20), 50nm , magnetron sputtered @ 600°C

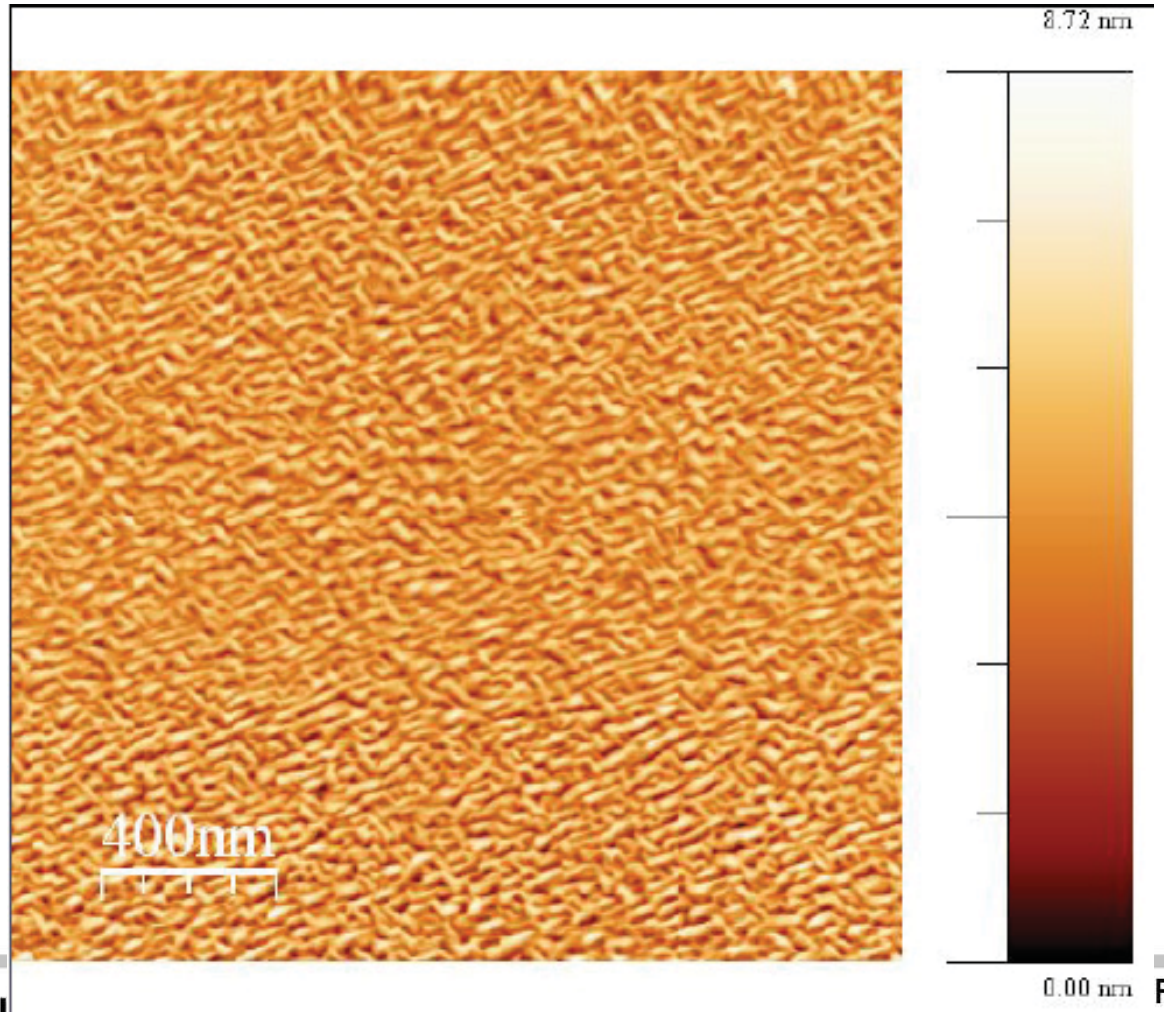

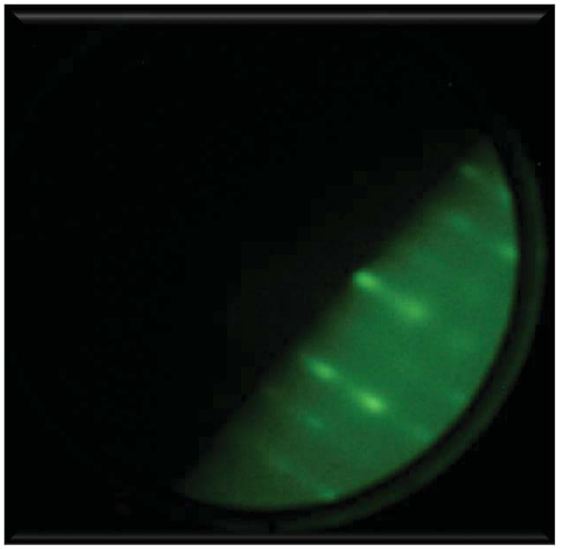

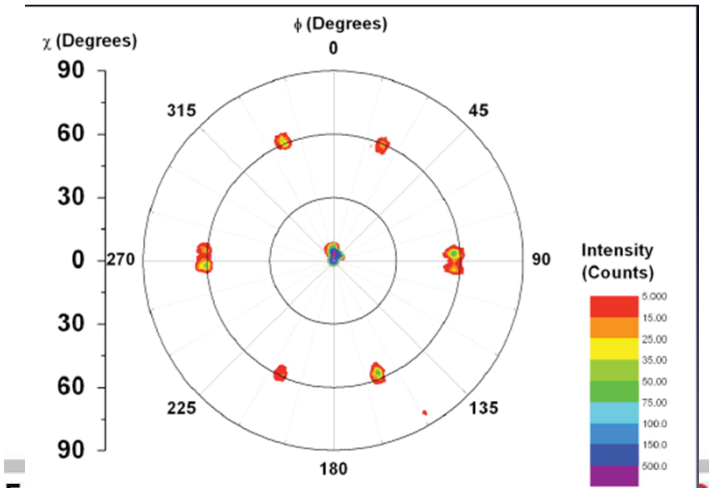

Nb/Al2O3 (11-20), 600nm , magnetron sputtered @ 600°C

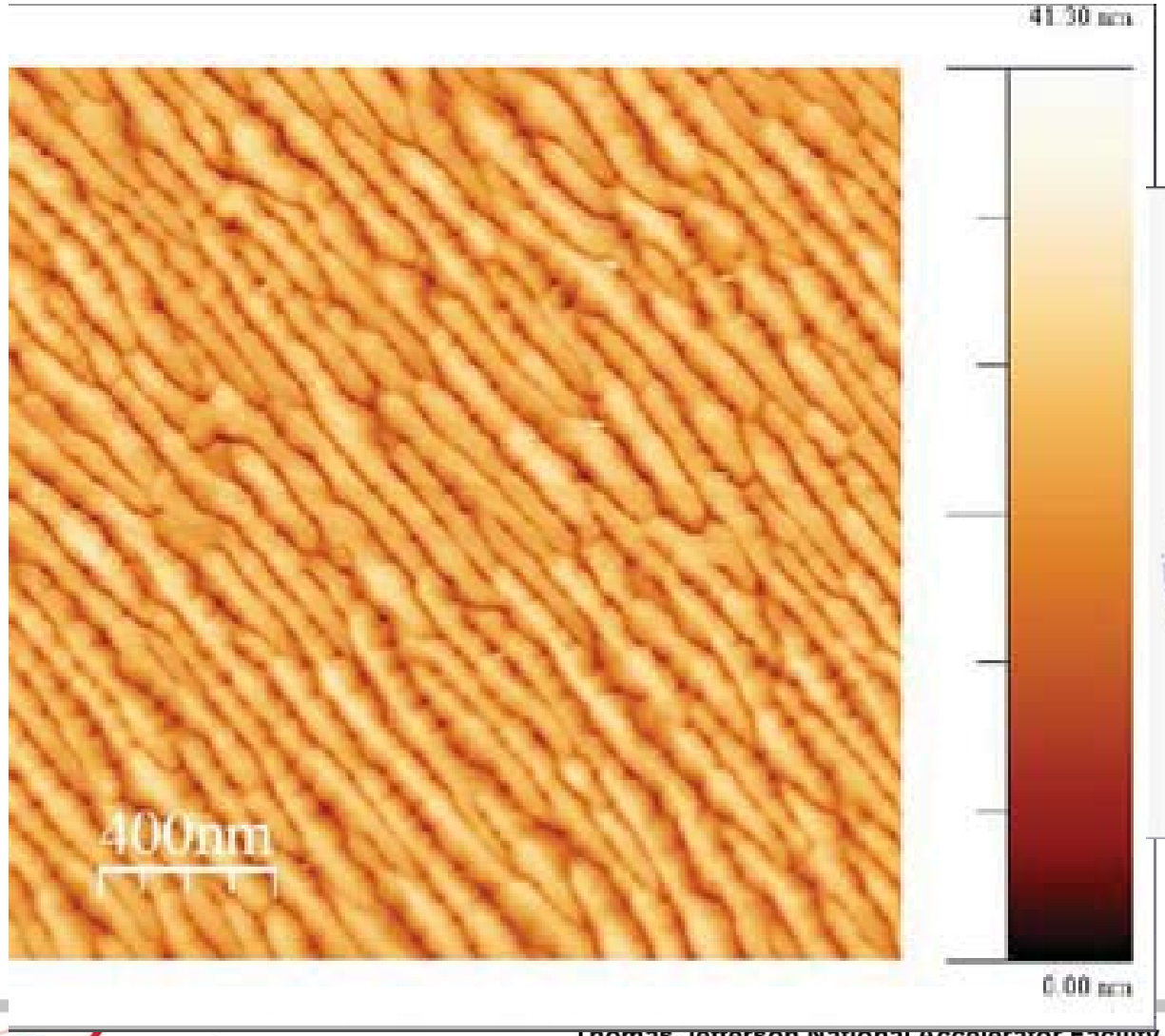

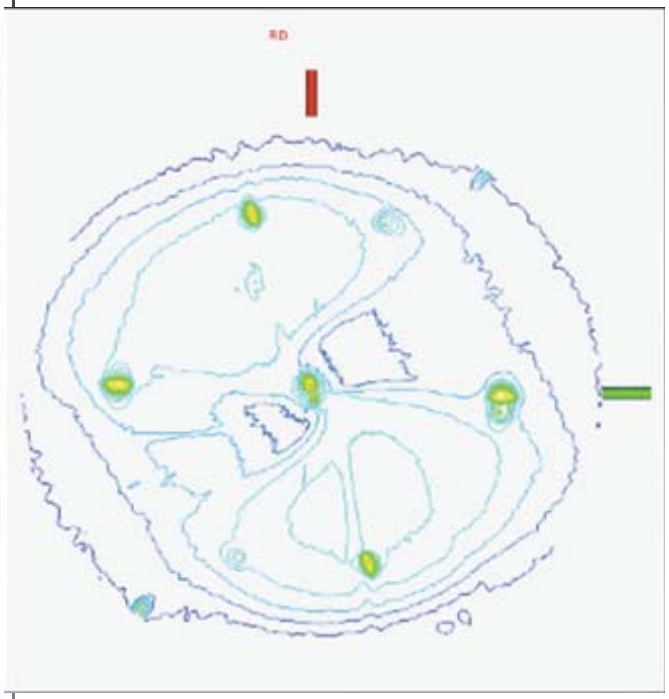

Nb/CuO – High Resolution TEM

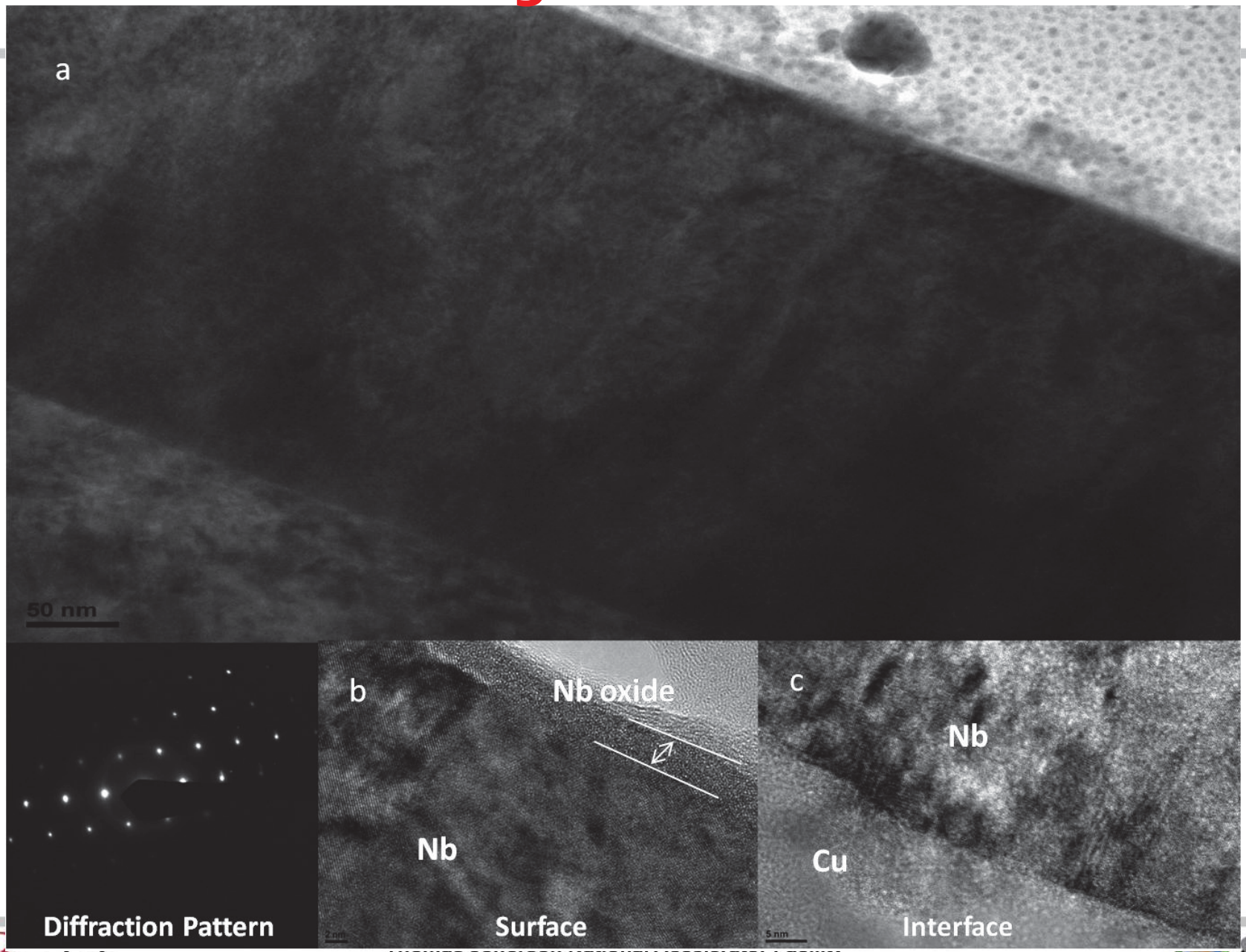

Effect of Bias Voltage for Nb/CuO

- Obvious advantage: no noble gas for plasma creation
- Sample tests: good RRR and Tc, 100-nm grain size, lower defect density and smooth surfaces

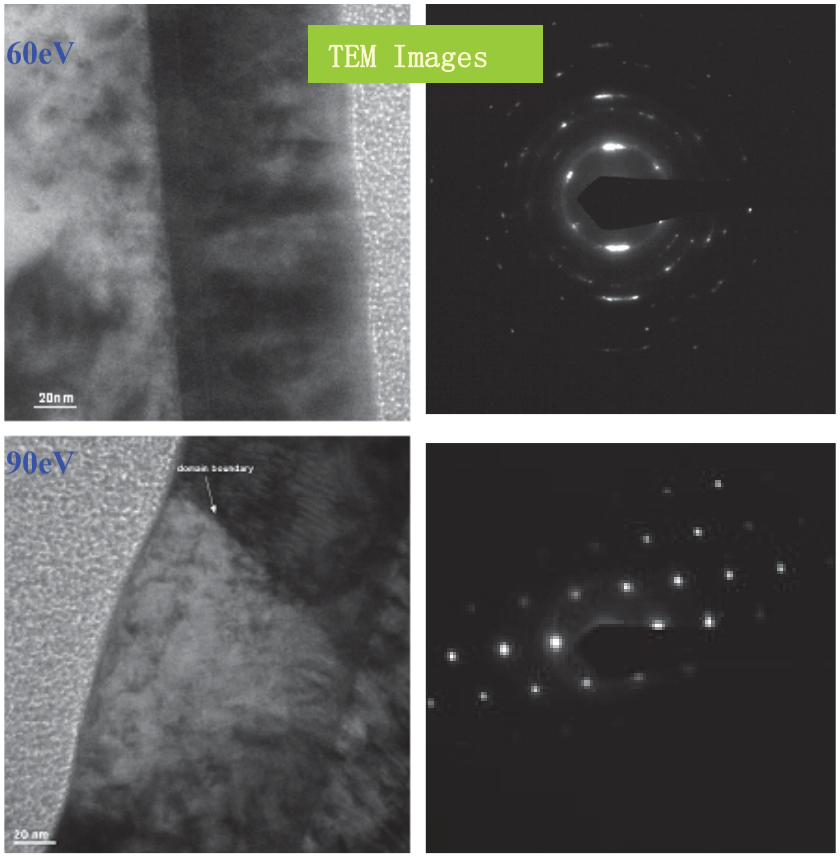

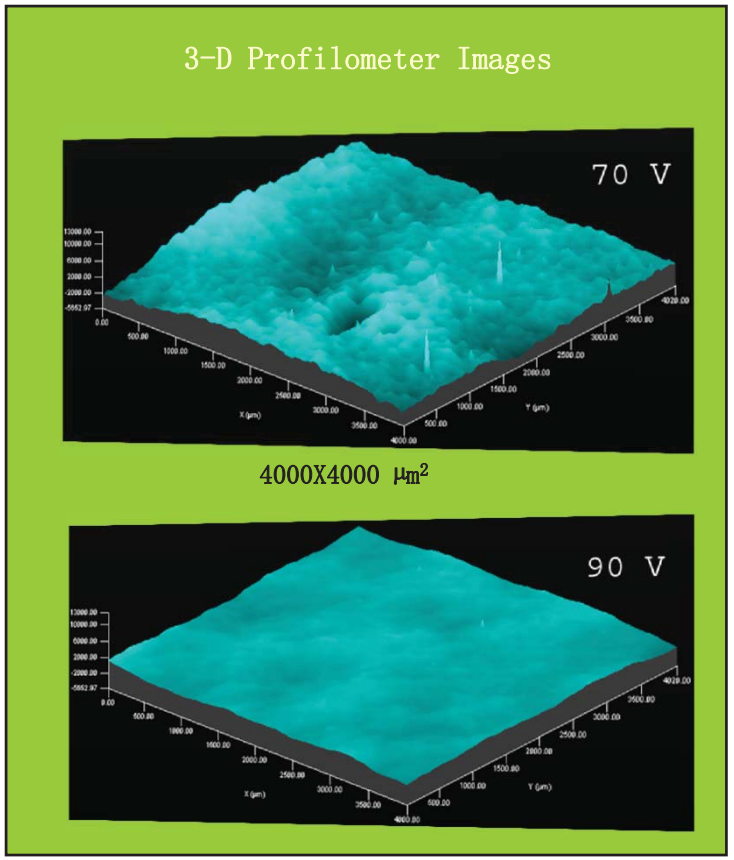

Effect of Bias Voltage for Nb/CuO

XRD – Bragg-Brentano

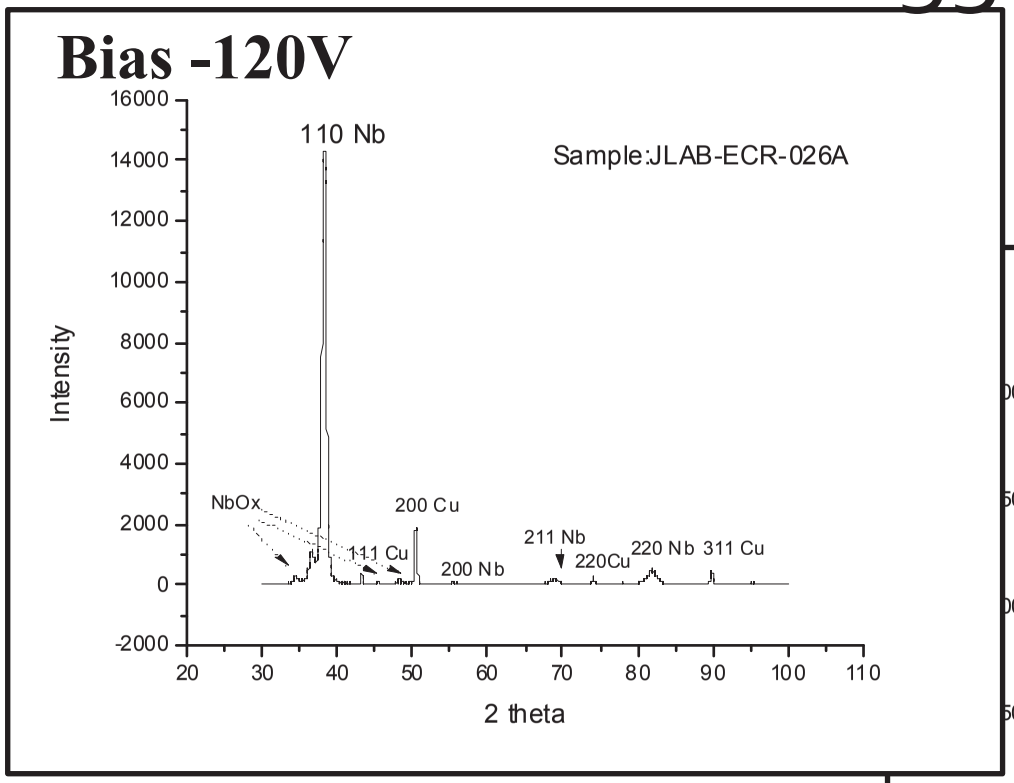

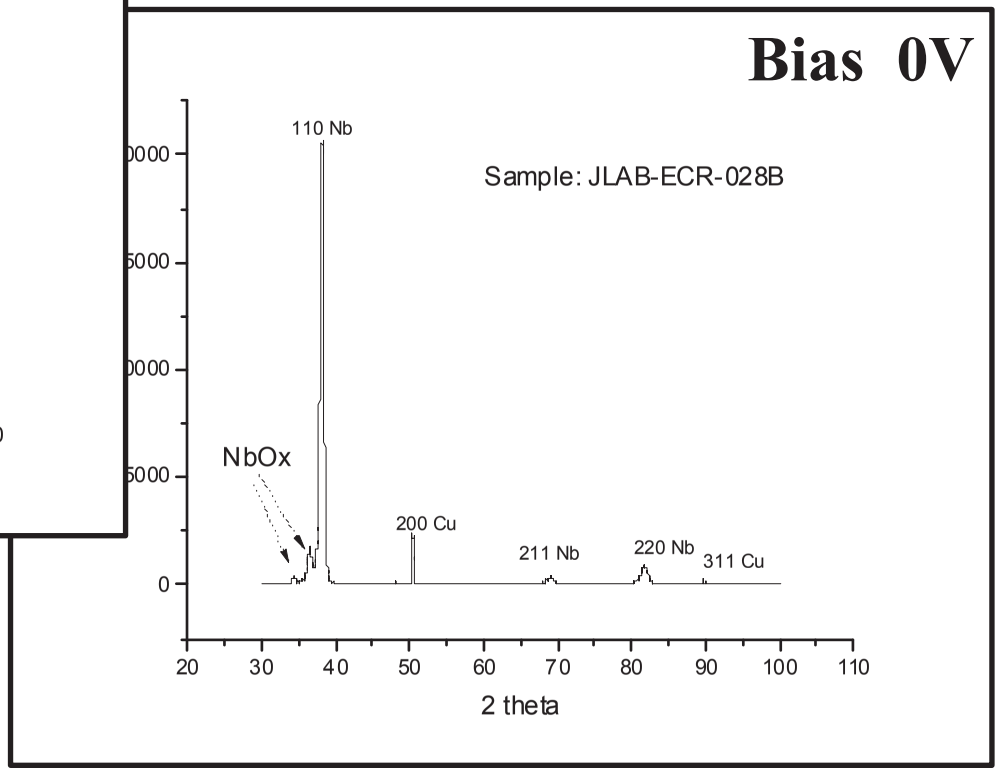

Nb/Cu

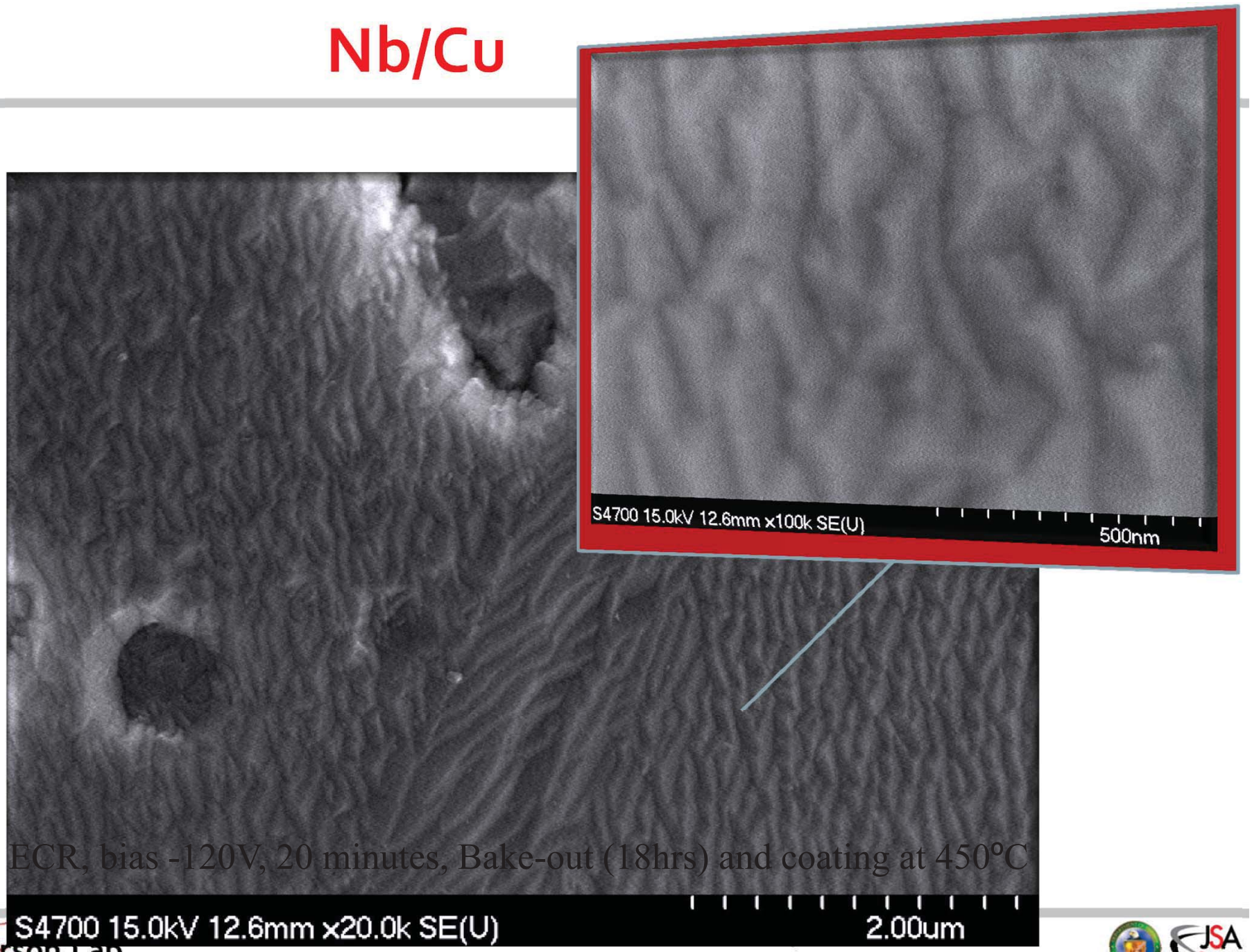

ECR, bias -120V, 20 minutes, Bake-out (18hrs) and coating at 450°C

Effect of Bias Voltage for Nb/Cu

150 x 150 µm, 1 µm resolution,
CI Avg. 0.71

Nb/Cu, Bias -120V

20', Bake-out (18hrs) and coating at 450°C

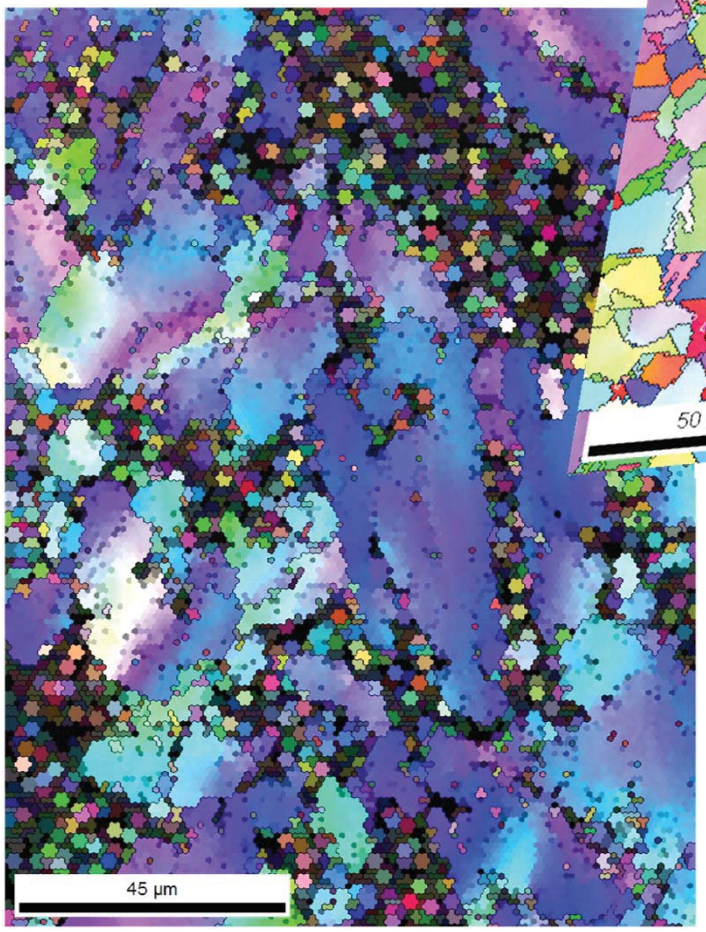

120 x 150 µm, 1 µm resolution, CI 0.23

Typical Cu substrate

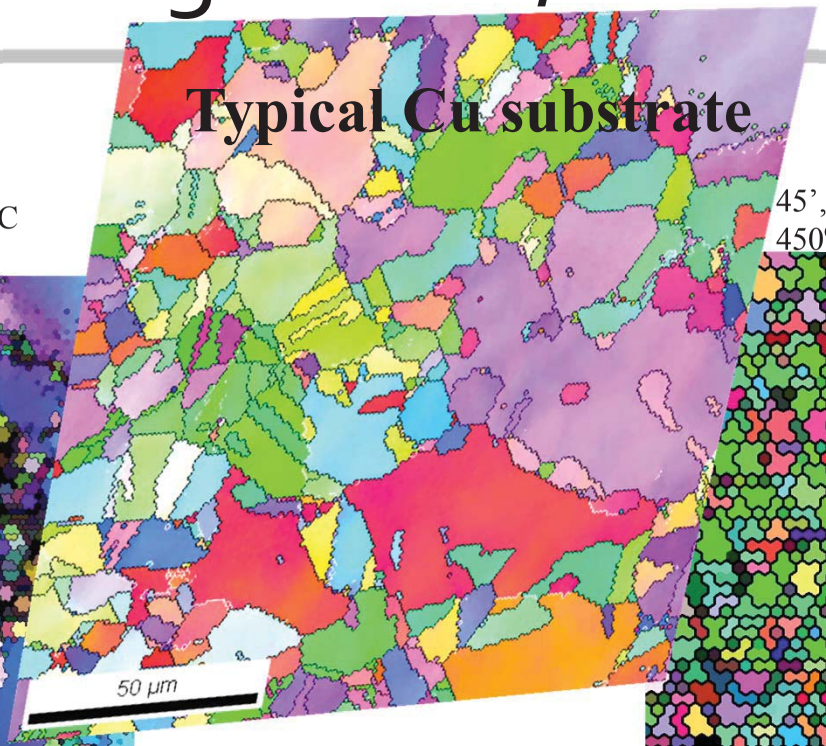

Nb/Cu, Bias oV

45', Bake-out (18hrs) and coating at 450°C

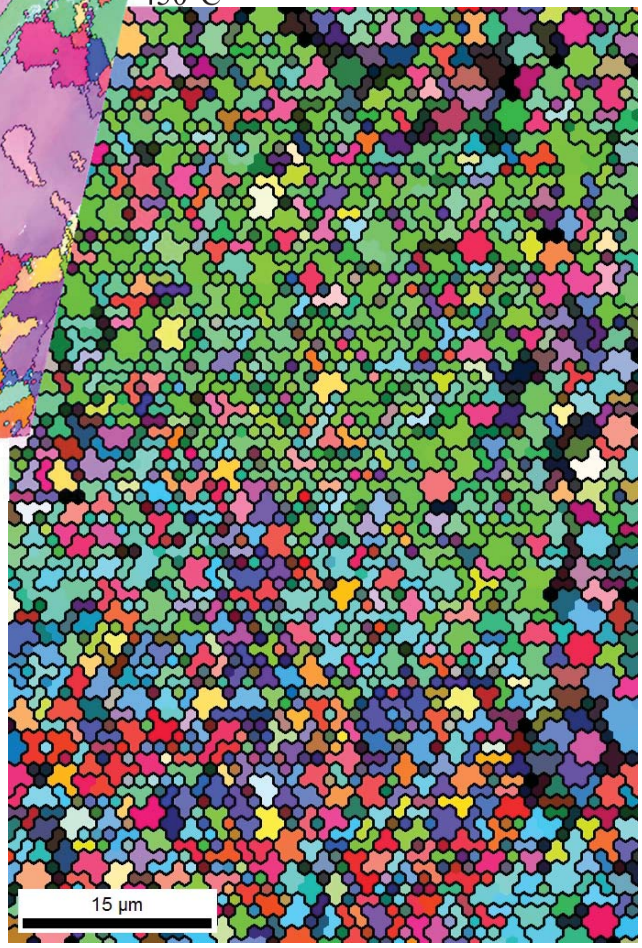

50 x 75 µm, 1 µm resolution, CI 0.16

1st SIC Measurements on Nb/CuO

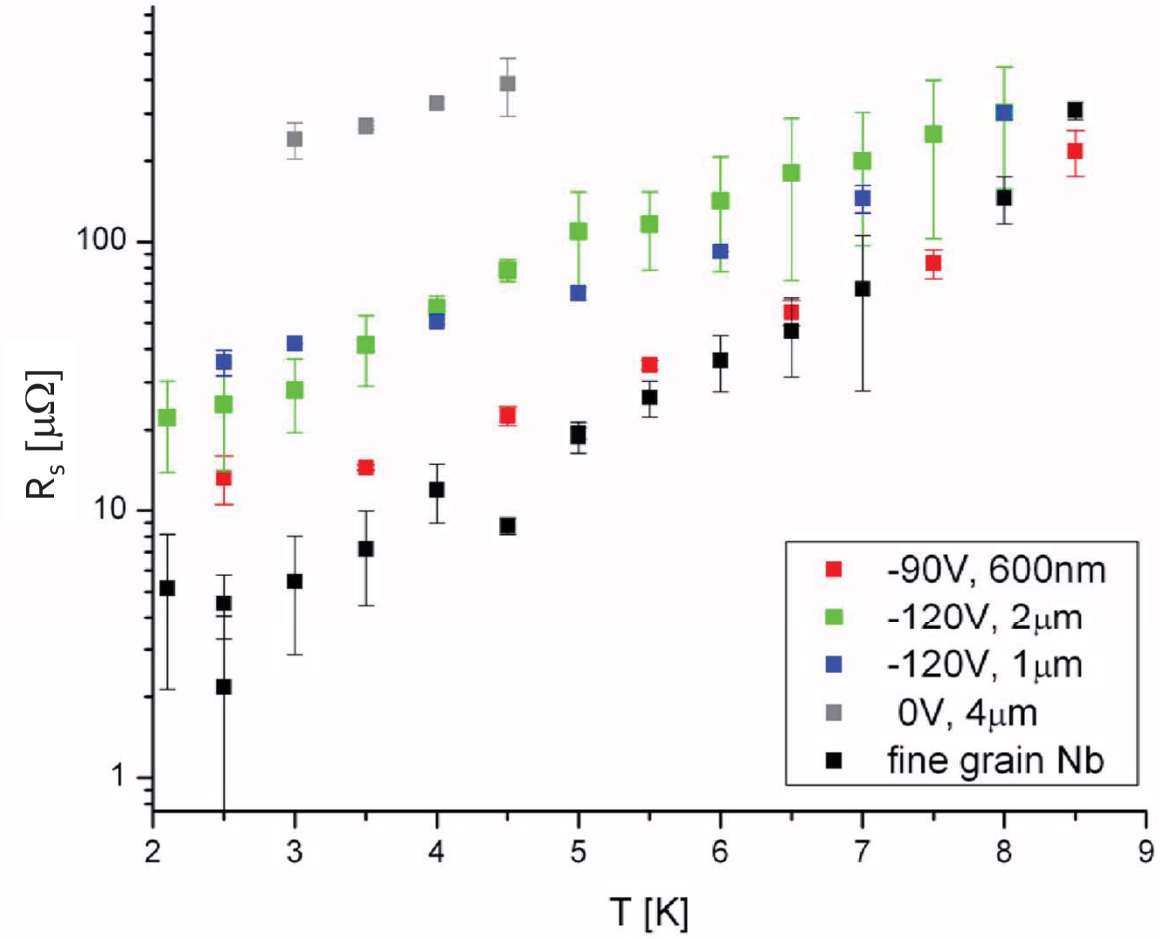

High quality Nb films

Run away heater: substrates heat treated to T>900°C
2′ coating at -120V bias & 450°C

Analyses on Nb/Cu and Nb/ Al_2O_3 (11-20)

T_c=9.25K, RRR = 73.5

Thickness: 234 nm for ~ 2′ coating!

Nb/ Al_2O_3 (11-20) displays high quality in crystallinity, very smooth.
Due to surface defect annealing on the substrate prior to coating?

Nb/Cu exhibits very large Nb grains due to the full re-crystallization of the Cu substrate. However, additionally to the roughness of the Cu substrate, the steps between grains are very high, most likely due to the re-crystallization process.
Sharp interface


100 nm

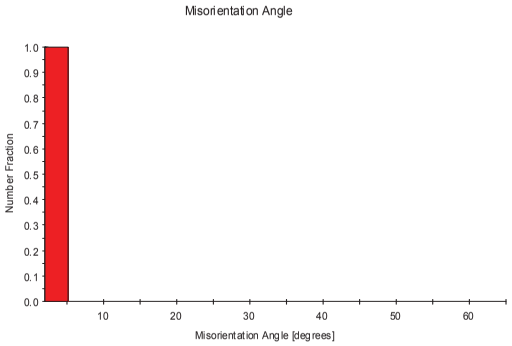
Misorientation Angle
Number Fraction
1.0
0.9
0.8
0.7
0.6
0.5
0.4
0.3
0.2
0.1
0.0
10
20
30
40
50
60
Misorientation Angle [degrees]

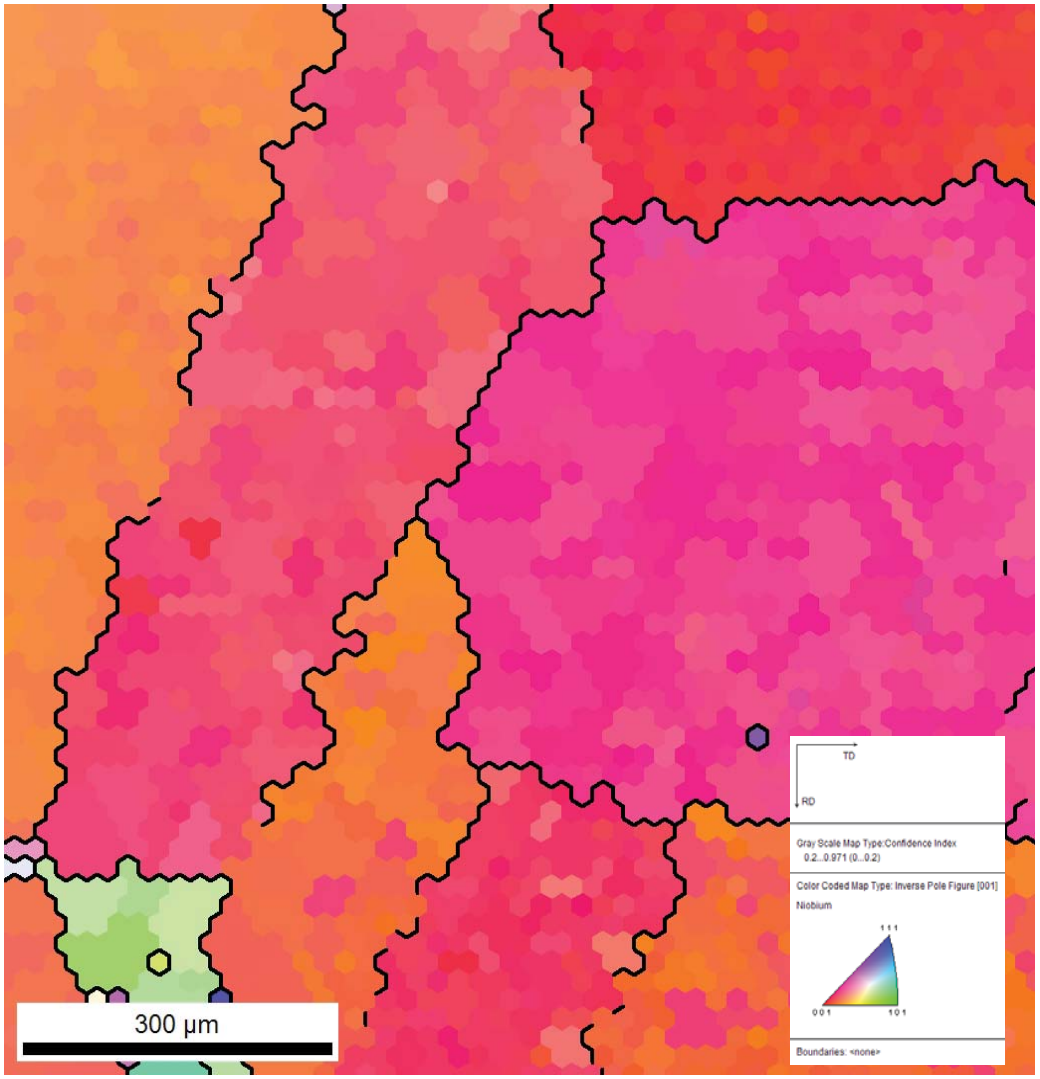
300 µm
TD
RD
Gray Scale Map Type:Confidence Index
0.2...0.971 (0...0.2)
Color Coded Map Type: Inverse Pole Figure [001]
Niobium
1 1 1
0 0 1
1 0 1
Boundaries: <none>

TF-JLAB-ECR-Nb-a-Al_2O_3-033

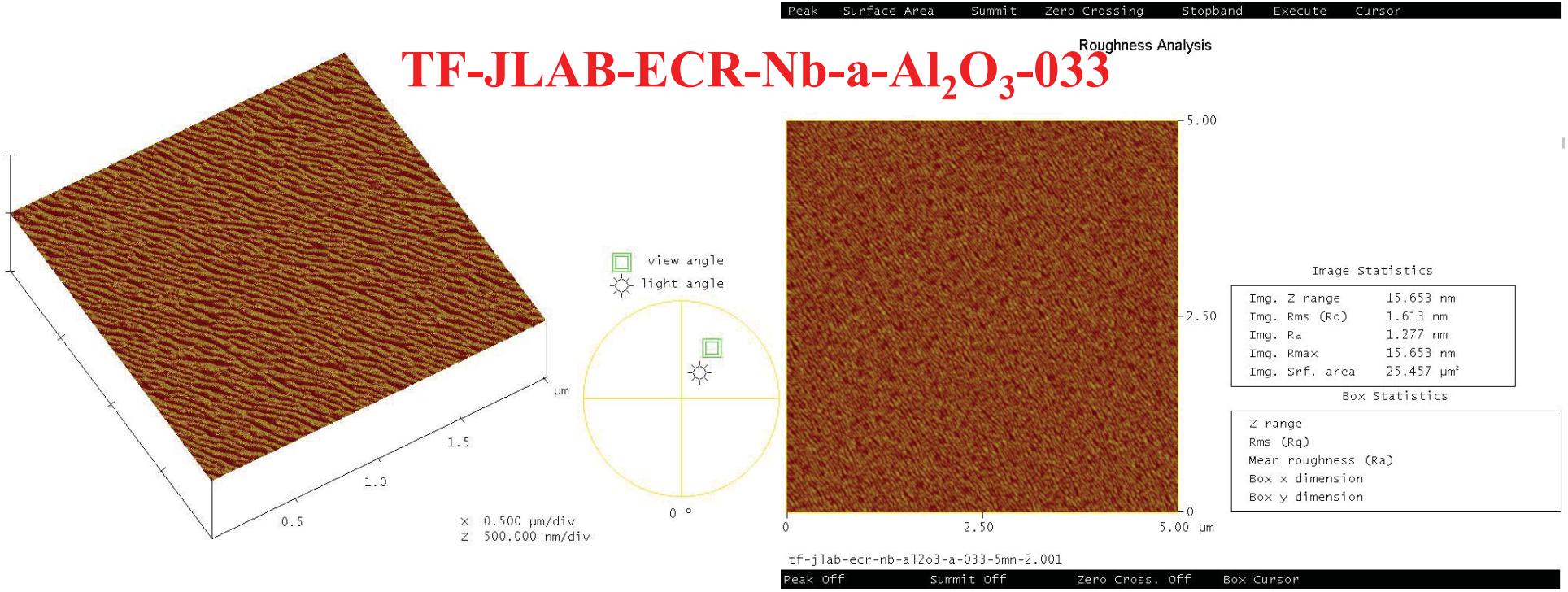

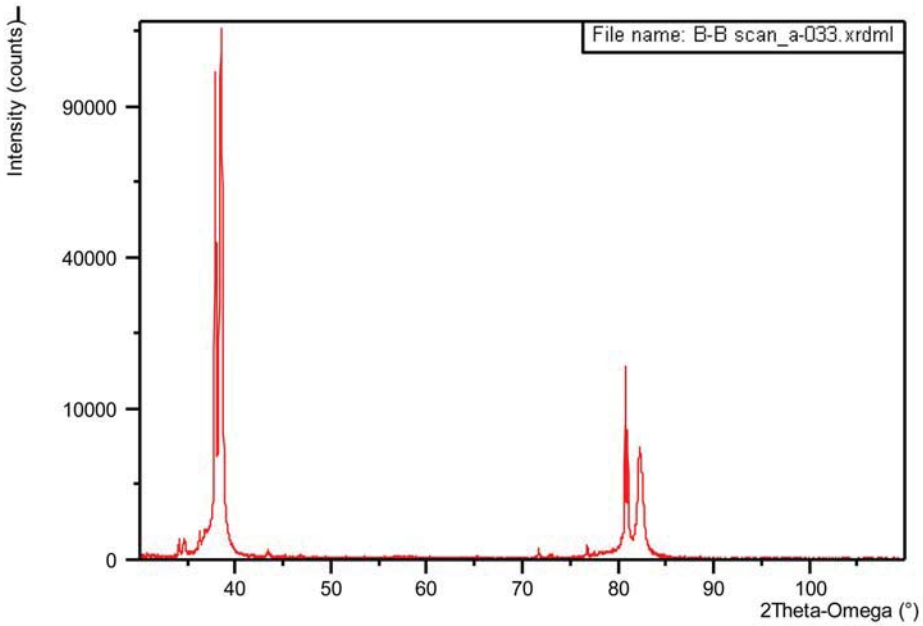

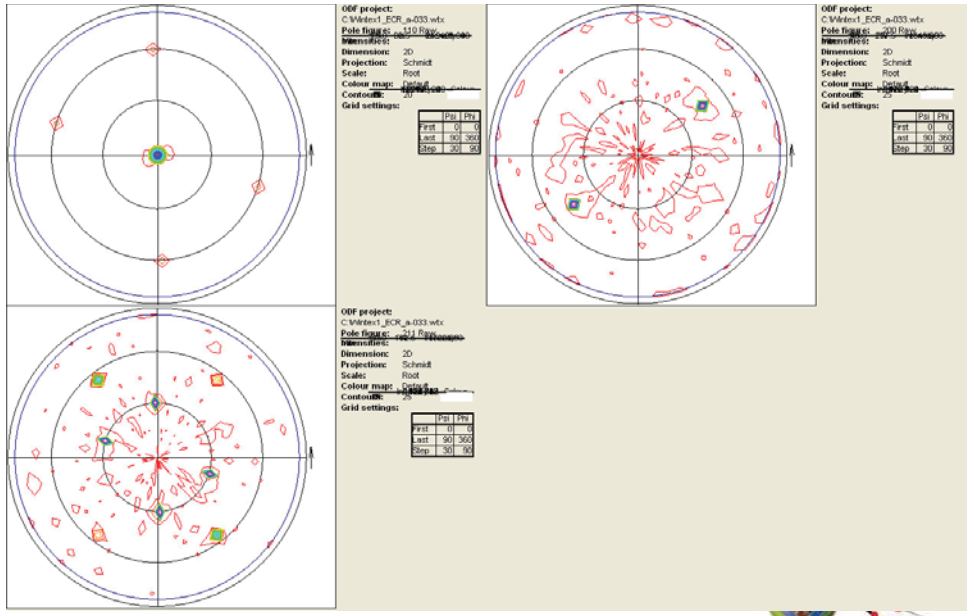

TF-JLAB-ECR-Nb-Cu-033

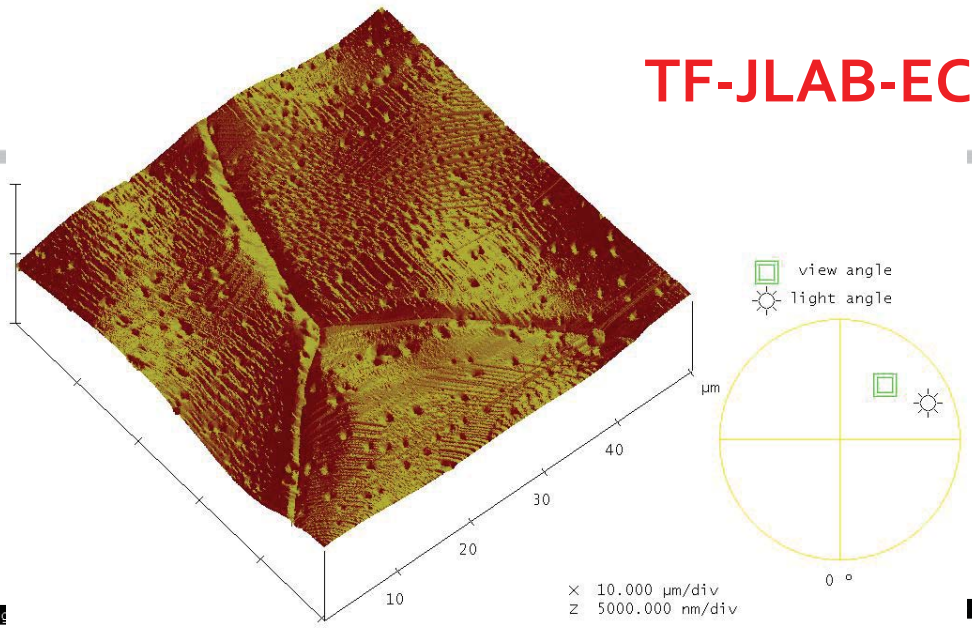

Peak Surface Area Summit Zero Crossing

Roughnes

Stopband Execute Cursor

s Analysis

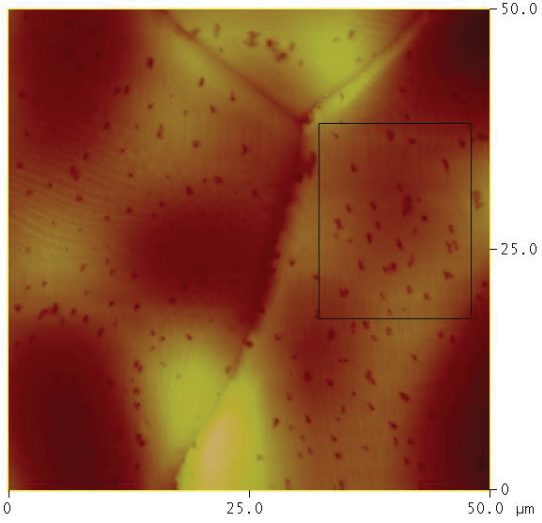

Image Statistics

Img. Z range	2.169 μm
Img. Rms (Rq)	320.36 nm
Img. Ra	242.46 nm
Img. Rmax	2.169 μm
Img. Srf. area	2554.4 μm²

Box Statistics

Z range	883.33 nm
Rms (Rq)	96.380 nm
Mean roughness (Ra)	78.000 nm
Box x dimension	15.851 μm
Box y dimension	20.352 μm

tf-jlab-ecr-nb-cu-033b-50mn-2.000

Peak Off Summit Off Zero Cross. Off Box Cursor

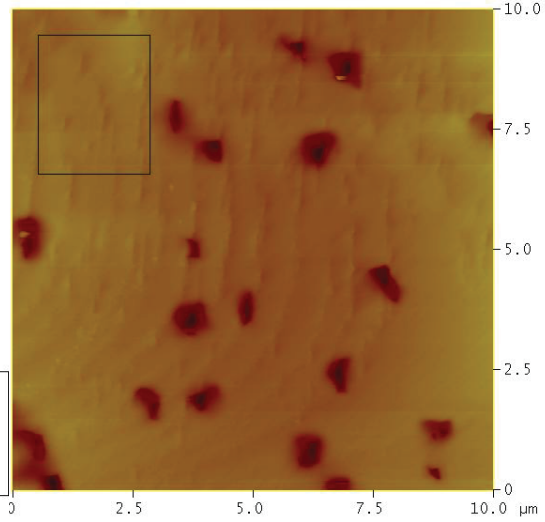

Image Statistics

Img. Z range	527.13 nm
Img. Rms (Rq)	45.359 nm
Img. Ra	27.733 nm
Img. Rmax	520.42 nm
Img. Srf. area	104.01 μm²

Box Statistics

Z range	69.973 nm
Rms (Rq)	11.501 nm
Mean roughness (Ra)	8.931 nm
Box x dimension	2.329 μm
Box y dimension	2.896 μm

tf-jlab-ecr-nb-cu-033b-10mn-1.001

Peak Off Summit Off Zero Cross. Off Box Cursor

Cursor Marker Spectrum Zoom Center Line Offset Clear

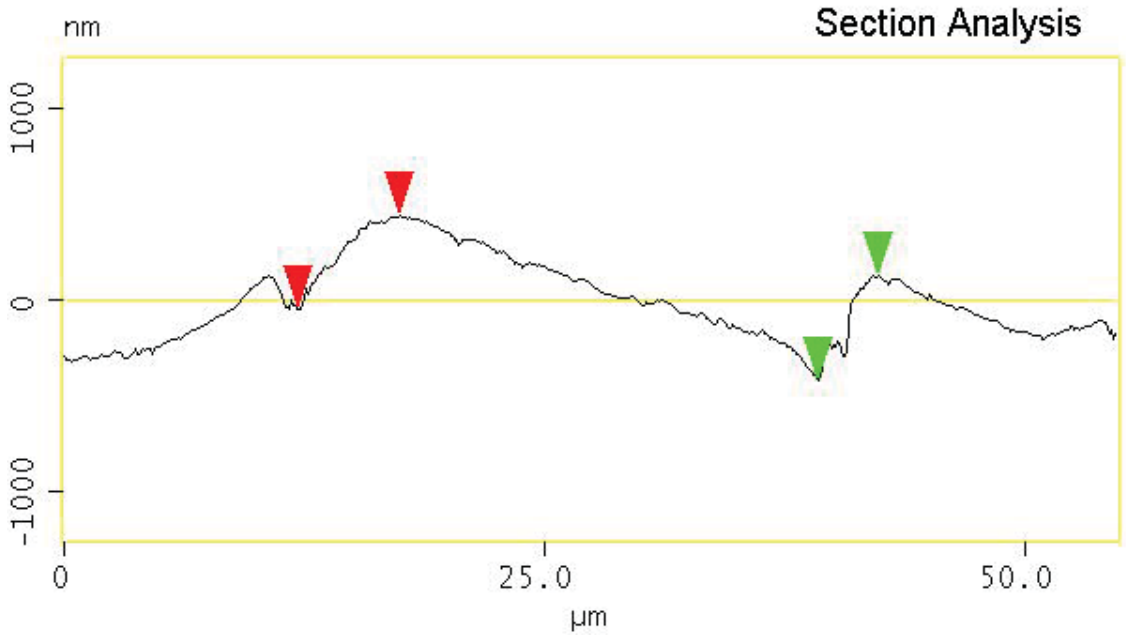

L	3.125 µm
RMS	176.74 nm
lc	DC
Ra(lc)	46.344 nm
Rmax	247.11 nm
Rz	181.70 nm
Rz Cnt	4
Radius	975.79 nm
Sigma	439.08 nm

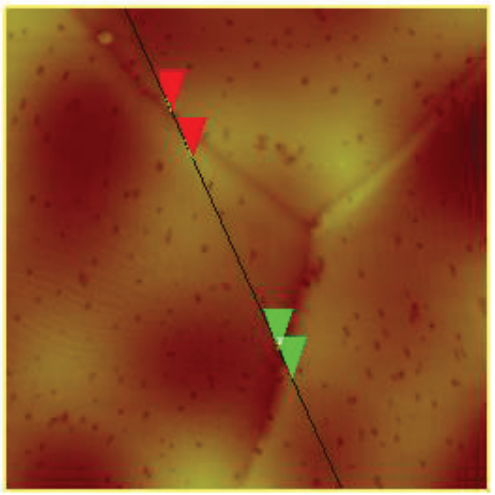

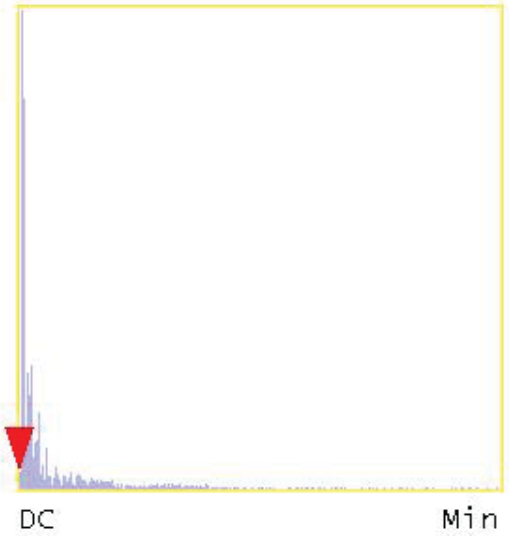

tf-jlab-ecr-nb-cu-033b-50mn-1.000

Surface distance	5.338 µm
Horiz distance(L)	5.273 µm
Vert distance	492.11 nm
Angle	5.331 °
Surface distance	3.354 µm
Horiz distance	3.125 µm
Vert distance	545.36 nm
Angle	9.899 °
Surface distance	
Horiz distance	
Vert distance	
Angle	
Spectral period	DC
Spectral freq	0 /µm
Spectral RMS amp	5.309 nm

Cursor: fixed Zoom: 2:1 Cen line: Off Offset: Off

CASE STUDY: EFFECT OF 120°C BAKE

Effect of 120 °C Bake

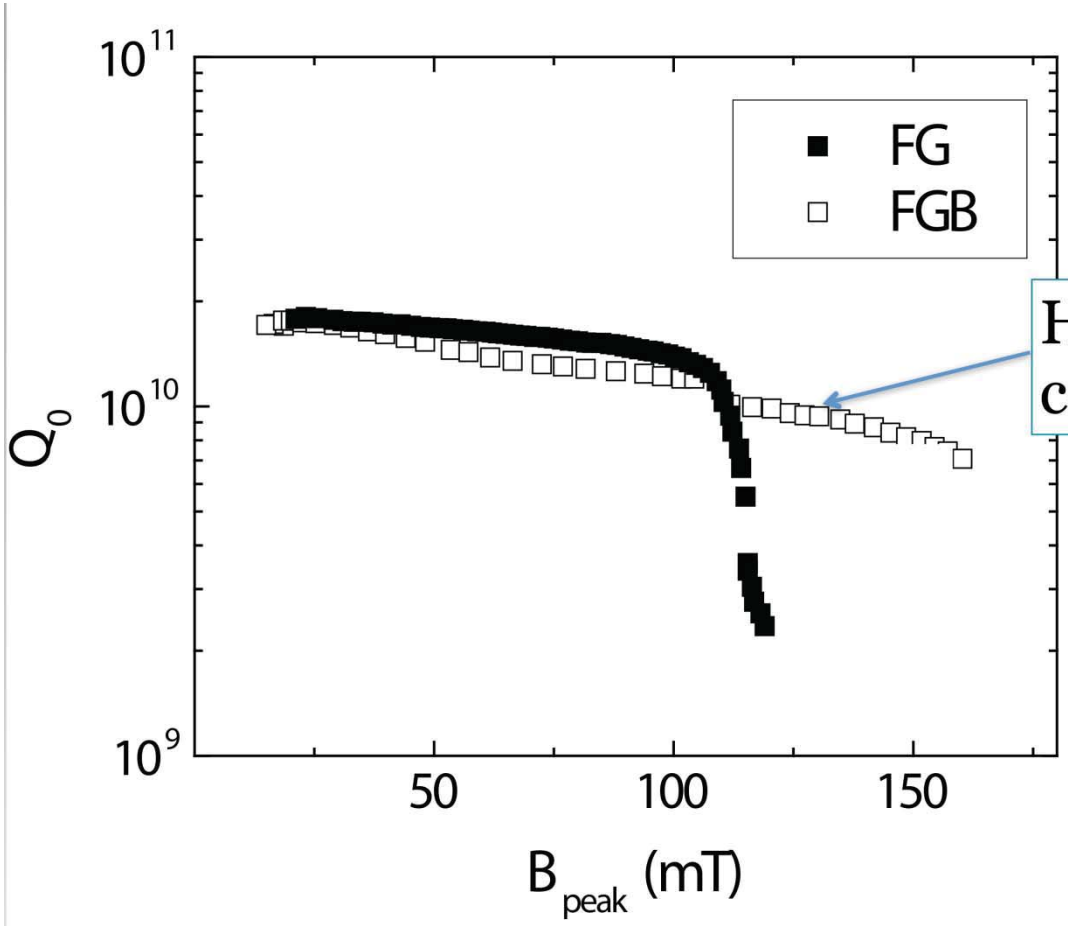

HFQS elimination in FG EP cavities after 120°C bake

Effect of 120 °C Bake

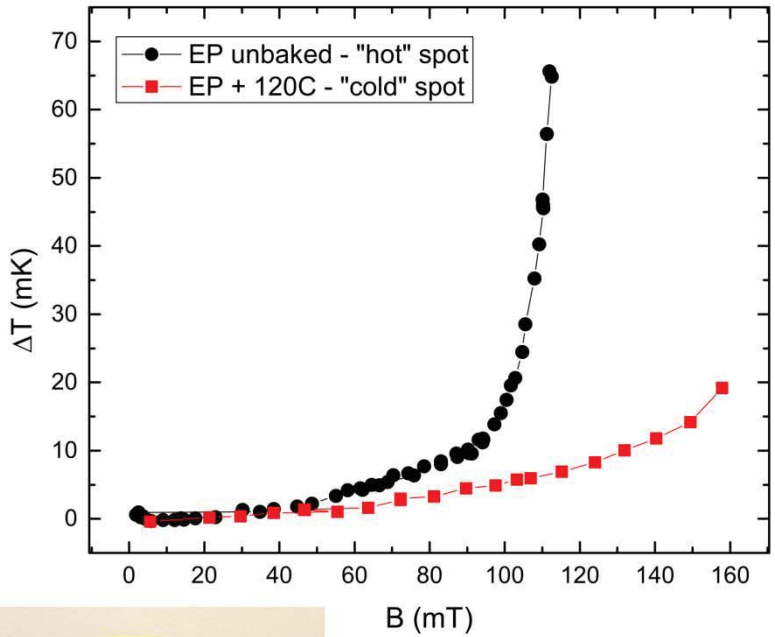

- **Hot spot**: from EP cavity
- **Cold spot**: from EP+120°C baked cavity

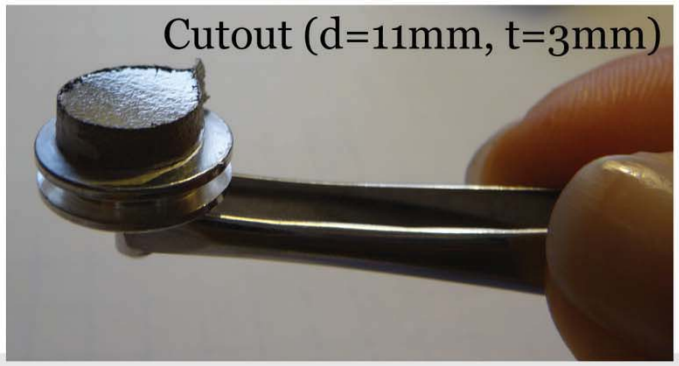

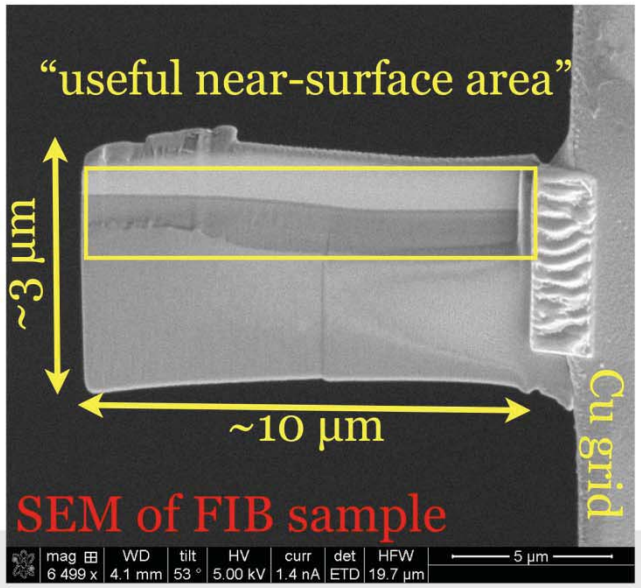

Effect of 120 °C Bake

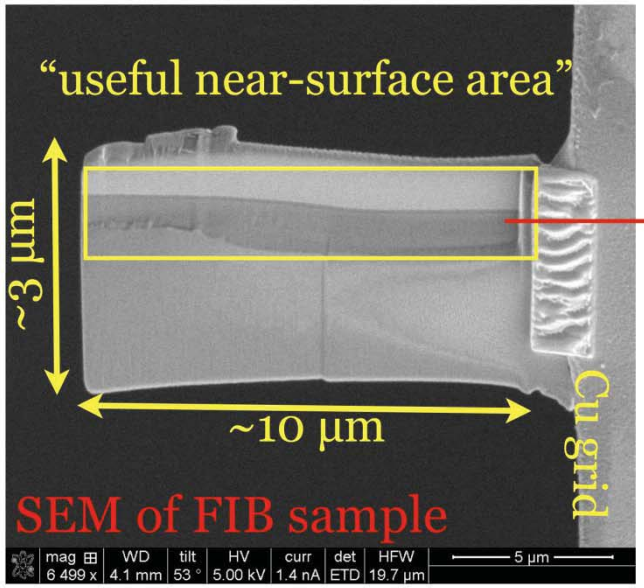

NED: Hot (not baked) and Cold (baked) spot at room T

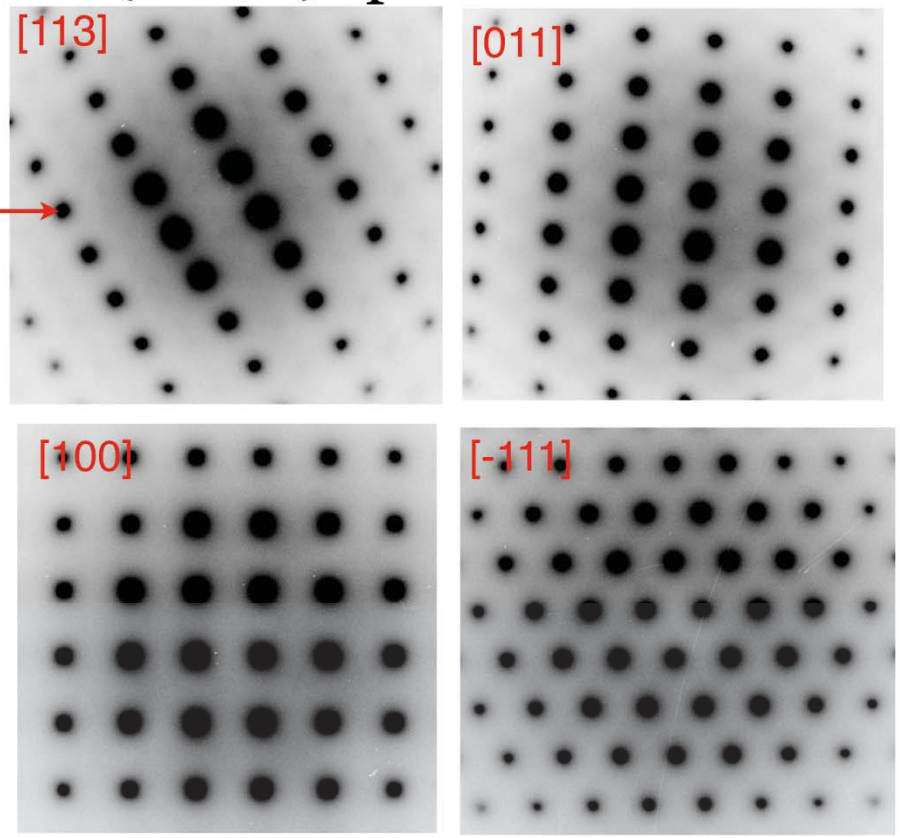

Electron diffraction: only Nb at room T
H in solid solution (α-phase)

Effect of 120 °C Bake

Diffraction mapping with low intensity beam

Hot (not baked) spot at 94K

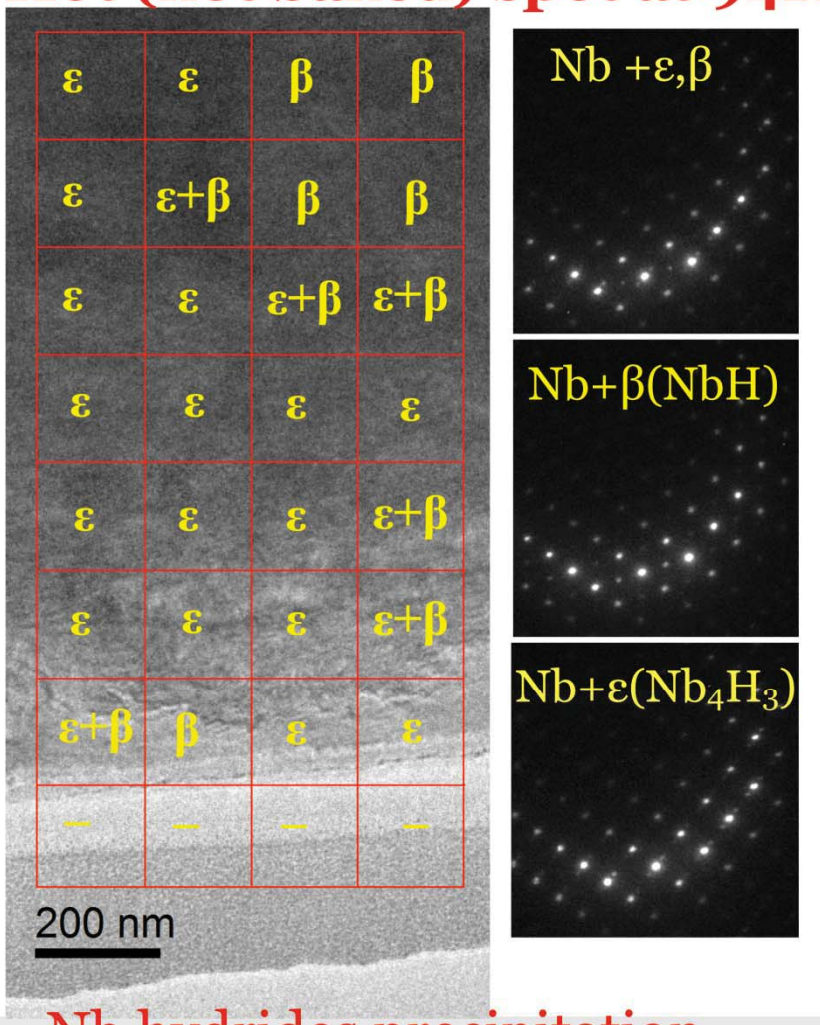

Nb hydrides precipitation

120°C baked stop at 94K

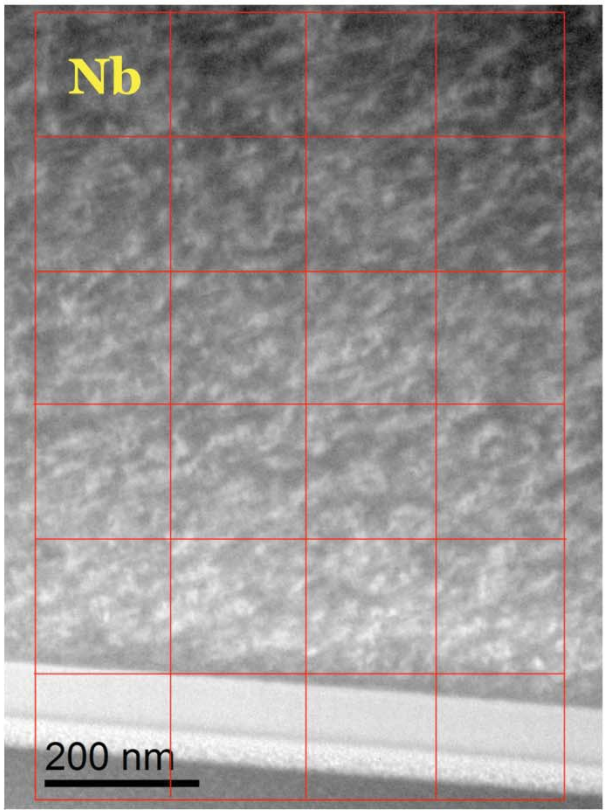

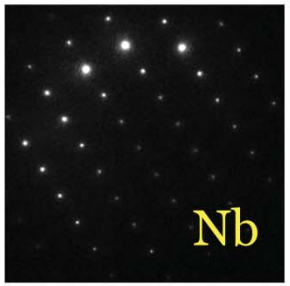

NO Nb hydrides precipitation

Effect of 120 °C Bake

Diffraction with brighter beam, better S/N

Hot (not baked) at 94K

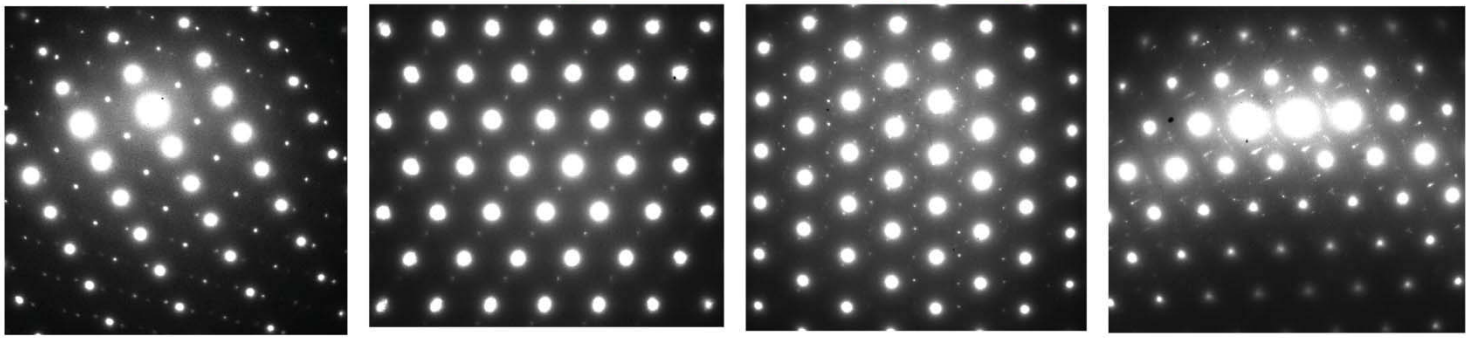

44%-68% probed spots

120°C baked stop at 94K

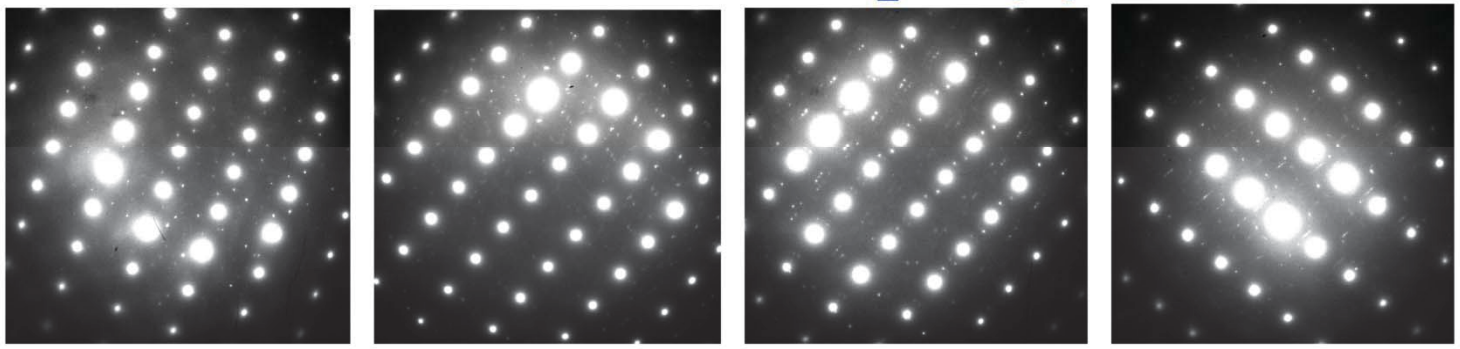

26%-29% probed spots

NED: Nb hydrides precipitation in **all cutouts**, amount and/or size of NbHx is different

Grain Boundary Investigation

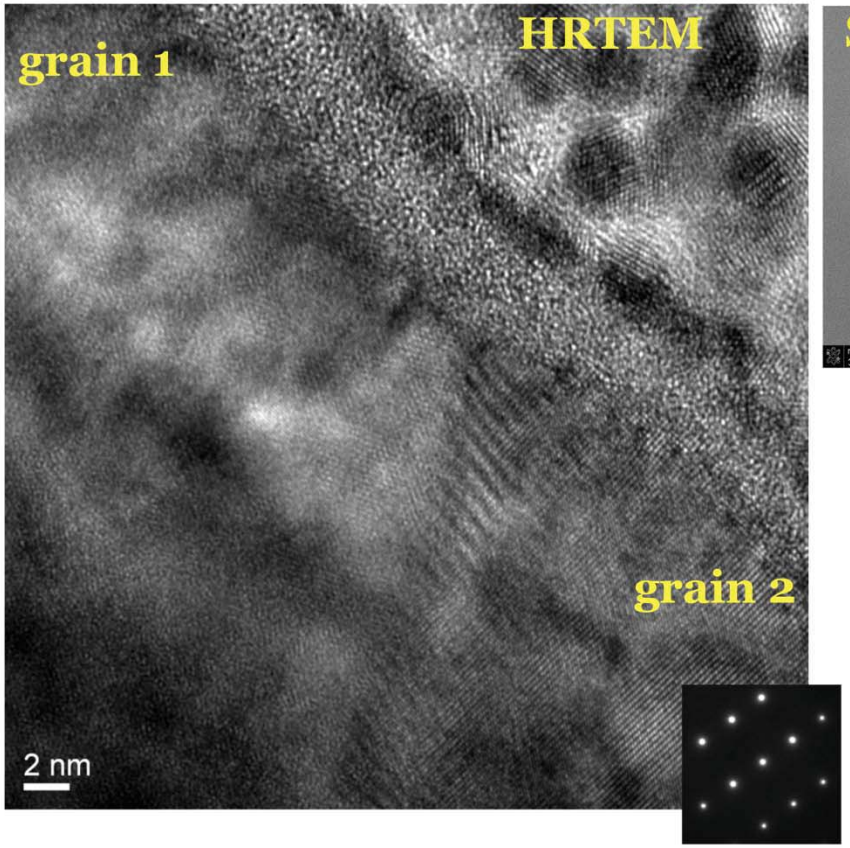

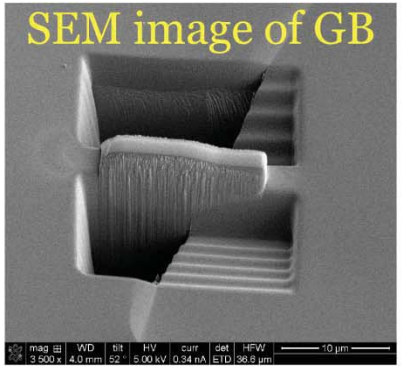

No evidence!

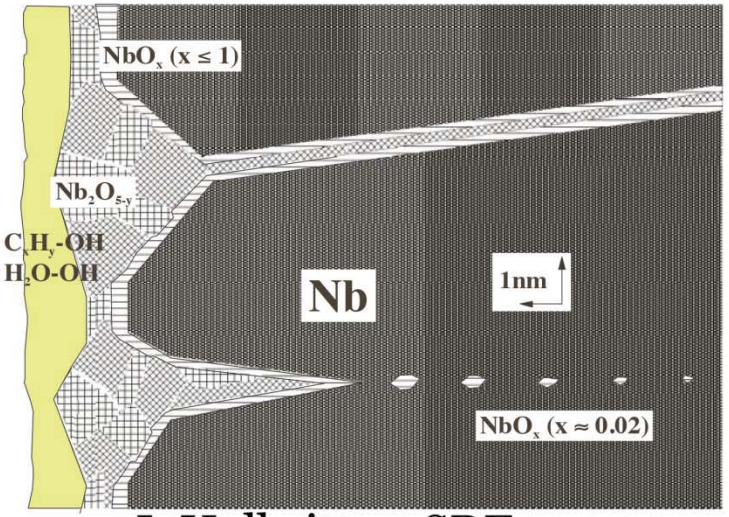

J. Halbritter, SRF 2001

HRTEM: No visible oxide layer along GB